



**KLIMA- OG
FORURENSNINGS-
DIREKTORATET**

Statlig program for forurensningsovervåking
Rapportnr. 1117/2012

Monitoring of greenhouse gases and aerosols at Svalbard and
Birkenes: Annual report 2010

TA
2902
2012

Utført av NILU – Norsk institutt for luftforskning

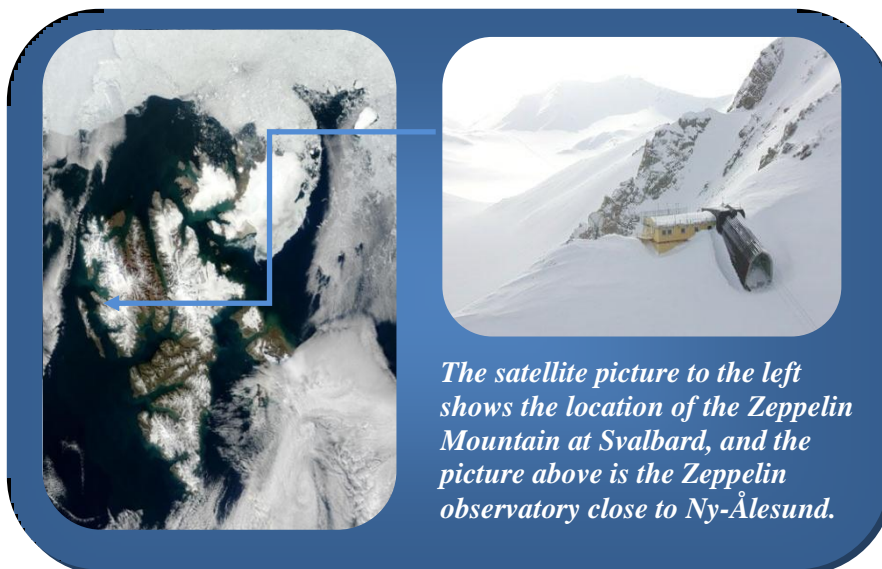


Preface

In 1999 The Climate and Pollution Agency (Klif, the former SFT) and Norwegian Institute for Air research (NILU) signed a contract commissioning NILU to run a programme for monitoring greenhouse gases at the Zeppelin station, close to Ny-Ålesund at Svalbard. This collaborative Klif/NILU programme includes monitoring of 23 greenhouse gases at the Zeppelin observatory in the Arctic. In 2009 NILU upgraded and extended the observational activity at the Birkenes Observatory in Aust-Agder. In 2010 the Klif/NILU monitoring programme was extended to also include the new observations from Birkenes of the greenhouse gases CO₂ and CH₄ and selected aerosol observations particularly relevant for the understanding of climate change.

The following greenhouse gases are regulated through the Montreal protocol and measured at the Zeppelin Observatory: chlorofluorocarbons (CFC), hydrochlorofluorocarbons (HCFC), and halones as well as other halogenated organic gases. Further the following gases included in the Kyoto protocol are monitored; methane (CH₄), nitrous oxide (N₂O) from 2010, hydrofluorocarbons (HFC), sulphurhexafluoride (SF₆). Additionally carbon monoxide (CO) and tropospheric ozone (O₃) are a part of the programme. The amount of particles in the air above the stations is also measured. The station is hosting measurements of carbon dioxide (CO₂) performed by ITM, University of Stockholm as well, but the availability of data is limited. This activity is funded by the Swedish Environmental Protection Agency.

The unique location of the Zeppelin observatory at Svalbard together with the infrastructure of the scientific research community at Ny-Ålesund makes it ideal for monitoring the global changes of the atmosphere. There are few local sources of emissions, and the Arctic location is also important as the Arctic is a particularly vulnerable region. The observations at the Birkenes Observatory complement the Arctic site. Birkenes Observatory is located in a forest area with few local sources. However, the observatory often receives long range transported pollution from Europe and the site is ideal to analyse the contribution of long range transported greenhouse gases and aerosol properties.



In 1987 the Montreal Protocol was signed and entered into force in 1989 in order to reduce the production and use of the ozone-depleting substances (ODS). The amount of most ODS in

the troposphere is now declining slowly and one expects to be back to pre-1980 levels around year 2050. It is crucial to follow the development of the concentration of these ozone depleting gases in order to verify that the Montreal Protocol and its amendments work as expected. Further these gases and their replacement gases are strong greenhouse gases making it even more important to follow the development of their concentrations. In December 1997 the Kyoto protocol was adopted. The target set by the Kyoto protocol is to reduce the total emissions of greenhouse gases from the industrialized countries during the period 2008 to 2012. The six most important groups of greenhouse gases included are: CO₂, CH₄, N₂O, fluorinated hydrocarbons (HFKs and PFKs) and sulphurhexafluoride (SF₆).

The Norwegian Institute for Air Research (NILU) is responsible for the operation and maintenance of the monitoring programme. The purpose of the programme is to:

- Provide continuous measurements of greenhouse gases in the Arctic region resulting in high quality data that can be used in trend analysis
- Provide continuous measurements of the greenhouse gases CO₂ and CH₄ at the Birkenes Observatory resulting in high quality data that can be used in trend analysis
- Provide trend analysis and interpretations of the observations from Zeppelin assess the influence regional anthropogenic emissions of greenhouse gases has on the radiative balance
- Provide information on the status and the development of the greenhouse gases with a particular focus on the gases included in the international conventions the Montreal and Kyoto protocol.
- Provide results of aerosol observations of relevance to the understanding of climate change
- Indicate sources regions with high influence on the measurements.

Observations and results from the monitoring programme are processed and used to assess the progress towards compliance with international agreements like the Kyoto and the Montreal Protocols. This report summarises the activities and results of the greenhouse gas and aerosol monitoring programme for the year 2010, and comprises a trend analysis for the period 2001-2010 including interpretation of the results.

Kjeller, March 2012

Cathrine Lund Myhre
Senior scientist and project manager

Table of Contents

Preface	1
1. Executive summary	5
2. Introduction	10
3. The Zeppelin and Birkenes Observatories; Norwegian Atmospheric supersites	13
3.1 Atmospheric supersites.....	13
3.2 The Zeppelin observatory.....	14
3.3 The Birkenes observatory.....	16
4. Observations and trends of greenhouse gases at the Zeppelin Observatory in the Norwegian Arctic	18
4.1 Greenhouse gases with natural and anthropogenic sources	19
4.1.1 Observations of methane in the period 2001-2010.....	19
4.1.2 Observations of Nitrous Oxide at the Zeppelin Observatory	23
4.1.3 Observations of Carbon Dioxide (CO ₂) in the period 1988-2010.....	24
4.1.4 Observations of Methyl Chloride in the period 2001-2010.....	26
4.1.5 Observations of Methyl Bromide in the period 2001-2010.....	27
4.1.6 Observations of tropospheric ozone in the period 1990-2010.....	29
4.1.7 Observations of CO in the period 2001-2010.....	30
4.2 Greenhouse gases with solely anthropogenic sources.....	32
4.2.1 Observations of Chlorofluorocarbons (CFCs) in the period 2001-2010	32
4.2.2 Observations of Hydrochlorofluorocarbons (HCFCs) in the period 2001-2010.....	34
4.2.3 Observations of hydrofluorocarbons (HFCs) in the period 2001-2010.....	36
4.2.4 Observations of halons in the period 2001-2010.....	39
4.2.5 Observations of other chlorinated hydrocarbons in the period 2001-2010	40
4.2.6 Perfluorinated compounds.....	41
5. Observations of greenhouse gases at the Birkenes Observatory in Aust-Agder	43
6. Aerosols and climate: Observations from Zeppelin and Birkenes Observatory	46
6.1 Observations of climate relevant aerosol properties: recent developments in Norway and internationally	47
6.2 Optical aerosol properties measured at Birkenes in 2010	49
6.3 Estimating the local, instantaneous direct aerosol radiative effect.....	51
6.4 Physical aerosol properties measured at Birkenes in 2010	52
6.5 Observations of the total aerosol load above Zeppelin and Birkenes observatories	55
6.5.1 Measurements of the total aerosol load above Ny-Ålesund.....	56
6.5.2 Measurements of the total aerosol load above the Birkenes observatory	59
7. Transport of pollution to the Zeppelin Observatory	62
8. References	64
Appendix I: Description of instruments, methods and trend analysis	67
Appendix II: Acknowledgments and affiliations of external authors	78

1. Executive summary

This annual report describes the activities and main results of the programme “Monitoring of greenhouse gases and aerosols at the Zeppelin Observatory, Svalbard, and Birkenes Observatory, Aust-Agder, Norway” for 2010. This is a part of the Governmental programme for monitoring pollution in Norway. The report comprises all natural well mixed greenhouse gases, the most important anthropogenic greenhouse gases as well as various particle’s properties with relevance to climate. Many of the gases also have strong ozone depleting effect.

Table 1: Key findings; Greenhouse gases measured at Ny-Ålesund; lifetimes in years¹, global warming potential (GWP), absolute change in concentrations since 2009, concentrations in 2010, their trends per year over the period 2001-2010, and relevance to the Montreal and Kyoto Protocols. All concentrations are mixing ratios in ppt_v, except for methane and carbon monoxide (ppb_v) and carbon dioxide (ppm_v).

Compound	Formula	Life-time	GWP ²	Change last year	2010	Trend / Year	Montreal or Kyoto Prot.	Comments on sources for the halocarbons
Methane	CH ₄	12 ³	25	>1	1892	+4.5	K	
Carbon monoxide	CO	Months		14.7	133	-0.26		
Carbondioxide ⁴	CO ₂		1	2.2	390	+2.1	K	
Chlorofluorocarbons								
CFC-11*	CCl ₃ F	45	4750	-1.8	241	-2.1	M phased out	foam blowing, aerosol propellant
CFC-12*	CF ₂ Cl ₂	100	10900	-3.7	534	-1.4	M phased out	temperature control
CFC-113*	CF ₂ CICFCl ₂	640	6130	-0.7	76	-0.7	M phased out	solvent, electronics industry
CFC-115*	CF ₃ CF ₂ Cl	1020	7370	0.0	8.4	+0.02	M phased out	temperature control, aerosol propellant
Hydrochlorofluorocarbons								
HCFC-22	CHClF ₂	11.9	1810	7.8	220.3	+6.8	M freeze	temperature control, foam blowing
HCFC-141b	C ₂ H ₃ FCI ₂	9.2	725	0.6	22.1	+0.5	M freeze	foam blowing, solvent
HCFC-142b*	CH ₃ CF ₂ Cl	17.2	2310	0.8	22.2	+0.9	M freeze	foam blowing
Hydrofluorocarbons								
HFC-125	CHF ₂ CF ₃	28.2	3500	1.3	9.2	+0.8	K	temperature control
HFC-134a	CH ₂ FCF ₃	13.4	1430	5.7	63.4	+4.6	K	temperature control, foam blowing, solvent, aerosol propellant
HFC-152a	CH ₃ CHF ₂	1.5	124	0.5	9.6	+0.8	K	foam blowing
Halons								
H-1211*	CBrClF ₂	16	1890	-0.1	4.3	-0.02	M phased out	fire extinguishing
H-1301	CBrF ₃	65	7140	0.0	3.3	+0.03	M phased out	fire extinguishing
Halogenated compounds								
Methylchloride	CH ₃ Cl	1.0	13	-6.0	520	+0.9		natural emissions (algae)
Methylbromide	CH ₃ Br	0.8	5	-0.4	7.3	-0.16	M freeze	agriculture, natural emissions (algae)
Dichloromethane	CH ₂ Cl ₂	0.38	8.7	3.3	41.7	+1.1		solvent
Chloroform	CHCl ₃	0.5	30	0.6	11.3	+0.01		Solvent, natural emissions
Methylchloroform	CH ₃ CCl ₃	5	146	-1.5	7.8	-3.31	M phased out	solvent
Trichloroethylene	CHClCCl ₂			0.1	0.6	-0.00		solvent
Perchloroethylene	CCl ₂ CCl ₂			0.2	3.1	-0.19		solvent
Sulphurhexafluoride* SF ₆		3200	22800	0.3	7.2	+0.25	K	Mg-production, electronics

* The measurements of these components have higher uncertainty. See Appendix I for more details.

¹ From Scientific Assessment of Ozone Depletion: 2010 (WMO, 2011b)

²GWP (Global warming potential) 100 years time period, CO₂ = 1

³ The lifetime for CH₄ are adjustment times including feedbacks of indirect effects on the lifetime. The lifetime is close to 9 year without adjustments.

⁴ Measurements of CO₂ is performed by Stockholm University. This is preliminary data and there is no trend calculation.

The lifetimes and GWPs in Table 1 are updated in accordance with the 4th Assessment Report of the IPCC and the last ozone Assessment report published in 2011 (WMO, 2011b). Trends are calculated for the period 2001–2010 and are given in mixing ratio (concentration) per year. Further details and interpretations are presented in section 3 of the report, and our observations are compared to updated results from the from the Assessment report (WMO, 2011b).

Greenhouse gases regulated through the Kyoto protocol – Key findings from the Zeppelin observatory

The report includes the 6 greenhouse gases or groups of gases regulated through the Kyoto protocol. The key findings are:

- **Methane – CH₄:** In 2010 the mixing ratios of methane increased to **new record levels both globally and at Zeppelin** where an annual mean value of 1892 ppb was reached. The increase in 2010 was however very small at Zeppelin; ca 1 ppb compared to the 29 ppb increase from 2005 to 2010. The methane increase at the Zeppelin observatory from 2005 to 2010 was 29 ppb or around 1.5%, whilst there was a 1,4 % increase globally. Both values seem to constitute a relatively large change compared to the evolution of the methane levels in the period from 1998-2005; the change was close to zero for this period both at Zeppelin and globally after a strong increase during the 20th Century according to IPCC (Forster et al., 2007).

There is yet no clear explanation for the global increase in methane that started in 2005, but a probable explanation could be increased methane emissions from wetlands, both in the tropics as well as in the Arctic region. This hypothesis is supported in recent studies published in 2011. Melting permafrost, both in terrestrial regions and at the sea floor, might introduce new possible methane emission sources initiated by the temperature increase the last years. According to recent studies in 2011, this does not seem to influence the observations at Zeppelin (Fisher et al. 2011). If this should be the case, it would be an alarming development, given the extensive stocks of methane in the permafrost.

To improve our understanding of the ongoing processes an immediate extension of the monitoring of methane is needed, in particular to identify possible sources in the Arctic. Methane from various sources has different isotopic ratios of ¹³C/¹²C. Isotopic measurements of methane at Zeppelin combined with transport modeling would be a very powerful tool to distinguish between methane from various sources as wetlands, oceans and exploitation of gas fields included gas transportation.

- **Nitrous Oxide –N₂O:** The global mean level of N₂O has increased from around 270 ppb prior to industrialization and up to an average global mean of 323.2 ppb in 2010 (WMO, 2011a) which is new record level. In 2009 NILU installed a new instrument at Zeppelin measuring N₂O to follow the evolution of this compound in the future in the Arctic. The instrument has been in full operation since April 2010 and the observations are presented in this report.

- **CO₂ reached new record level in 2010 both globally and at the Zeppelin Observatory in the Arctic.** The global abundance was 389.0 according to WMO (2011a) and the preliminary analysis of the Zeppelin measurements indicates a mixing ratio of 390 ppm.

The annual growth rates were slightly higher than to the last years, above 2 ppm per year both globally and at Zeppelin.

- **Hydrofluorocarbons:** These gases replace the strongly ozone depleting substances CFC's, and are relatively new gases emitted to the atmosphere. They are all of solely anthropogenic origin. The mixing ratios of HFC-125, HFC-134a, HFC-152a have **increased by as much as 360%, 206% and 237% respectively since 2001** at the Zeppelin observatory. However, their concentrations are still very low, thus the total radiative forcing of these gases since the start of their emissions around 1970 and up to 2010 is only about 0.013 W m^{-2} . For comparison: The forcing of a typical 2 ppm annual increase in CO_2 is around 0.03 W m^{-2} and the forcing of these HFCs is less than 1 % of the radiative forcing from the change in CO_2 since pre-industrial time. Thus the contribution from these manmade gases to the global warming is small today, but given the observed extremely rapid increase in the use and atmospheric concentrations, it is crucial to follow the development of these gases in the future.
- **The perfluorinated compound – SF_6 :** The only perfluorinated compound measured at Zeppelin is Sulphurhexafluoride, SF_6 . This is an **extremely potent greenhouse gas**, but the concentration is still very low. However, measurements show that the concentration has increased more than 45% since 2001.

Greenhouse gases regulated through the Montreal protocol – Key findings

All gases regulated through the Montreal protocol are substances depleting the ozone layer. In addition they are all greenhouse gases. The amount of most of the ozone-depleting substances (ODS) in the troposphere is now declining slowly globally and is expected to be back to pre-1980 levels around the year 2050. The gases included in the monitoring programme at Zeppelin are the man-made greenhouse gases called chlorofluorocarbons (CFCs), the hydrogen chlorofluorocarbons (HCFCs), which are CFC substitutes, and halons.

- **CFCs:** In total the development of the CFC gases measured at the global background site Zeppelin give reason for optimism. The concentrations of the observed CFCs, **CFC-11, CFC-12 and CFC-113 are declining, whilst CFC-115 is at the same level as in 2009**. The mixing ratios of three of the gases are now at a lower level than in 2001 when measurements started at Zeppelin.
- **HCFCs:** The CFC substitutes **HCFC-22, HCFC-141b and HCFC-142b all had a relatively strong increase in the levels measured at Zeppelin from 2001-2010**. HCFC-22 used for temperature control and foam blowing had the largest growth rate. This is the most abundant substance of the HCFCs and is currently increasing at a rate of 6.8 ppt/year which is almost 4% per year, and as much as 38% increase since 2001. HCFC-142b had the strongest relative increase with more than 21% since 2007 and more than 50% since 2001.
- **Halons:** Halons are the Bromine containing halocarbons. The levels of the two gases monitored have been relatively stable over the observation period at Zeppelin. The recent results indicate that there was a maximum in 2004 for halon-1211 at Zeppelin, and a small decline after that. According to the last Ozone Assessment (WMO, 2011b) the total stratospheric Bromine concentration is no longer increasing, and Bromine from halons

stopped increasing during the period 2005-2008. Also our last observations indicate that the growth has stopped.

Greenhouse gases not regulated through the protocols – Key findings

The monitoring programme also includes five greenhouse gases not regulated through any of the two protocols.

- **Chlorinated greenhouse gases:** These are the following 5 chlorinated gases: methylchloride (CH_3Cl), dichloromethane (CH_2Cl_2), chloroform (CHCl_3), trichloromethane (CHClCCl_3), perchloroethylene (CCl_2CCl_2). The concentrations of these gases show small variations from year to year and four of them have increased the last years. A considerable increase in chloroform is evident at Zeppelin from 2009-2010, and since 2009 the component has increased with ca 10%. The reason for this is not yet clear. **Dichloromethane shows an increase of almost 34% since 2001**, and as much as 8.5 % the last year. The main use of this compound is as an active ingredient in paint removers.

Long range transport of pollutions; aerosols and reactive gases – Key findings

- **Aerosols:** Aerosols are small particles in the atmosphere. Major sources of anthropogenic aerosols are burning of fossil fuel, coal and biomass including waste from agriculture and forest fires. Aerosols can have a cooling or warming effect depending on the chemical compositing. Globally the cooling effect dominates and has offset the warming of the greenhouse gases since the year 1750 by around 1/3. However, this is connected with considerable uncertainty and the uncertainty with respect to the effects of aerosols on the radiative balance and climate is one of the reasons for the large uncertainty in IPCC's projected range of the increase in global temperature. Measuring a wide range of aerosol variables is therefore crucial for improved understanding of global warming and its mitigation.

Observations of the total amount of aerosol particles above Ny-Ålesund show increased concentration levels during spring time compared to the rest of the year. This is called Arctic haze which is due to transport of pollution from lower latitudes (mainly Europe and Russia) during winter/spring. In 2010 this aerosol pollution was at approximate the same level as previous years. There were also shorter episodes with elevated levels of particles later than springtime. Aerosol particles are short-lived climate forcing agents, some with cooling, and some with warming effects. Their concentrations and combined effects can change relatively fast. An extension of the aerosol observations at Zeppelin by including measurements of the aerosol absorption properties will be very useful to improve the knowledge about the different types of aerosols and their effects in the Arctic atmosphere.

Starting in 2010 aerosol observations from the Birkenes observatory are included in the program. The aerosols observed at Birkenes are characterized by long-range transport from Great Britain, Central Europe, and the Arctic, with occasional long-range transport episodes also from North America including forest fire aerosol. In addition to the long range transported aerosols, also aerosols from local or regional emissions, either natural or anthropogenic are observed. With respect to local or regional influence on the forming of aerosol particles, it seems like natural emissions from vegetation dominate in summer,

whereas anthropogenic emissions dominate in winter at Birkenes. The climate effect of aerosols observed at Birkenes seems in average for the whole year to be cooling , but the strength reveals seasonal variations. The chemical composition of aerosols in Norway is more thoroughly discussed in Aas et al. (2011).

- **Reactive gases:** Tropospheric ozone and CO have elevated levels in polluted regions like central Europe. They are suitable indicators for long range transport of pollution from the continents to Svalbard, and CO is also a proper tracer for transport of emissions from biomass burning and other fire events. There were several episodes with elevated levels of ozone and CO in 2010 at Zeppelin indicating long range transport. No episode was as extreme as the one in 2006. In general there has been **a reduction in the CO concentration at Zeppelin from 2003-2009, but a considerable increase from 2009 to 2010**. The reason for this is not yet understood. The annual mean value for 2010 was 133 ppb compared 118 ppb in 2009. The results for ozone is more thoroughly discussed in Aas et al. (2011).

2. Introduction

The greenhouse effect is a naturally occurring process in the atmosphere caused by trace gases, especially water vapour (H₂O), carbon dioxide (CO₂), methane (CH₄) and nitrous oxide (N₂O) that naturally occur in the atmosphere. The content of the last three gases in the atmosphere are closely related to emissions from main sources, whilst the water content varies mainly with temperature. Without these gases the global mean temperature would have been much lower. These gases absorb infrared radiation and thereby trap energy emitted by the Earth. Due to this energy trapping the global mean temperature is approximately 13.7°C, more than 30 degrees higher than it would have been without these gases present (IPCC, 2007). This is the natural greenhouse effect. The enhanced greenhouse effect refers to the additional effect of the greenhouse gases from human activities. In the industrial era, after 1750, the concentration of greenhouse gases in the atmosphere has increased significantly. The global atmospheric mean mixing ratios of CO₂ has increased by 39% (from 280 ppm as a pre-industrial concentration to 389 ppm in 2010) and methane has increased by as much as 158% from 700 ppb to 1808 ppb in 2010) according to WMO (WMO, 2011a). 2011 showed new record levels of both these gases. The overall changes in the concentrations of the greenhouse gases are the main cause of the global mean temperature rise of 0.74°C over the last century reported by IPCC (2007). Depending on the various emission scenarios used and natural feedback mechanisms the temperature is predicted to increase with 1.1-6.4°C approaching the year 2100, according to IPCC (2007).

Radiative forcing⁵ is a useful tool to estimate the relative climate impacts of various components inducing atmospheric radiative changes. The influence of external factors on the climate can be broadly compared using this concept. Revised global-average radiative forcing estimates from the 4th IPCC assessment report are shown in Figure 1 (IPCC, 2007). The estimates represent radiative forcing caused by changes in anthropogenic factors since pre-industrial time and up to the year 2005.

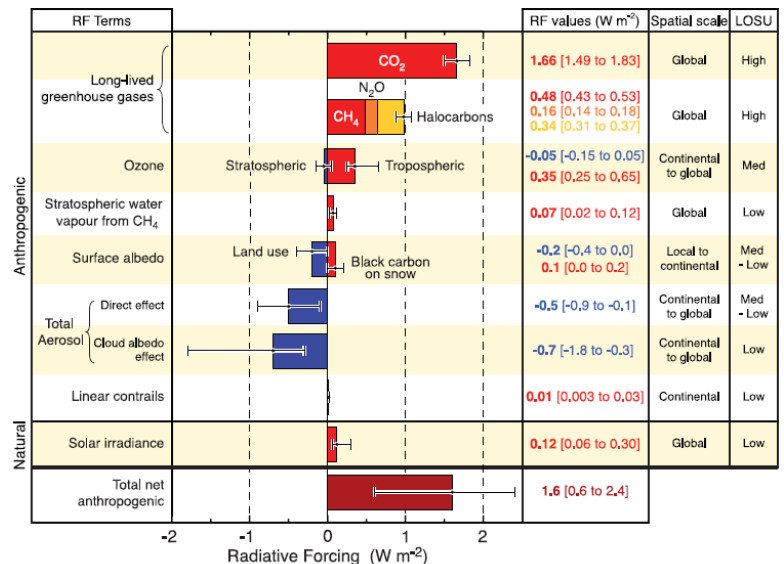


Figure 1: Global-average radiative forcing (RF) estimates for important anthropogenic agents and mechanisms together with the typical spatial scale of the forcing and the assessed level of scientific understanding (LOSU).

⁵ Radiative forcing is a measure of the influence a factor has in altering the balance of incoming and outgoing energy in the Earth-atmosphere. It is an index of the importance of the factor as a potential climate change mechanism. It is expressed in Wm⁻² and positive radiative forcing tends to warm the surface. A negative forcing tends to cool the surface.

The most important greenhouse gas emitted from anthropogenic activities is CO₂ with a radiative forcing of 1.66 W m⁻² given in the 4th IPCC report (IPCC, 2007). This is an increase of 0.2 W m⁻² since the IPCC report from 2001. CH₄ and N₂O are other components with strong forcings of 0.48 W m⁻² and 0.16 W m⁻² respectively. It is worth noting that even the change in CO₂ radiative forcing since 2001 is stronger than the total forcing of e.g. N₂O since 1750, emphasising the importance of CO₂.

The joint group of halocarbons is also a significant contributor to the radiative forcing. Halocarbons include a wide range of components. The most important ones are the ozone depleting gases regulated through the Montreal protocol. This includes the CFCs, the HCFCs, chlorocarbons, bromocarbons and halons. Other gases are the HFC (fluorinated halocarbons), PFCs (per fluorinated halocarbons), and SF₆. These fluorinated gases are regulated through the Kyoto protocol. The total forcing of the halocarbons is 0.337 Wm⁻², and the single component CFC-12 is presently stronger than N₂O, but the concentration of CFC-12 seems to have reached its peak value. The trend for CFC-12, seemingly to lower concentrations, gives reason for optimism for this substance. Observations of the halocarbons and methane are central activities at the Zeppelin observatory. Most of the halocarbons have now a negative trend in the development of the atmospheric mixing ratios.

The diagram below shows the relative contribution (in percent) of the long-lived greenhouse gases and ozone to the anthropogenic greenhouse warming since pre-industrial times (1750). The numbers are based on the radiative forcing estimates in the last IPCC report. The diagram shows that CO₂ has contributed to 55% of the changes in the radiative balance while methane has contributed 16% since pre-industrial times. The halocarbons have contributed 11% to the direct radiative forcing of all long-lived greenhouse gases.

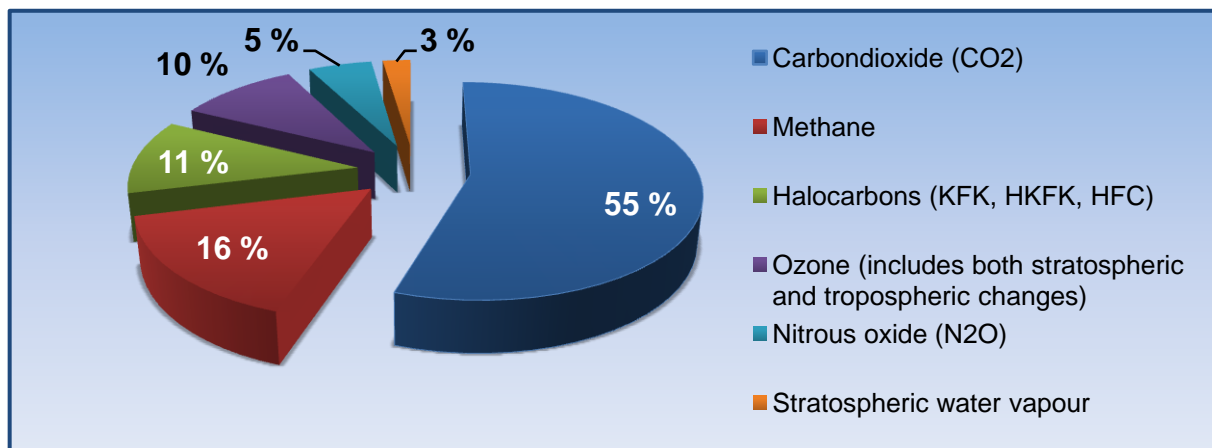


Figure 2: The relative contribution in percent of the long-lived greenhouse gases and ozone to the anthropogenic warming since pre-industrial times (1750). The numbers are based on the radiative forcing estimates in the last IPCC report.

According to the last IPCC report (IPCC, 2007), a large source of uncertainty in climate predictions is caused by insufficient understanding of the atmospheric aerosol processes and historic evolution.

There are two dominant pathways for atmospheric aerosols to influence climate, both exerting a cooling effect in most cases. On one hand, aerosol scatter incoming solar radiation back into

space, preventing it from reaching the ground and warm the surface. This is the so-called direct aerosol climate effect. Additionally, aerosols are activated to cloud particles. Increasing the number of aerosols will in turn increase the cloud particles and also the reflectivity and lifetime of the cloud, again with a cooling effect. This is called indirect aerosol climate effect. Both effects are quantified by negative aerosol radiative forcing in Figure 1 leading to cooling of the surface. The negative aerosol radiative forcing partially offsets the positive, warming radiative forcing by greenhouse gases. In this way the aerosols mask the warming of the greenhouse gases, the magnitude is still uncertain.

The main objective of NILU's monitoring programme is to observe, analyse and interpret the changes in the atmospheric concentrations of the gases included in the Montreal protocol and the Kyoto protocol. An overview of all gases observed together with their trends, lifetime and GWP is given in Table 1 in the Summary. Furthermore the programme shall provide relevant information about aerosols observations important for increased understanding of climate change.

The international collaboration regarding the protection of the ozone layer leading to the Montreal protocol started with the Vienna convention in 1985. Two years later the Montreal protocol was signed and for the first time there was an international agreement forcing the participating countries to reduce and phase out anthropogenic substances. Halocarbons and their relation to the Montreal protocol are indicated in Table 1. Today more than 190 countries have ratified the protocol and many countries have also ratified the later additions to the protocol. The Montreal protocol has goals and strategies for all of the ozone reducing substances and the protocol is a part of the UN environmental program UNEP. According to the last ozone assessment report from WMO (WMO, 2011b) the total combined abundance of anthropogenic ozone-depleting gases in the troposphere has continued to decrease from the peak value observed in the 1992-1994 time period. However, the decrease is slower than previous projected due to slower decrease in CFC-11 and CFC12, and also larger increase in HCFC than anticipated. The reduction is around 28% relative to the peak value. In the stratosphere the peak is later, around 200-2002, and the reduction since then is close to 10% (WMO, 2011b).

The target set by the Kyoto protocol is to reduce the total emissions of greenhouse gases from the industrialized countries during the period 2008 to 2012. The four most important greenhouse gases and two groups of gases are included: CO₂, CH₄, N₂O, SF₆ (sulphur-hexafluoride), hydrofluorocarbons (HFCs) and perfluorocarbons (PFCs). The emissions are calculated as annual mean values during the period 2008-2012. The gases are considered jointly and weighted in accordance with their global warming potentials as given by IPCC (2007) and shown in Table 1.

A Norwegian introduction to the Montreal and Kyoto protocol can be found at "Miljøstatus Norge" (<http://www.miljostatus.no>). The English link to the Montreal protocol is http://ozone.unep.org/Ratification_status/montreal_protocol.shtml whereas the Kyoto protocol can be found at http://unfccc.int/essential_background/kyoto_protocol/items/1678.php.

3. The Zeppelin and Birkenes Observatories; Norwegian Atmospheric supersites

3.1 Atmospheric supersites

There are considerable future challenges connected with the understanding of atmospheric change, and the effects of this. This includes the evolution and assessments of long-lived greenhouse gases (LLGHG) as well as the understanding of short-lived climate forces (SLCF). SLCF includes aerosols and tropospheric ozone in particular, and related gases as CO, NO_x, methane and volatile organic compounds (VOC). Furthermore also the interaction between aerosols and clouds is largely unknown. A key point in the analysis and understanding of these variables are quality assured and harmonised measurements within Europe, as well as on larger geographical scale. NILU acts as the Chemical Coordinating Centre for EMEP⁶ and coordinates the atmospheric monitoring work under the Convention on Long-Range Transboundary Air Pollution (under United Nations Economic Commission for Europe). This is a scientifically based and policy driven programme with high relevance for the institute's involvement in, and relation to, international research infrastructure projects and ESFRI (European Strategy Forum on Research Infrastructures) research infrastructures. There are mutual benefits and close links between selected infrastructure programs in EU and EMEP. In particular NILU has been highly involved in EUSAAR (European Supersites for Atmospheric Aerosol Research, ended this year), and now ACTRIS (Aerosols, Clouds, and Trace gases Research InfraStructure Network, www.actris.net) but also the new infrastructure project InGOS (Integrated non-CO₂ greenhouse gases observing system). The importance of these projects is high for the development of optimised observational infrastructures (both with respect to equipments, analysis and cost) to meet the future needs for studying atmospheric compositional change. The projects are focusing on both long-lived and short-lived climate forcers. International collaboration and harmonisation of these types of

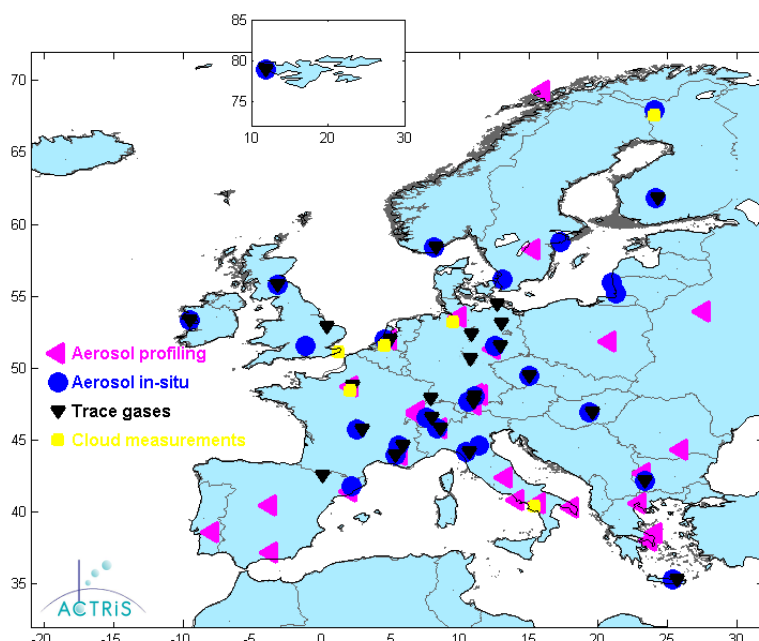


Figure 3: The map shows sites in ACTRIS and the distribution of various types atmospheric measurements.

observations are crucial for processes understating and satisfactory quality to assess trends. NILU is also involved in ICOS (Integrated Carbon Observation System) and has two atmospheric sites that will become ICOS sites if national funding is established (At Birkenes and Zeppelin). The map in Figure 3 shows the sites include in the research infrastructure project ACTRIS (www.actris.net). This project started 1. April 2011.

⁶ EMEP: European Monitoring and Evaluation Programme: <http://www.emep.int/>



Figure 4: Location of NILU's the atmospheric sites measuring long lived greenhouse gases.

Trough different monitoring programmes, NILU operates many measurements sites, and three of these are comprehensive observatories measuring various long lived greenhouse gases illustrated in Figure 4. The national monitoring programme of greenhouse gases has only included measurements from Zeppelin from 2001, but in 2010 measurements of CO₂ and CH₄ at Birkenes was also included. Additionally, NILU performs measurements of CO and CO₂ at Andøya from 2010 through the *Marine Pollution Monitoring Programme*.

Norway has a national interest and particular responsibility to develop harmonized and high quality GHG observation infrastructures in the northern region including the Sub-arctic and Arctic areas. Long range transport of air pollution from the central-European continent is occurring, and of high relevance. There is also transport from the North-American continent, China and other Asian regions (Stohl, 2006) detected at Zeppelin. Furthermore, the industrial development in the Arctic regions, particularly the increase in oil, gas, and ship activities, will influence the GHG levels in this vulnerable region. Moreover, possible emission from the

huge reservoirs of methane in the Arctic region is crucial to follow over long time. These are typical emissions from regions with thawing of permafrost, changes in wetlands and thaw lakes, and methane hydrates at the sea floor. All are sensitive to global warming, with strong positive feedbacks.

The measurement activities at the Zeppelin and Birkenes Observatories contribute to a number of global, regional and national monitoring networks:

- EMEP (European Monitoring and Evaluation Programme under "UN Economic Commission for Europe")
- AGAGE (Advanced Global Atmospheric Gases Experiment)
- Global Atmospheric Watch (GAW under WMO)
- Network for detection of atmospheric change (NDAC under UNEP and WMO)
- Arctic Monitoring and Assessment Programme (AMAP)

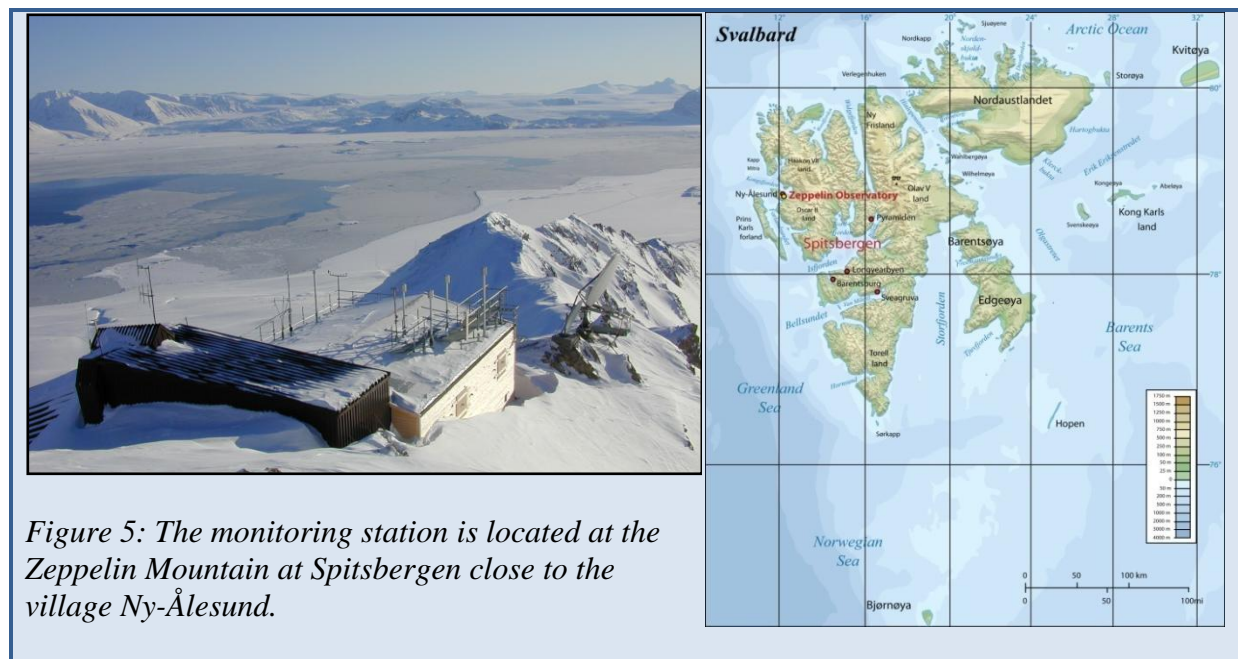
Most data are public available through the international data base hosted at NILU: <http://ebas.nilu.no>.

3.2 The Zeppelin observatory

The monitoring observatory is located in the Arctic on the Zeppelin Mountain, close to Ny-Ålesund at Svalbard. At 79° north the station is placed in an undisturbed arctic environment, away from major pollution sources. Situated 474 meters a.s.l and most of the time above the inversion layer, there is minimal influence from local pollution sources in the nearby small community of Ny-Ålesund.

The unique location of the station makes it an ideal platform for the monitoring of global atmospheric change and long-range transport of pollution. The main goals of NILU's research activities at the Zeppelin station are:

- Studies of climate related matters and stratospheric ozone
- Exploration of atmospheric long-range transport of pollutants. This includes greenhouse gases, ozone, persistent organic pollutants, aerosols and others.
- Characterization of the arctic atmosphere and studies of atmospheric processes and changes



The Zeppelin station is owned and maintained by the Norwegian Polar Institute. NILU is co-ordinating the scientific activities at the station. The station was built in 1989-1990. After 10 years of use, the old building was removed to give place to a new modern station that was opened in May 2000. The building contains several separate laboratories, some for permanent use by NILU and Stockholm University, others intended for short-term use like measurement campaigns and visiting scientists. A permanent data communication line permits on-line contact with the station for data reading and instrument control.

NILU performs measurements of more than 20 greenhouse gases including halogenated greenhouse gases, methane and carbon monoxide. In Appendix I there are more details about sampling techniques and frequency of observations. Methane and CO are sampled 3 times per hour. This high sampling frequency gives valuable data for the examination of episodes caused by long-range transport of pollutants as well as a good basis for the study of trends and global atmospheric change. Close cooperation with AGAGE-partners on the halocarbon instrument and audits on the methane and CO-instruments (performed by EMPA on the behalf of GAW/WMO) results in show data of high quality.

The amount of particles in the air is monitored by a Precision-Filter-Radiometer (PFR) sun photometer. This instrument gives the aerosol optical depth (AOD). AOD is a measure of the aerosols attenuation of solar radiation in the total atmospheric column.

The station at Zeppelin Mountain is also used for a wide range of other measurements, which are not directly related to climate gas monitoring, including daily measurements of sulphur and nitrogen compounds (SO_2 , SO_4^{2-} , $(\text{NO}_3^- + \text{HNO}_3)$ and $(\text{NH}_4^+ + \text{NH}_3)$, main compounds in precipitation (performed in Ny-Ålesund), total gaseous mercury, particulate heavy metals, persistent organic pollutants (HCB, HCH, PCB, DDT, PAH etc.) in air, as well as tropospheric ozone. Zeppelin observatory is also widely used in campaigns as during the International Polar Year.

At the Zeppelin station carbon dioxide (CO_2) is measured by Stockholm University (SU) (Institute of Applied Environmental Research, ITM). SU maintain an infrared CO_2 instrument measuring CO_2 continuously. The instrument has been in operations since 1989. The continuous data are enhanced by the weekly flask sampling programme in co-operation with NOAA CMDL. Analysis of the flask samples provide CH_4 , CO , H_2 , N_2O and SF_6 data for the Zeppelin station in addition to CO_2 .

3.3 The Birkenes observatory

Birkenes is located in Southern-Norway at 58° 23'N, 8° 15'E, 190 m a.s.l. Birkenes atmospheric observatory in Aust-Agder fills a central position in the Norwegian climate monitoring programme since it represents Norway's South also downwind from Europe receiving long range transported air pollution. The observatory has been in operation since 1971 and is one of the longest-running sites in Europe, and it is one of the core EMEP sites. In 2009, the aerosol observation programme at Birkenes Atmospheric Observatory received a major upgrade along with the upgrade of the general station infrastructure. The observatory was moved a few hundred meters and considerably upgraded in 2009 now measuring CO_2 and CH_4 with a Picarro instrument and a comprehensive aerosol program. The old station was situated in a hollow with limited line of sight to the oncoming flow. Since summer 2009, the observations are housed in a container assembly on the top of a hill a, with free line of sight to the oncoming flow in all directions (see Figure 6). The land use in the close vicinity of the site is characterized by 65% forest, 10% meadow, 15% freshwater lakes, and 10% agricultural areas (low intensity). This relocation improved the regional representativeness of the station significantly. The observation programme concerning atmospheric aerosol parameters was augmented by measurements of coarse mode particle size distribution, spectral particle scattering coefficient, and aerosol optical depth. It meets now EUSAAR⁷ and GAW standards, and comprises now almost all observations considered by the GAW aerosol scientific advisory group as relevant for aerosol climate effect assessments. This upgrade is also an important improvement of the Norwegian observation programme of climate forcing agents, which so far was more focussed on the polar regions. Accurate observations of climate relevant aerosol properties are a prerequisite for better climate predictions for this region.

All electrical and data infrastructure is new and upgrade with Near-Real-Time measurements controlled at NILU. Data from Birkenes (e.g. daily measurements SO_2 , SO_4^{2-} , $\text{NO}_3^- + \text{HNO}_3$ and $\text{NH}_4^+ + \text{NH}_3$, main compounds in precipitation, mercury and other heavy metals, persistent organic pollutants, tropospheric ozone) have been essential for the study of long-range transport and deposition of air pollution to Scandinavia. The monitoring at this site, together with other central European regional sites, has provided the necessary background for establishing international binding agreements for targeting emission reductions, c.f. the convention for long-range transboundary air pollutions (CLTRAP) and the protocols

⁷ EUSAAR: European Supersites for Atmospheric Aerosol Research <http://www.eusaar.net>

hereunder. Personnel is visiting the observatory on a daily basis, and engineers from NILU are present at the station regularly (approximately once per month).

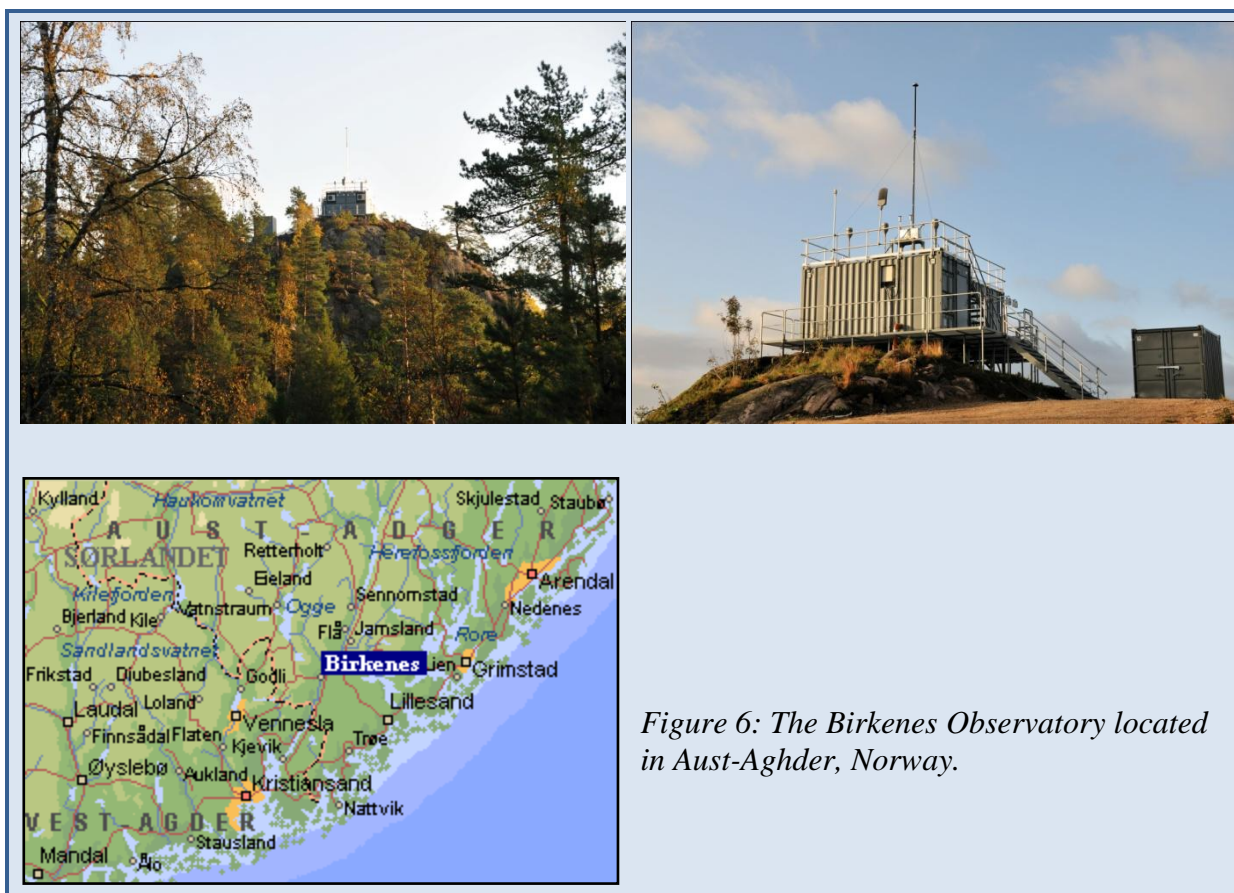


Figure 6: The Birkenes Observatory located in Aust-Agder, Norway.

4. Observations and trends of greenhouse gases at the Zeppelin Observatory in the Norwegian Arctic

NILU measures 23 greenhouse gases at the Zeppelin observatory at Svalbard. The results from the measurements, analysis and interpretations are presented in this chapter. Also observations of CO₂, which are performed by the Stockholm University - Department of Applied Environmental Science (ITM), are included in the report.

Table 2 presents the main results with annual mean values since the beginning of the observation period in 2001. Also trend per year and change (acceleration) in the trend for each component is given. The acceleration in the trend show how the growth rate has changed the last few years, and indicates the expected change in the coming years⁸, assuming the same development in the emissions.

Table 2: Yearly average concentration levels of greenhouse gases measured at the Zeppelin station for the years 2001-2010. All concentrations are in ppt_v, except for methane and carbon monoxide (ppb_v) and CO₂ (ppm_v). The trends are calculated from observations for the period 2001-2010.

Compound	Formula	2001	2005	2010	Trend / year	Change in trend
Methane	CH ₄	1858	1863	1892	+4.5	+0.75
Carbon monoxide	CO		132.6	133	-0.26	-0.72
Carbon dioxide**	CO ₂	371	380	390	2.1**	-0.15**
Chlorofluorocarbons						
CFC-11*	CFCl ₃	259	251	241	-2.1	-0.05
CFC-12*	CF ₂ Cl ₂	547	547	534	-1.4	-0.6
CFC-113*	CF ₂ ClCFCl ₂	82	79	76	-0.7	0.1
CFC-115*	CF ₃ CF ₂ Cl	8.3	8.6	8.4	+0.02	-0.00
Hydrochlorofluorocarbons						
HCFC-22	CHF ₂ Cl	159	181	220	+ 6.8	-0.5
HCFC-141b	CH ₃ CFCl ₂	16.5	19.6	22.1	+ 0.5	-0.06
HCFC-142b*	CH ₃ CF ₂ Cl	14.5	17.1	22.2	+ 0.90	+0.06
Hydrofluorocarbons						
HFC-125	CHF ₂ CF ₃	2.0	4.5	9.5	+0.8	+0.08
HFC-134a	CH ₂ FCF ₃	20.7	40.0	63.4	+4.60	-0.01
HFC-152a	CH ₃ CHF ₂	2.8	5.6	9.6	+0.80	-0.01
Halons						
H-1211*	CF ₂ ClBr	4.4	4.5	4.3	- 0.02	-0.02
H-1301	CF ₃ Br	3.0	3.2	3.3	+ 0.03	-0.01
Halogenated compounds						
Methyl Chloride	CH ₃ Cl	505	521	520	+0.87	-1.00
Methyl Bromide	CH ₃ Br	9.1	8.7	7.3	-0.16	-0.07
Dichloromethane	CH ₂ Cl ₂	31.0	32.1	41.7	+1.1	+ 0.28
Chloroform	CHCl ₃	10.8	10.5	11.3	+0.01	+0.05
Methylchloroform	CH ₃ CCl ₃	38.3	19.1	7.8	-3.31	+0.55
Trichloroethylene	CHClCCl ₂	0.7	0.4	0.6	-0.00	+0.03
Perchloroethylene	CCl ₂ CCl ₂	4.4	3.1	3.1	-0.19	+0.09
Sulphurhexafluoride*	SF ₆	4.9	5.8	7.2	+0.25	+0.01

The measurements of these components are not within the required precision of AGAGE. See Appendix I for more details.

***Measurements of Carbon dioxide are performed by Stockholm University, Department of Applied Environmental Science (ITM).*

⁸ As the time series still are short and the seasonal and annual variations are large for many of the components, there are considerable uncertainties connected with the results.

Greenhouse gases have numerous sources both anthropogenic and natural. Trends and future changes in concentrations are determined by their sources and the sinks, and in section 4.1 are observations and trends of the monitored greenhouse gases with both natural and anthropogenic sources presented in more detail. In section 4.2 are the detailed results of the gases with purely anthropogenic sources presented. These gases are not only greenhouse gases but also a considerable source of chlorine and bromine in the stratosphere, and are thus responsible for the ozone depletion and the ozone hole discovered in 1984. The ozone depleting gases are controlled and regulated through the successful Montreal protocol. Section 3 describes the Zeppelin observatory at Svalbard where the measurements take place and the importance of the unique location. Zeppelin observatory is a unique site for observations of changes in the background level of atmospheric components. All peak concentrations of the measured gases are significantly lower at Ny-Ålesund than at other sites, due to the stations remote location. A description of the instrumental and theoretical methods applied is included in Appendix I.

4.1 Greenhouse gases with natural and anthropogenic sources

All gases presented in this section (methane, carbon dioxide, methyl chloride, methyl bromide, carbon monoxide and tropospheric ozone) have both natural and anthropogenic sources. This makes it complex to interpret the observed changes as the sources and sinks are numerous. Moreover, several of these gases are produced in the atmosphere from chemical precursor gases and often also dependant on the solar intensity.

4.1.1 Observations of methane in the period 2001-2010

Methane (CH₄) is the second most important greenhouse gas from human activity after CO₂ with a radiative forcing of 0.48 W m⁻² since 1750 and up to 2005. The average CH₄ concentration in the atmosphere is determined by a balance between emission from the various sources at the earth's surface and reaction and removal by free hydroxyl radicals (OH) in the troposphere. In addition to be a dominating greenhouse gas, methane also plays a significant role in the atmospheric chemistry. The atmospheric lifetime of methane is ca 9 years and about 12 years when indirect effects are included (Forster et al., 2007).

In the atmosphere methane is destroyed by the reaction with the hydroxyl radical (OH) giving water vapour and CO₂. A small fraction is also removed by surface deposition. The stratospheric impact of CH₄ is due to the fact that CH₄ contributes to water vapor buildup in this region of the atmosphere influencing the ozone layer. Since the reaction with OH also represents a significant loss path for the oxidant OH, additional CH₄ emission will suppress OH and thereby increase the CH₄ lifetime, implying further increases in atmospheric CH₄ concentrations (Isaksen and Hov, 1987; Prather et al., 2001). This positive chemical feedback is estimated to be significant in the current atmosphere with a feedback factor of about 1.4⁹ (Prather et al., 2001). The OH radical has a crucial role in the tropospheric chemistry by reactions with many emitted components and is responsible for the cleaning of the atmosphere (like removal of CO, hydrocarbons, HFCs, and others).

The atmospheric mixing ratio of methane has, after a strong increase during the 20th century, been relatively stable over the period 1998-2005. The global average change was close to zero for this period according to IPCC (Forster et al, 2007), and also at our site for the short observation period 2001-2004. 2003 was an exception globally and at Zeppelin; a maximum

⁹ This means that with current atmospheric chemical distribution a 10 % increase in emission of methane, the atmospheric composition increases will reach 14 %.

annual mean of 1870 ppb at Zeppelin was obtained, considerable higher than the other years. This was probably caused by increased precipitation in the tropical regions leading to increased methane emissions from wetland areas and a global rise in the concentration. Recently an increase in the methane levels is evident from both our observations, and observations at other sites (Rigby et al., 2008; WMO, 2009). The year 2010 showed new record globally, but same level at Zeppelin as in 2009. Figure 7 presents the observations of methane at Zeppelin since the start in 2001.

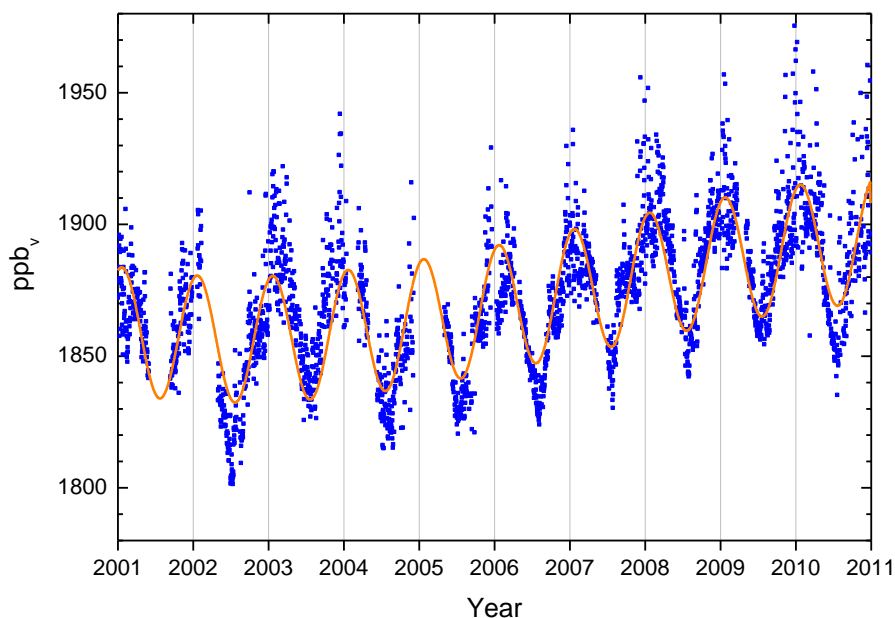


Figure 7: Observations of daily averaged methane concentrations for the period 2001-2010 at the Zeppelin observatory. Blue dots: observations, orange solid line: modelled background methane mixing ratio.

As can be seen from Figure 7 there has been an increase in the concentrations of methane observed at Zeppelin the last years. The pronounced increase started in November/December 2006 and continued throughout the years 2007 - 2009, and is particularly evident in the late summer-winter 2007, and late autumn 2009. A maximum methane mixing ratio as high as 1975 ppb was observed 26th December 2009. This was 2.9% above the modelled background value, and the highest value ever recorded at Zeppelin. There were no values nearly as high as this in 2010. Note that for 2010 there are lower values during summer than for 2009.

To retrieve the annual trends in the methane levels for the entire period the observations have been fitted by an empirical equation as described in Appendix I. The modelled methane values are included as the orange solid line in Figure 7. Only the observations during periods with clean air arriving at Zeppelin are used in the model, thus the model represents the background level of methane at the site.

During 1980s when the methane concentration showed a large increase, the annual change was around 15 ppb ppb_v per year. At Zeppelin the average annual growth rate was +4.5 ppb_v per year for the period 2001-2010. This corresponds to an increase of 0.18% per year. In 2009 there has been an acceleration of 0.75 in the trend (see Table 2), a slowdown in the change compared to 2001-2009. The development in the future is connected with large uncertainty as

the reason for the observed increase since 2005 is not clear, and additionally, the seasonal and annual variations are large and the time series still short.

The increase in the methane levels the last years is visualized in Figure 8 showing the CH₄ annual mean mixing ratio for the period 2001-2010. The annual means are based on a combination of the observed methane values and the modelled background values; during periods with lacking observations we have used the modelled background mixing ratios in the calculation of the annual mean.

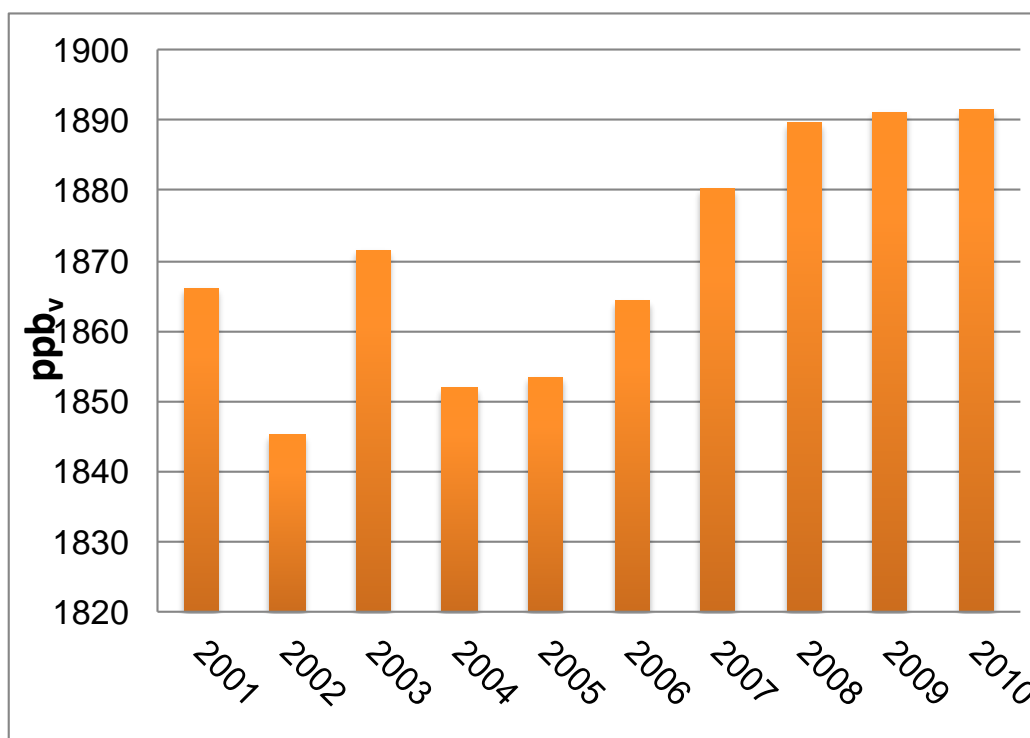


Figure 8: Development of the annual mean mixing ratio of methane measured at the Zeppelin Observatory for the period 2001-2010.

This diagram clearly illustrates the increase in the concentrations of methane during 2004-2008, with 2010 at the same level as for 2009. Unfortunately more data had to be rejected in October-December 2010 than previous years due to a problem with ventilation at the station. This has led to high uncertainty in the calculated annual mean, particularly because there are strong seasonal variations in methane. This might have resulted in slightly too low annual mean for 2010. The annual mean mixing ratio for 2010 was 1892 ppb while the level was 1891 ppb_v in 2009. The increase since 2005 at Zeppelin is 29 ppb (ca. 1.5 %) which is considered as relatively large compared to the development of the methane mixing ratio in the period from 1999-2005 both at Svalbard and globally. It is also larger than the global mean increase since 2005 which is 25 ppb (WMO, 2009; 2011a).

Also stations at other locations show a significant increase in methane for the year 2007, 2008, and 2009 at both hemispheres. According to WMO (WMO, 2010) there has been a global increase in the methane concentration by 7 ppb from 2006 to 2007 and a continuation of the increase up to a new record level in 2010. The global mean absolute increase from

2009-2010 was 5 ppb. Thus the global increase is higher than what we observed at Zeppelin for 2010.

The main sources of methane include boreal and tropical wetlands, rice paddies, emissions from ruminant animals, biomass burning, and fossil fuels combustion. Further, methane is the principal component of natural gas and e.g. leakage from pipelines, off-shore and on-shore installations are known source of atmospheric methane. The distribution between natural and anthropogenic sources is approximately 40% natural sources, and 60% of the sources are direct a result of anthropogenic emissions. Of natural sources there is a large unknown potential methane source at the ocean floor, so called methane hydrates. Other sources include mud volcanoes which are connected with deep geological faults, and also emissions from plants are suggested (Keppler et al., 2006). Further a large unknown amount of methane is bounded in the permafrost layer in Siberia and North America and this might be released if the permafrost layer melts as a feedback to climate change. According to a recent paper in Nature (Schoor and Abbot, 2011), there is a high risk of permafrost thaw and substantial realisation of both CO₂ and CH₄. They estimated a release of 30-63 billion tonnes carbon from Arctic soil before the year 2040 as response to a predicted Arctic temperature increase of 7.5°C by the year 2100. This is 1.7-5.2 times larger than previous estimates. They assume that most of the carbon release will be as CO₂, and less than 3% will be emitted as CH₄. However, because CH₄ has much higher global warming potential (25 compared to CO₂), almost half of the climate effect will be caused by CH₄. According to the last IPCC report (Alley et al., 2007) the temperature of the top of the permafrost layer has generally increased by up to 3°C since 1980s.

The recent observed increase in the atmospheric methane concentrations has led to enhanced focus and intensified research to improve the understanding of the methane sources and changes particularly in responses to global and regional temperature increase. Currently the observed increase the last years is not explained or understood. The high level observed in 2003 was a global feature, and is still not fully understood. It is essential to find out if the increase since 2005 is due to large point emissions or if it is caused by newly initiated processes releasing methane to the atmosphere like e.g. the thawing of the permafrost layer. Recent and ongoing scientific discussions point in the direction of increased emissions from wetlands located both in the tropical region and in the Arctic region.

One valuable method to study various methane sources is to exploit isotopic measurements. Many arctic methane sources have different isotopic ratios of ¹²C_{CH₄} ¹³C_{CH₄}. Combined with model studies of air transport to Zeppelin it is possible to improve the quantification of emission from wetlands, gas from fossil fuel, and emission from methane hydrates at the sea floor. This has been done in selected periods during 2008 and 2009 at Zeppelin and the results are described in Fischer et al. (2011). The study shows that the dominant Arctic summer CH₄ source in 2008 and 2009 was from wetlands. During winter time fossil gas emissions dominated the CH₄ input. Submarine emissions along the West Spitsbergen slope was found to have negligible CH₄ input to the atmosphere in summer, despite the fact that it was possible to identify methane bubbles in the sea from the sea floor. Gas hydrates at the sea floor are widespread in thick sediments in this area between Spitsbergen and Greenland. If the sea bottom warms, this might initiate further emissions from this source. Our results presented in Fisher et al. (2011) are in agreement with the findings of Bousquet et al. (2011). They have used models to study global source attribution to the changes in atmospheric methane for 2006-2008. Their conclusions were that in 2007 tropical wetland contributed 2/3 to the global

increase, but with a significant contribution also from wetlands at high latitudes boreal regions.

Wetland CH₄ emissions respond rapidly to warming. In particular, Arctic and boreal wetlands are likely to respond immediately to sustained heatwaves and increases in precipitation. Fire CH₄ is also more likely with elevated temperatures. There is a strong need for more regular CH₄ isotopic measurements in the high Arctic. Isotopic data can then be used to constrain emissions in both regional and global inversion models. Continuous monitoring of carbon isotopes of methane at several of Arctic sites will be important for the understanding and quantification of future changes in Arctic methane sources. High effort should be put on the issue to understand the increase in the CH₄ concentrations as the consequence might be severe. Currently NILU has two research projects¹⁰ financed by Norwegian Research Council where the objectives are to understand greenhouse gas budgets and establish isotopic methane measurements at Zeppelin.

4.1.2 Observations of Nitrous Oxide at the Zeppelin Observatory

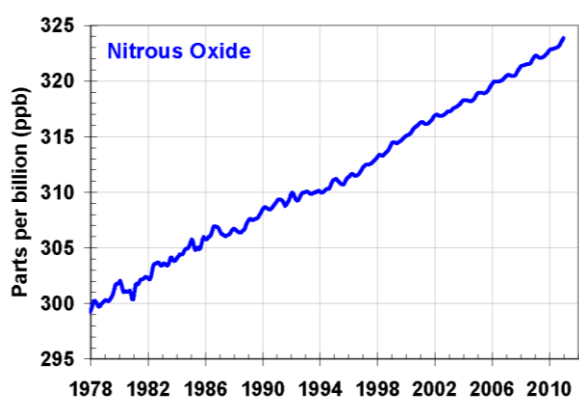


Figure 9: Global average abundances of, nitrous oxide from the NOAA global air sampling network are plotted since the beginning of 1979. <http://www.esrl.noaa.gov/gmd/aggi/>

Nitrous Oxide (N₂O) is a greenhouse gas with both natural and anthropogenic sources. The sources include oceans, tropical forests, soil, biomass burning, cultivated soil and use of fertilizer, and various industrial processes. There are large uncertainties in the major soil, agricultural, combustion and oceanic sources of N₂O and also frozen peat soils in Arctic tundra is reports as a potential significant source (Repo et al., 2009). N₂O has a lifetime of ca 114 years and the GWP is 310 (Forster et al, 2007). Thus N₂O is an important greenhouse gas with a radiative forcing of 0.16 W m⁻² since 1750 contributing around 5-6 % to the overall long lived greenhouse gas

forcing over the industrial era. The gas is regulated through the Kyoto protocol. Additionally, N₂O is also the major source of the ozone-depleting nitric oxide (NO) and nitrogen dioxide (NO₂) in the stratosphere thus the component is also influencing the stratospheric ozone layer. The recent Assessment of the ozone depletion (WMO, 2011b) suggests that current emissions of N₂O are presently the most significant substance that depletes ozone.

N₂O has increased from around 270 ppb prior to industrialization and up to an average global mean of 323.2 in 2010 (WMO, 2011a). The acreage growth rate from 2005-2008 was 0.8 ppn/year (WMO, 2011b). Figure 9 is taken from NOAA and shows the average global development of N₂O since 1978. The mean growth rate has been 0.77 ppb/yr the last 10 according to WMO. The NOAA observations are based on flask samples with mostly weekly or lower time resolution. There are few continuous observations of N₂O, and particularly in the Arctic region. In 2009 NILU installed a new instrument at Zeppelin to measure N₂O with

¹⁰ GAME: Causes and effects of Global and Arctic changes in the MEthane budget: <http://game.nilu.no>
GHG-Nor: Greenhouse gases in the North: from local to regional scale

high time resolution; 15 mins. The instrument was in full operation in April 2010 and the results for 2010 are presented in Figure 10.

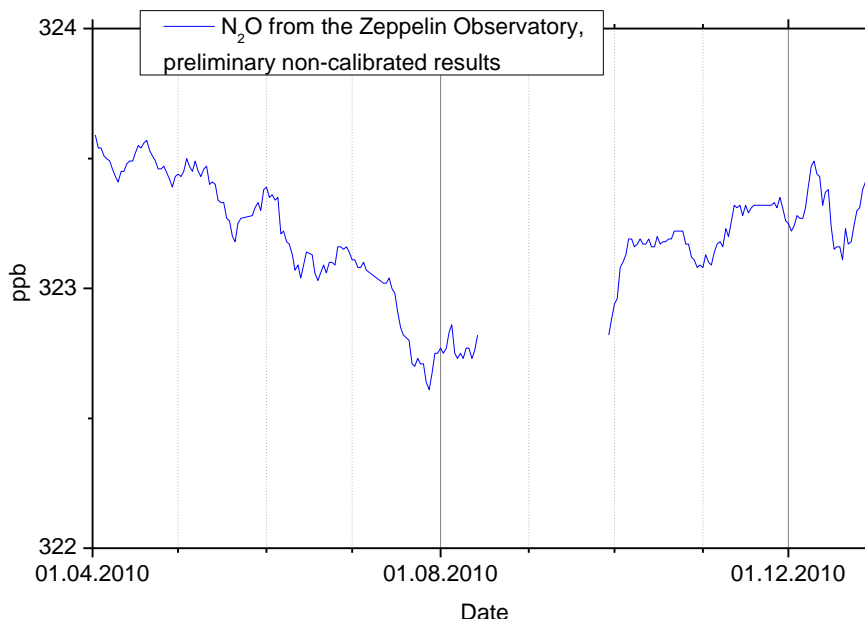


Figure 10: Measurements of N₂O at the Zeppelin Observatory for 2010.

4.1.3 Observations of Carbon Dioxide (CO₂) in the period 1988-2010

CO₂ is the most important greenhouse gases with a radiative forcing of 1.66 W m⁻² since 1750 and an increase in the forcing of as much as 0.2 W m⁻² since the IPCC report from 2001 (Forster et al., 2007). CO₂ is the end product in the atmosphere of the oxidation of all main organic compounds and has shown an increase of as much as 39 % since the pre industrial time (WMO, 2011a).

Norway do not perform own measurements of CO₂ at the Zeppelin Observatory. The atmospheric CO₂ concentration measured at Zeppelin Observatory for the period 2001-2010 is presented in Figure 11. These data are provided by ITM University of Stockholm and we acknowledge the effort they are doing in monitoring CO₂ at the site. Note that the data are preliminary and have not undergone full quality assurance.

The results show a continues increase since the start of the observations and in Figure 12 is the development of the annual mean concentrations measured at Zeppelin observatory for the period 1988-2010 shown.

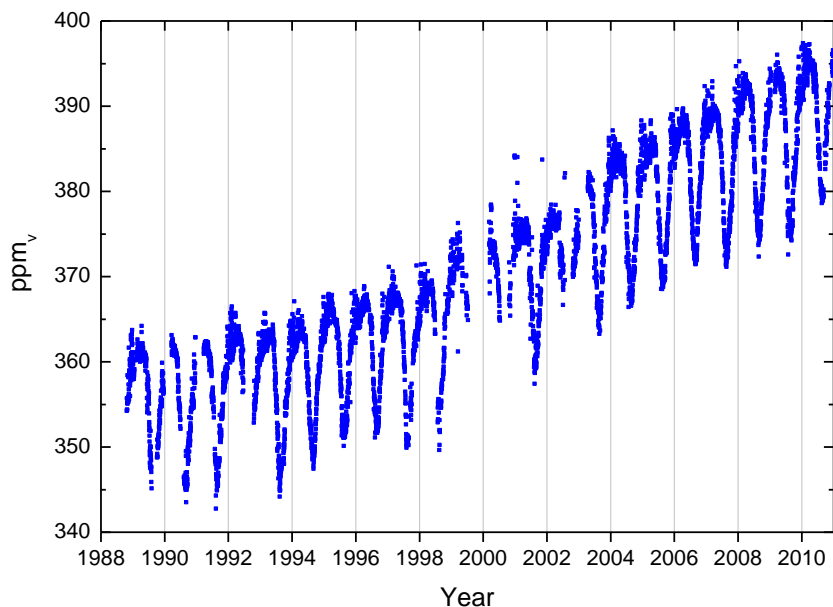


Figure 11: The CO₂ concentration measured at Zeppelin Observatory for the period 2001-2010.

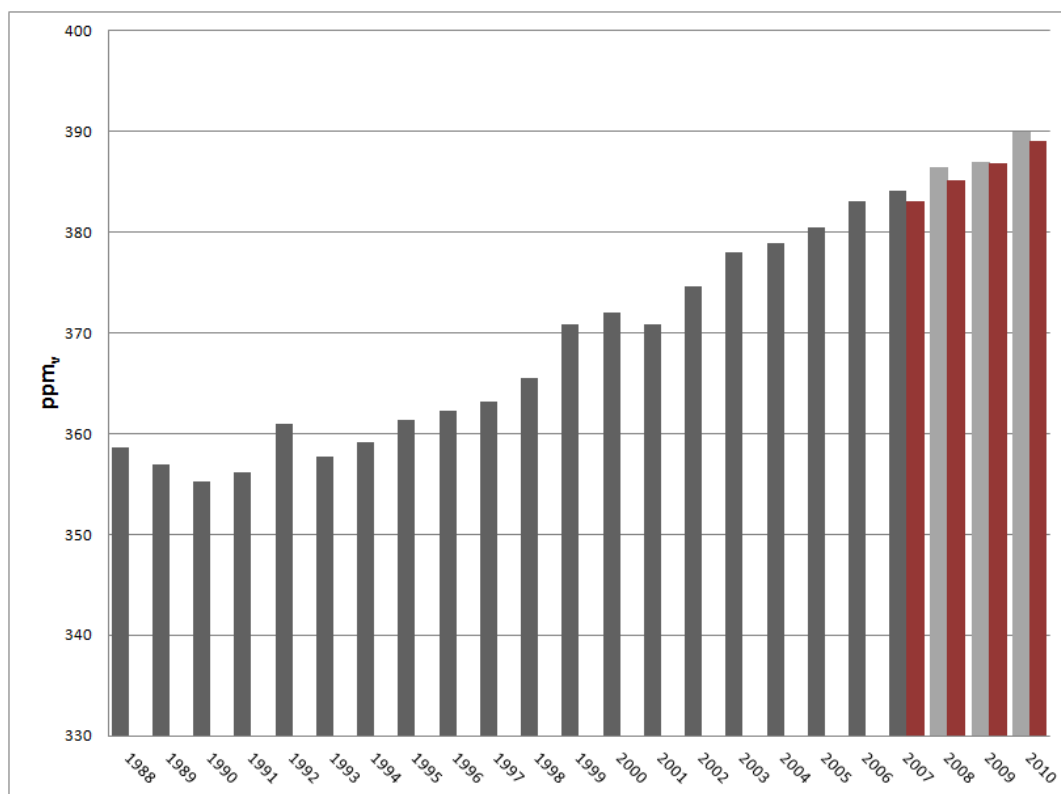


Figure 12: Development of the annual mean mixing ratio of CO₂ measured at Zeppelin observatory for the period 1988-2010. The light grey bars are the preliminary results, and the red bars show the global annual mean for 2007-2010 (WMO, 2011a).

The preliminary results show that 2010 is a new record year for the annual mixing ratio of CO₂ at Zeppelin, and the increase is considerable larger than the global mean increase with an

increase at Zeppelin of 3.0 ppb and a global mean increase of 2.3 ppb (WMO 2011a). This is the largest yearly increase at Zeppelin since 2003. The preliminary results indicated an increase of only 0.6 ppb from 2008 to 2009. ITM University of Stockholm have not completed their analysis of the observations, thus the mean values for the last years are preliminary. It is shown as a light grey bars in the Figure. The global mean value for 2010 is 389.0 ppb (WMO, 2011a). This is an increase of 2.3 ppb since 2009, and considerable higher than the increase from 2008-2009 (1.6 ppb). The main reason why the CO₂ level is higher at Zeppelin than globally is that in general the CO₂ emissions is lower in the Southern hemisphere, and the global mixing takes a certain time.

4.1.4 Observations of Methyl Chloride in the period 2001-2010

Methyl chloride (CH₃Cl) is the most abundant chlorine containing organic gas in the atmosphere, and it contributes 16% to the total Chlorine from the long lived gases in the troposphere (WMO, 2011b). The main sources of Methyl Chloride in the atmosphere are natural and dominating source is thought to be emissions from warm coastal land, particularly from tropical islands are shown to be a significant source but also algae in the ocean, and biomass burning. Several of these sources are vary with global temperature change (WMO, 2011b). Due to the dominating natural sources, this compound is not regulated trough any of the Montreal or Kyoto protocols, but is an important natural source of Chlorine to the stratosphere.

The results of the observation of this substance for the period 2001-2011 are shown in Figure 13.

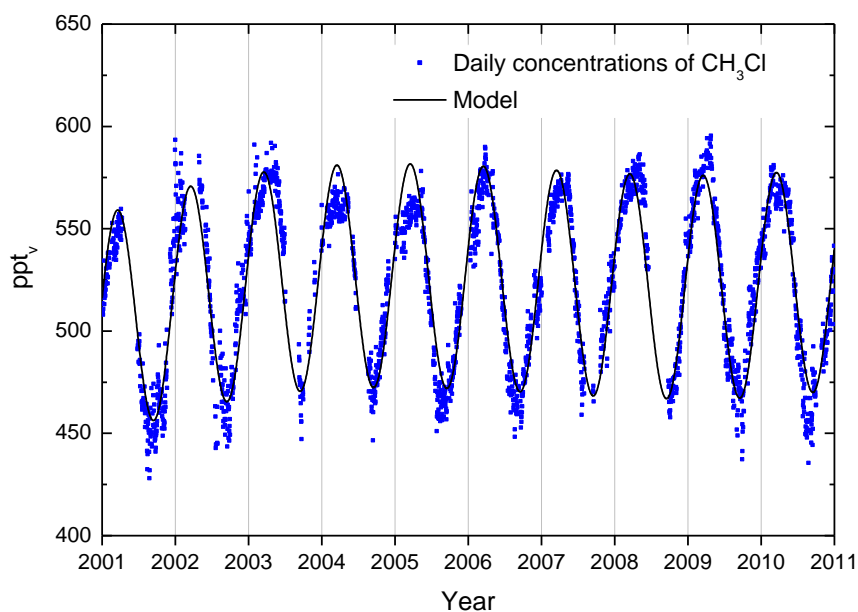


Figure 13: Observations of methyl chloride, CH₃Cl, for the period 2001-2011 at the Zeppelin observatory. Dots: daily averaged concentrations from the observations, solid line: modelled background mixing ratio.

There is a remarkable decrease the last year. The lifetime of the compound is only 1 year resulting in large seasonal fluctuations as shown in the Figure and rapid response to changes in sources. The degradation of the compound is dependent on solar intensity. To reach the stratosphere, the lifetime in general needs to be in the order of 2-4 years to have significant

chlorine contribution, but this is also dependant on the source strength and their regional distribution. Methyl Chloride has relatively high mixing ratios, and contributes to the stratospheric Chlorine burden. With respect to the warming potential this substance is 16 times stronger than CO₂ per kg gas emitted.

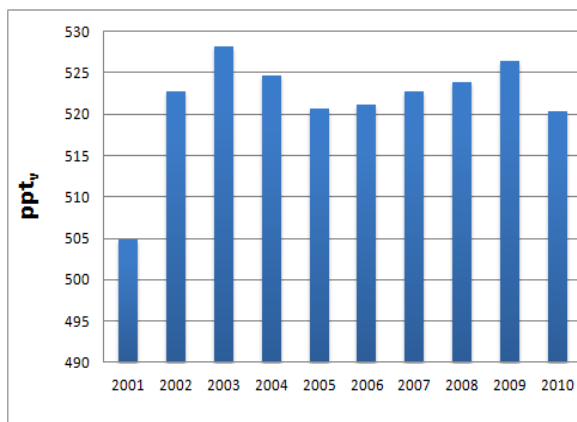


Figure 14: Development of the annual means methyl chloride measured at the Zeppelin Observatory for the period 2001-2010.

back to the 2006 level. The reason for this is not understood, and a closer study of sources variation for this compound is recommended, also by WMO (WMO 2011b) as sources are also related to atmospheric temperature change.

4.1.5 Observations of Methyl Bromide in the period 2001-2010

The sources of Methyl Bromide (CH₃Br) are both from natural and anthropogenic activities. The natural sources such as the ocean, plants, and soil, can also be a sink for this substance. Additionally there are also significant anthropogenic sources; it is used in a broad spectrum of pesticides in the control of pest insects, nematodes, weeds, pathogens, and rodents. Biomass burning is also a source and it is also used in agriculture primarily for soil fumigation, as well as for commodity and quarantine treatment, and structural fumigation. While methyl bromide is a natural substance, the additional methyl bromide added to the atmosphere by humans contributes to the man made thinning of the ozone layer. Total organic bromine from halons and methyl bromide peaked in 1998 and has declined since. The tropospheric abundance of bromine is decreasing, and the stratospheric abundance is no longer increasing (WMO, 2011b). This observed decrease was solely a result of declines observed for methyl bromide. Bromine (Br) from halons continues to increase, but at slower rates in recent years, see section 4.2.4 on page 39.

The results of the daily averaged observations of this compound for the period 2001-2010 are shown in Figure 15.

By use of the model described in Appendix I we have calculated the annual trend, and the change in the trend is also given in Table 2. The trend for the period 2001-2010 is 0.87 ppt per year, and the change in the trend is -1, last year show an apparent change in the development.

The development of the annual means of methyl chloride for the period 2001-2011 is presented in Figure 14. The last years there has been a stabilisation of the level of this gas globally, but from 2006 there is an increase of 1.4%, but from 2009-2010 there was a decrease of as much as 6 ppt,

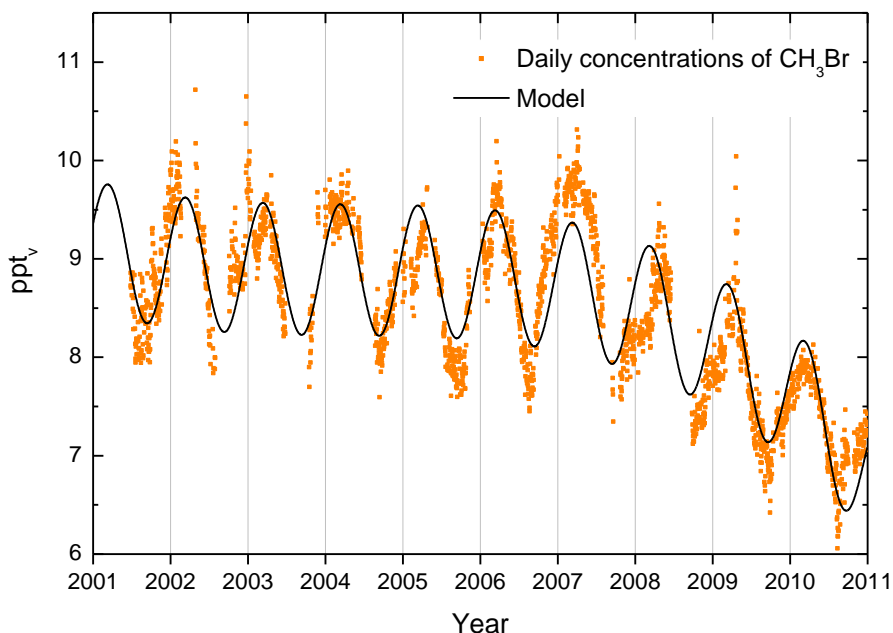


Figure 15: Observations of methyl bromide, CH_3Br , for the period 2001-2010 at the Zeppelin observatory. Dots: daily averages mixing ratios from the observations, solid line: modelled background mixing ratio.

A relatively large change is evident after the year 2007, a reduction of more than 17.5% since that year in our observations. Methyl bromide is a greenhouse gas with a lifetime of 0.8 years and it is 5 times stronger than CO_2 , if the amount emitted of both gases were equal. The short life time explains the large annual and seasonal variations of this compound.

We have calculated the annual trend by use of the model described in Appendix I. The trend and change in the trend is given in Table 2. For the period 2001-2010 there is a reduction in the mixing ratio of -0.16 ppt per year, with acceleration in the trend of -0.07. However, note that the observed changes are small (ca 1.5 ppt since 2007) and the time period relatively short thus the seasonal and annual variations of the trends are uncertain.

The development of the annual means for the period 2001-2010 is presented in Figure 16, clearly illustrating the decrease the last years. In general atmospheric amounts of methyl bromide have declined since the beginning in 1999 when industrial production was reduced as a result of the Montreal protocol. The global mean mixing ratio was 7.3-7.5 ppt in 2008, slightly lower than at Zeppelin and also the annual mean reduction is slower than at Zeppelin, 0.14 ppt/year (WMO, 2011b). The differences are explained by slower inter hemispheric

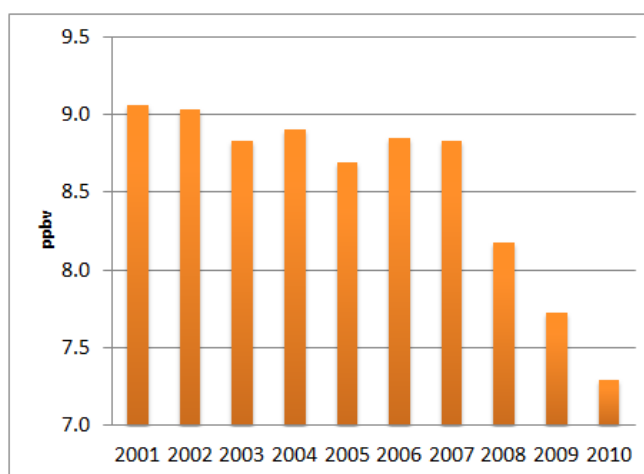


Figure 16: Development of the annual means of Methyl Bromide measured at the Zeppelin Observatory for the period 2001-2010.

mixing. The recent reduction is explained by considerable reduction in the use of this compound; in 2008 the use was 73% lower than the peak year late 1990s (WMO, 2011b).

4.1.6 Observations of tropospheric ozone in the period 1990-2010

Tropospheric ozone (which is the ozone in the lower part of the atmosphere) is a natural constituent of the atmosphere and plays a vital role in many atmospheric processes. It also a short-lived greenhouse gas with a radiative forcing of $+0.35 \text{ W m}^{-2}$ (IPCC, 2007) due to man made changes in the concentrations since 1750. This is 10% of the overall global radiative forcing since 1750 making this component as the third most influencing greenhouse gas (see Figure 1 on page 10). Tropospheric ozone is a central short-lived climate forcer (SLCF) receiving enhanced focus the last years in both research and monitoring internationally. In a recent report UNEP¹¹ advocates for SLCF mitigation strategies to complement CO₂ reductions. In addition to ozone, SLCF includes aerosols, black carbon (in aerosols) and sometime also direct or indirect effects of methane. Ozone is not emitted directly to the atmosphere, but it is rather produced from precursor gases; the formation of ozone is due to a large number of photochemical reactions taking place in the atmosphere and depends on the temperature, humidity and solar radiation as well as the primary emissions of nitrogen oxides, CO and volatile organic compounds. Anthropogenic emissions of VOC and nitrogen oxides have increased the photochemical formation of ozone in the troposphere. Until the end of the 1960s the problem was basically believed to be one of the big cities and their immediate surroundings. In the 1970s, however, it was found that the problem of photochemical oxidant formation is much more widespread. The ongoing monitoring of ozone at rural sites throughout Europe shows that episodes of high concentrations of ground-level ozone occur over most parts of the continent every summer. Future observations and understanding of precursors gases is targeted both by EMEP and the EU infrastructure project ACTRIS (see section 3.1). As there are no direct anthropogenic sources for ozone; the component is not regulated by the Kyoto protocol.

The 1999 Gothenburg Protocol is designed for a joint abatement of acidification, eutrophication and ground-level ozone. The critical levels defined by ECE for protection of vegetation are $150 \mu\text{g}/\text{m}^3$ for hourly mean, $60 \mu\text{g}/\text{m}^3$ for eight-hour mean and $50 \mu\text{g}/\text{m}^3$ for seven-hour mean (9 a.m. - 4 p.m.) averaged over the growing season (April-September).

The observed ozone mixing ratios at the Zeppelin Observatory for the period 1990-2010 are shown in Figure 16.

¹¹ http://www.unep.org/dewa/Portals/67/pdf/Black_Carbon.pdf

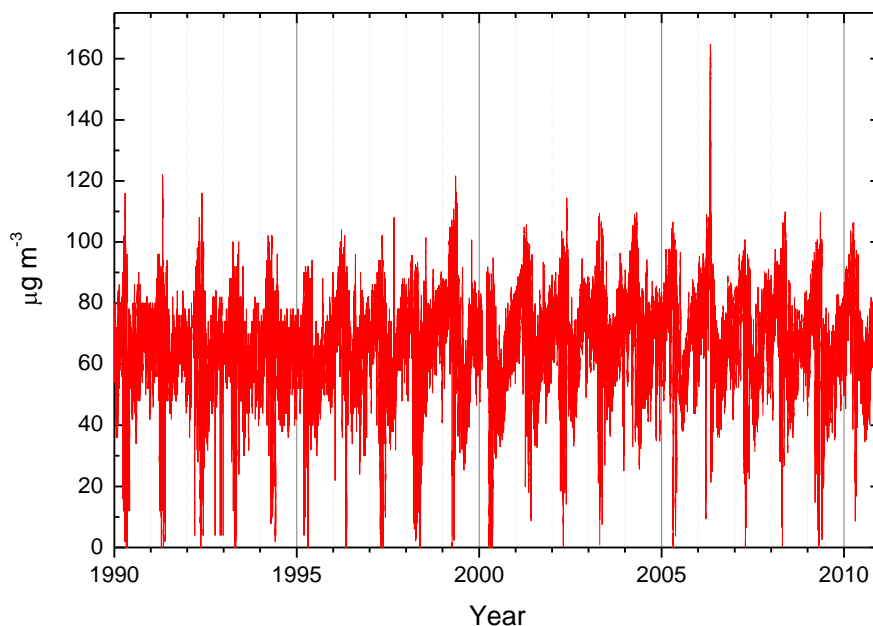


Figure 17: Observations of ozone in the troposphere for the period 1990-2010 at the Zeppelin observatory. Red dots: hourly average concentrations.

There are large seasonal variations due to relatively short lifetime and the dependency on solar radiation and interactions with precursor gases. In 2006 there was an extreme episode with transport of pollution into the Arctic region and ozone levels as high as $\sim 160 \mu\text{g m}^{-3}$. This was above all critical levels. In 2010 there have been few strong episodes, and the maximum ozone level observed was $106 \mu\text{g m}^{-3}$ at 1^h of April 2010 in the evening. Analysis of the air transport to the Zeppelin Observatory this day shows that the air arrived from Central-Russia. The ozone variations at several sites in Norway is more thoroughly discussed in Aas et al. (2011).

4.1.7 Observations of CO in the period 2001-2010

Carbon monoxide (CO) is not considered as a direct greenhouse gas, mostly because it does not absorb terrestrial thermal IR energy strongly enough. However, CO is able to modulate the level of methane and production tropospheric ozone which are both very important climate components. CO is closely linked to the cycles of methane and ozone and, like methane; CO plays a key role in the control of the OH radical.

The observed CO mixing ratio for the period September 2001-2010 is shown in Figure 11.

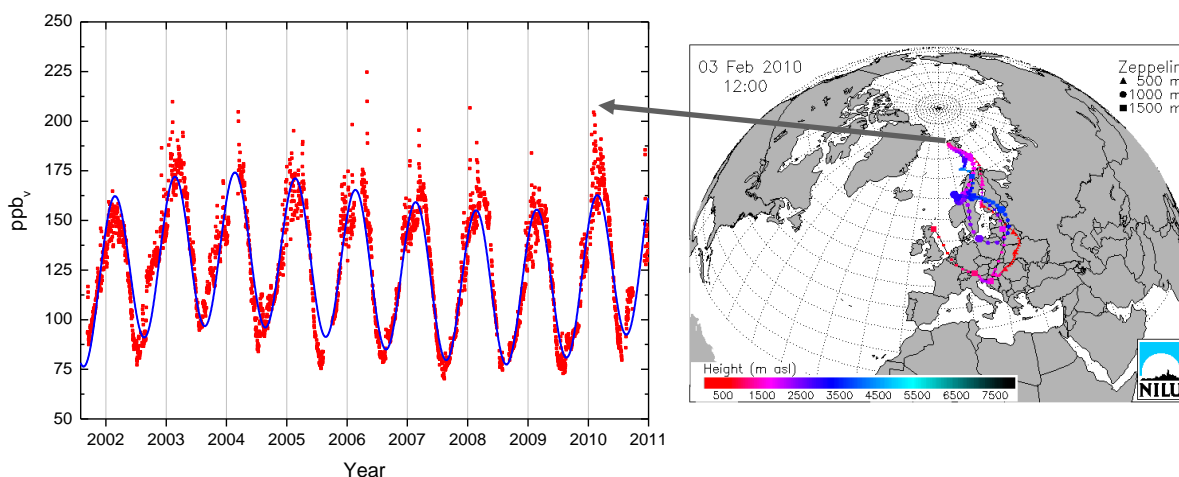


Figure 18: Observations of carbon monoxide (CO) from the September 2001 to 31.12.2010 at the Zeppelin observatory. Red dots: daily averaged observed mixing ratios. The solid line is the modelled background mixing ratio. The maximum value in 2010 is caused by transport of pollution from Europe as illustrated to the right.

The concentrations of CO show characteristic seasonal variations with large amplitudes in the Northern Hemisphere and small ones in the Southern Hemisphere. This seasonal cycle is driven by variations in OH concentration as a sink, emission by industries and biomass burning, and transportation on a large scale.

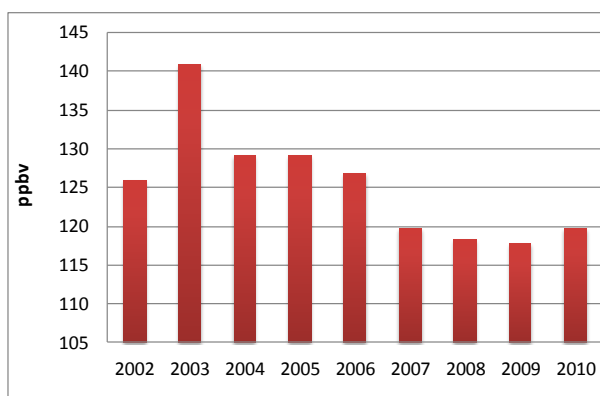


Figure 19: Development of the annual means of CO measured at the Zeppelin Observatory for the period 2001-2010.

The maximum daily average value in 2010 was observed on the 3th of February and was 204 ppb. The maximum value is caused by transport of pollution from Europe as illustrated to the right in the Figure. The highest mixing ratio ever observed at Zeppelin; is 217.2 ppb on the 2nd of May 2006. These peak values were due to transport of polluted air from lower latitudes; urban pollution (e.g. combustion of fossil fuel). CO is an excellent tracer for transport of smoke from fires (biomass burning, agricultural- or forest fires). In general the CO concentrations measured at Zeppelin show a decrease during the period 2003 to 2009, and 2009 has the lowest for the period investigated. For 2010 a small increase is evident as shown in Figure 19. The difference in the mixing ratio of CO between the peak year 2003 and 2009 is 16%. CO is central to monitor as the sources of CO are numerous and complex, and the level of this compound is important for the ozone and methane levels. The compound is very valuable in the interpretation of other variables at Zeppelin. Atmospheric CO sources are oxidation of various organic gases (volatile organic compounds, VOC) from sources as fossil fuel, biomass burning, and also oxidation of methane is important. Additionally emissions from plants and ocean are important sources.

The global levels of CO were increasing until the mid-1980s. Thereafter the levels have declined with an averaged global growth rate -0.9 ppb/year for the period from 1992 to 2001.

The variability of the growth rates is large. High positive growth rates and subsequent high negative growth rates were observed in northern latitudes and southern low latitudes from 1997 to 1999. We calculated a trend at Zeppelin of -0.25 ppb per year for the period 2002-2009. The development of the annual means for the period 2002-2010 is presented in Figure 19, clearly illustrating a maximum in the year of 2003, and a decrease from 2003-2009 with an new increase the last year.

4.2 Greenhouse gases with solely anthropogenic sources

All the gases presented in this chapter have solely anthropogenic sources. These are the man-made greenhouse gases and are called CFCs, HCFCs, HFCs PFCs, SF₆ and halons and most of the gases did not exist in the atmosphere before the 20th century. All these gases except for SF₆ are halogenated hydrocarbons. Although the gases have much lower concentration levels than most of the natural gases mentioned in the previous section, they are strong infrared absorbers, many of them with extremely long atmospheric lifetimes resulting in high global warming potentials; see Table 1 on page 5. Together as a group the gases contribute 11% to the overall global radiative forcing since 1750.

Some of these gases are ozone depleting, and consequently regulated through the Montreal protocol. Additional chlorine and bromine from CFCs, HCFCs and halons added to the atmosphere contributes to the thinning of the ozone layer, allowing increased UV radiation to reach the earth's surface, with potential impact not only to human health and the environment, but to agricultural crops as well. In 1987 the Montreal Protocol was signed in order to reduce the production and use of these ozone-depleting substances (ODS) and the amount of ODS in the troposphere reached a maximum around 1995. The amount of most of the ODS in the troposphere is now declining slowly and one expects to be back to pre-1980 levels around year 2050. In the stratosphere the peak is reached somewhat later, around the year 2000, and observations until 2004 confirm that the level of stratospheric chlorine has not continued to increase (WMO, 2007).

The CFCs, consisting primarily of CFC-11, -12, and -113, accounted for ~62% of total tropospheric Chlorine in 2004 and accounted for a decline of 9 ppt Chlorine from 2003-2004 (or nearly half of the total Chlorine decline in the troposphere over this period) (WMO, 2007).

There are two generations of substitutes for the CFCs, the main group of the ozone depleting substances. The first generation substitutes is now included in the Montreal protocol as they also influence the ozone layer. This comprises the components called HCFCs listed in Table 1 and Table 2. The second-generation substitutes, the HFCs, are included in the Kyoto protocol. The situation now is that the CFCs have started to decline, while their substitutes are increasing, and many of them have a steep increase.

4.2.1 Observations of Chlorofluorocarbons (CFCs) in the period 2001-2010

This section includes the results of the observations of the CFCs: CFC-11, CFC-12, CFC-113, CFC-115. These are the main ozone depleting gases, and the anthropogenic emissions started around 1930s and were restricted in the first Montreal protocol. Figure 20 shows the daily averaged observed mixing ratios of these four CFCs. The current instrumentation is not in accordance with recommendations and criteria of AGAGE for measurements of CFCs and there are larger uncertainties in the observations of these compounds, see also Appendix I. As a result also the trends are connected with larger uncertainties. From September 2009 we have

new and improved instrumentation installed at Zeppelin providing better observations of these compounds.

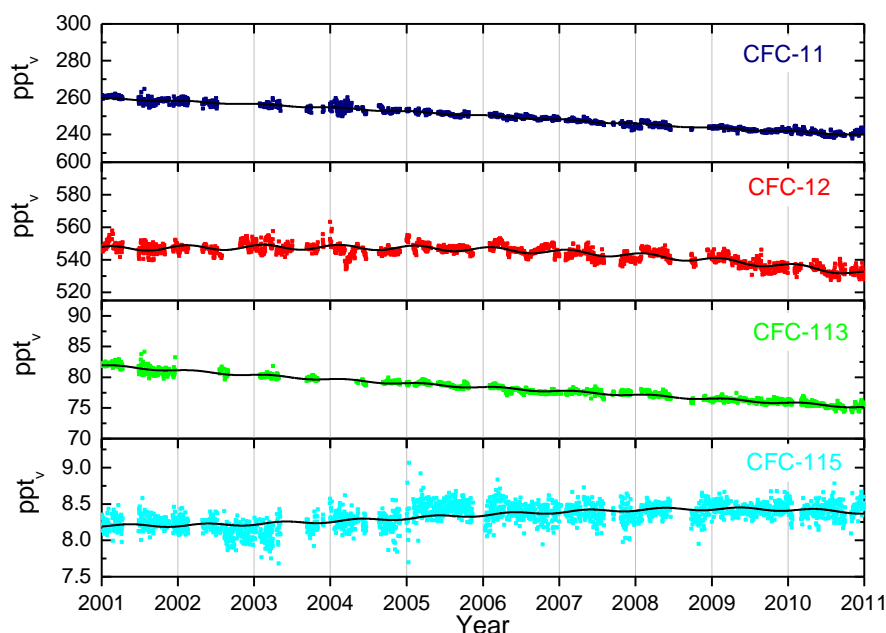


Figure 20: Daily averaged mixing ratios of the monitored CFCs: CFC-11 (dark blue), CFC-12 (red), CFC-113 (green) and CFC-115 (light blue) for the period 2001-2010 at the Zeppelin observatory. The solid lines are modelled background mixing ratio.

The main sources of these compounds were foam blowing, aerosol propellant, temperature control (refrigerators), solvent, and electronics industry. The highest production of the observed CFCs was around 1985 and maximum emissions were around 1987. The life times of the compounds is long as given in Table 1, and also the GWP due to the life time and strong infrared absorption properties is very high.

We have used the model described in Appendix I in the calculation of the annual trends, and changes in the trends. The trends per year for the substances CFC-11, CFC12 and CFC-113 are now all negative given in Table 2, and the changes in the trends are also negative indicating acceleration in the decline¹². For the compound CFC-115 the trend is still slightly positive, +0.03 ppt/year, but the change in trend is negative and thus we expect the trend for to be negative in few years. In total the development of the CFC levels at the global background site Zeppelin is now very promising.

According to WMO (WMO, 2011b) the global mean mixing ratios of CFC-11 are decreasing with approximately 2.0 ppt +/-0.01 ppt and CFC-113 are decreasing by approximately 0.7 ppt from 2007-2008. This is relatively close to our results at Zeppelin for CFC-113 for the period 2001-2010 (-0.7 ppt/yr for 2001-2010), and also for CFC-11 (2.1 ppt/year). The global mean reduction for CFC-12 was -2.2 ppt/year for 2007-2008. For Zeppelin the reduction was 1.3 ppt/year over the period 2001-2010, and 1.8 ppt from 2007-2008.

¹² The current instrumentation is not in accordance with recommendations and criteria of AGAGE for measurements of the CFCs and there are larger uncertainties in the observations of this compound, see also Appendix I.

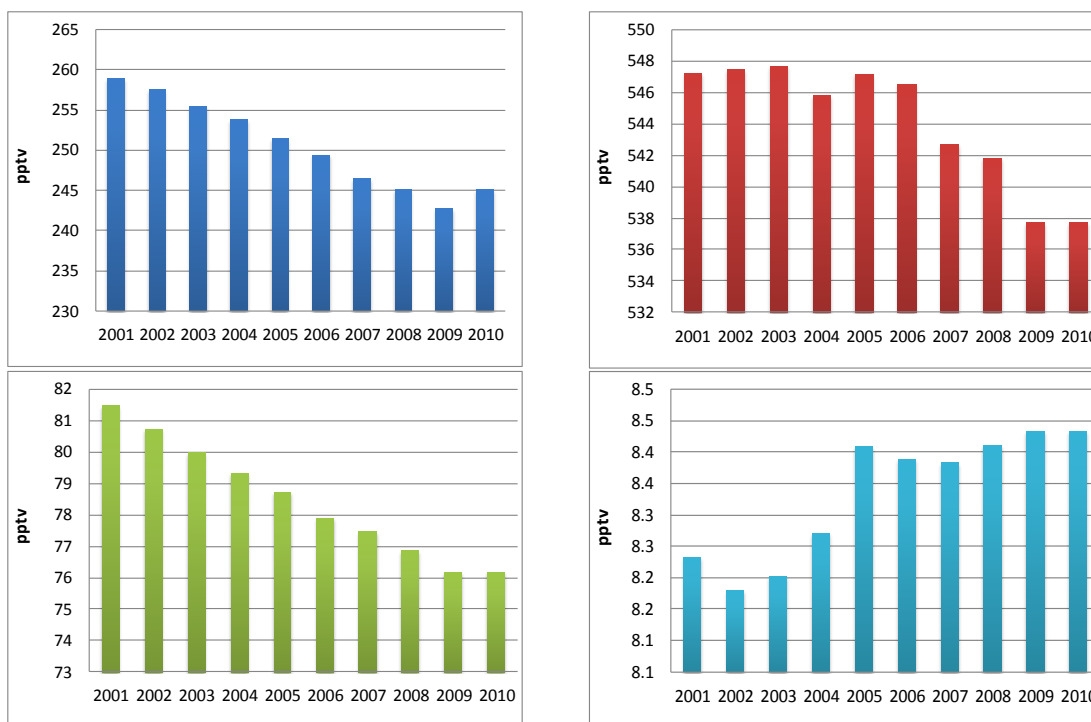


Figure 21: Development of the annual means all the observed CFCs at the Zeppelin Observatory for the period 2001-2010. Upper left panel: CFC-11, upper right panel: CFC-12, lower left panel: CFC-113, lower right panel: CFC-115. See Appendix I for data quality and uncertainty.

The development of the annual means for all the observed CFCs is shown in Figure 21, and it shows a similar tendency for all the compounds; a weak increase in the beginning of the period and a decrease the recent years. The results of CFC-11 show an increase from 2009-2010, which is not expected. This reflects the uncertainty and too low precision of the observations. As described in Appendix I there is now a new instrument at Zeppelin giving better and more accurate observations of CFCs. The old and new observations are harmonised and as described in the appendix. CFC-12 (the red diagram) is the gas with the highest GWP of the CFCs, 10600, and the second highest of all gases observed at Zeppelin. This means that the warming potential of 1 kg emitted CFC-12 gas has 10600 times stronger warming effect than 1 kg emitted CO₂ gas. The global averaged atmospheric mixing ratio of CFC-12 has been decreasing at a rate of 0.5% over the year 2004-2008 (WMO, 2011b). This fits well with our observations as illustrated in Figure 21 as CFC-12 has the maximum in 2003-2004, but the variations since 2001 is larger than the global average variation, and there seem to be a clear reduction the last years.

4.2.2 Observations of Hydrochlorofluorocarbons (HCFCs) in the period 2001-2010

This chapter includes the observations of the following components: HCFC-22, HCFC-141b and HCFC-142b. These are all first generation replacement gases for the CFCs and their lifetimes are rather long. This means that they have potentially strong warming effects, depending on their concentrations and absorption properties; their GWPs are high (see Table 1). The compound HCFC-142b is the strongest of these gases, and the warming potential is 2400 times stronger than CO₂, per kg gas emitted. These gases do also contain chlorine, and thus are contributing to the depletion of the ozone layer. The HCFCs accounted for 7.5% of the total tropospheric chlorine in 2004 versus 6% of the total in 2004 (WMO, 2011b).

The daily averaged observations of these gases are shown in Figure 22 for the period 2001-2010¹³. As a result also the trends are connected with larger uncertainties. From September 2009 we have new and improved instrumentation installed at Zeppelin providing better observations of these compounds.

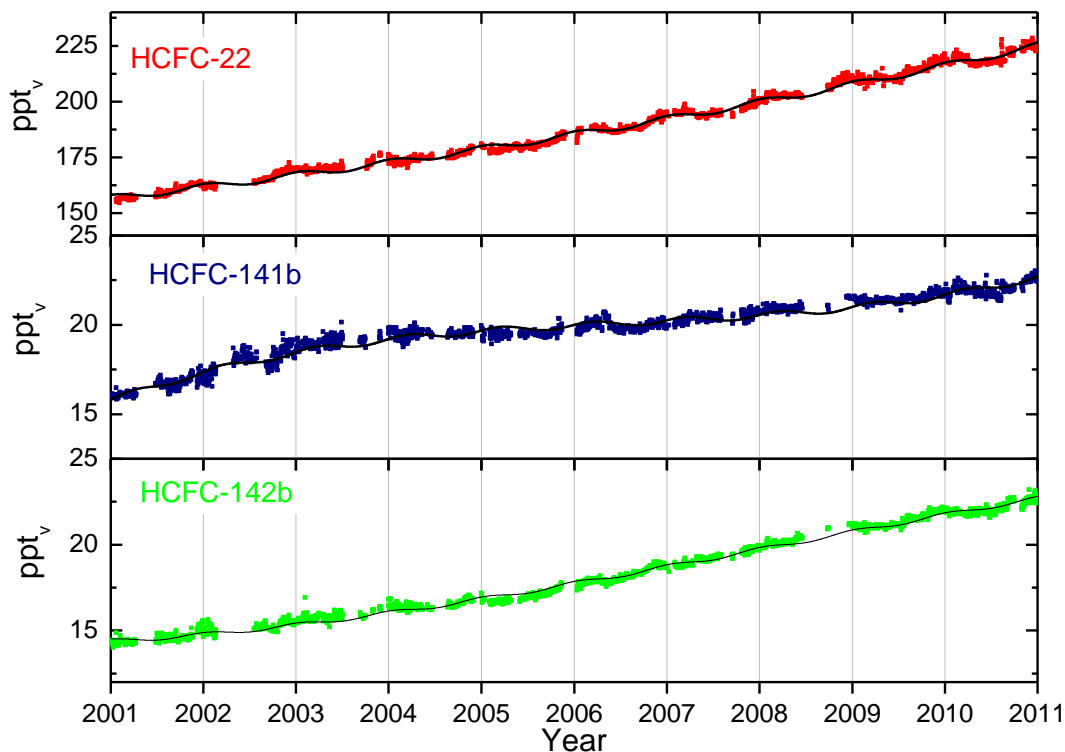


Figure 22: Daily average mixing ratios of the monitored HCFCs: HCFC-22 (red), HCFC-141b (dark blue) HCFC-142b⁶ (green) for the period 2001-2010 at the Zeppelin observatory. The solid lines are modelled background mixing ratio.

The trends per year for the compounds HCFC-22, HCFC-141b and HCFC-142b are all positive, and HCFC-22 has the largest change as given in Table 2. HCFC-22 is the most abundant of the HCFCs and is currently increasing at a rate of 6.8 ppt/year over the period 2001-2010. In comparison, the global mean increase for 2007-2008 was +ca 8 ppt according to WMO, (WMO, 2011b). Our result for Zeppelin showed an increase of 8.4 ppt for 2007-2008, in close agreement with the annual mean. The mixing ratios of HCFC-141b and HCFC-142b have increased by 0.5 ppt/yr and 0.8 ppt/year, respectively over the same period.

It is worth mentioning that the changes in trends close to zero for HCFC-22 and HCFC-141b, indicating that the yearly increases in the concentrations is stable. The rates of increase for three of these HCFC substances are stronger than or comparable to the scenarios projected in the Ozone Assessment 2006 (WMO, 2011b).

¹³ The current instrumentation is not in accordance with recommendations and criteria of AGAGE for measurements of the HCFC-142b and there are larger uncertainties in the observations of this compound, see also Appendix I.

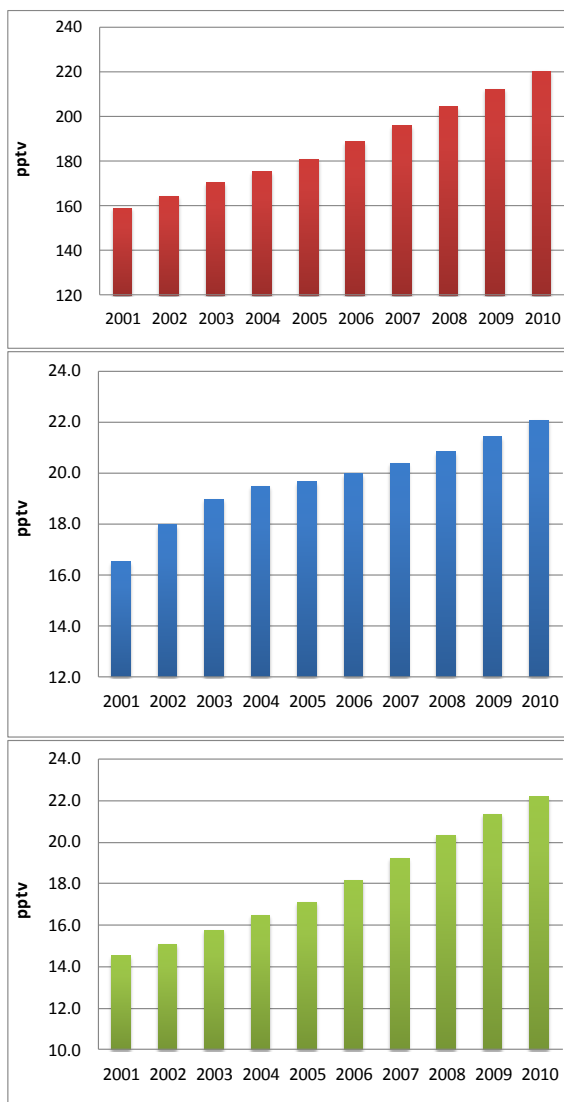


Figure 23: Development of the annual means the observed HCFCs at the Zeppelin Observatory for the period 2001-2010. Red: HCFC-22, Blue: HCFC-141b, and green: HCFC-142b.

Figure 23 shows the annual means for the full period for the three compounds, clearly illustrating the development; an considerable increase. The main sources of these gases are temperature control (refrigerants), foam blowing and solvents, as for the CFCs, which they suppose to replace. All these gases are regulated through the Montreal protocol as they all contain Chlorine. The use of the gases is now frozen, but they are not completely phased out. With lifetimes in the order of 10-20 years it is central to monitor the levels in the future as they have an influence both on the ozone layer, and are strong climate gases.

4.2.3 Observations of hydrofluorocarbons (HFCs) in the period 2001-2010

The substances called HFCs are the so called second generation replacements of CFCs, which means that they are considered as better alternatives to the CFCs with respect to the ozone layer than HCFCs. This sub-section includes the following components: HFC-125, HFC-134a, HFC-152a with lifetimes in the order of 1.5-29 years. These substances do not contain chlorine thus they do not have a direct influence on the ozone layer, but they are infrared absorbers and contribute to the global warming.

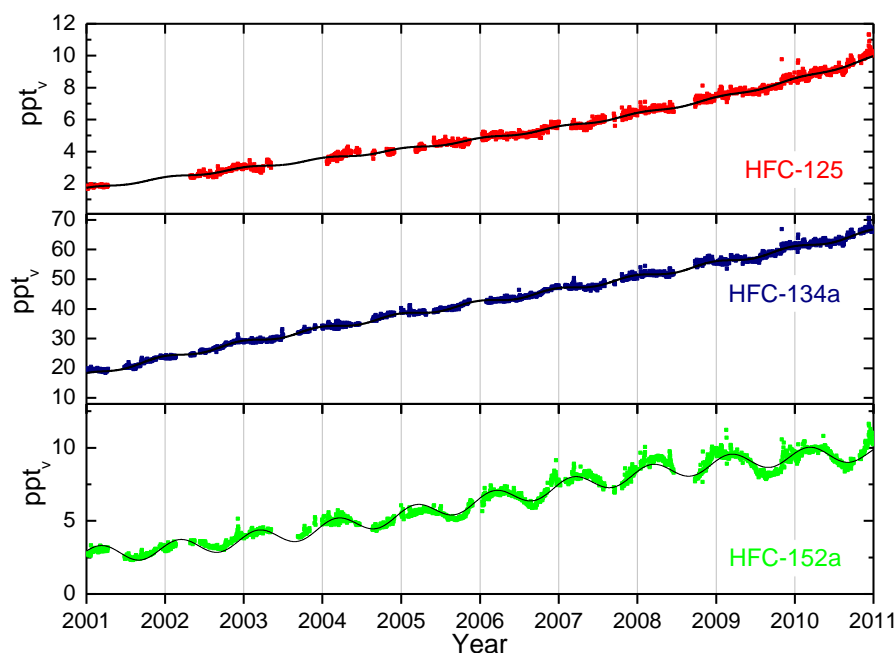


Figure 24: Daily average concentrations of the monitored HFCs: HFC-125 (red), HFC-134a (dark blue), HFC-152a (green) for the period 2001-2010 at the Zeppelin observatory. The solid lines are modelled background mixing ratio.

HFC-152a has the shortest life time and is mainly destroyed in the lowest part of the atmosphere by photolysis and reactions with OH. The seasonal cycle in the observed mixing ratios of these substances is caused by the variation in the incoming solar radiation and is clearly visible in the time series shown in Figure 24 for HFC-152a.

Even if these compounds are better alternatives for the protection of the ozone layer as they do not contain chlorine or bromine, they are still problematic as they are highly potent greenhouse gases. 1 kg of the gas HFC-125 is as much as 3400 times more powerful greenhouse gas than CO₂. However, still their mixing ratios are rather low, but the background mixing ratios are increasing steeply as our results show. This is also clearly illustrated in Figure 25 showing the development of the annual means. The gases are continuously increasing at a constant rate per year as earlier.

The three main HFCs are HFC-23 (measured at Zeppelin from 2010, not a part of the national monitoring program), HFC-134a and HFC-152a. HFC-134a is the most widely used refrigerant (temperature control), and also in air conditioners in cars. Since 1990, when it was almost undetectable in the atmosphere, concentrations of HFC-134a have risen massively. For the period 2001-2010 we find an annual increase per year of 4.6 ppt, which leaves this compound as the one with the second highest change per year of the all the halocarbons measured at Zeppelin. The mixing ratios of HFC-125, HFC-134a and HFC-152a have increased by as much as 360%, 206% and 2037% respectively since 2001. This is a rapid average increase in the interval from ~20-36 % per year. The last ozone Assessment report (WMO, 2011b) does not include these compounds as they are not affecting the ozone layer directly.

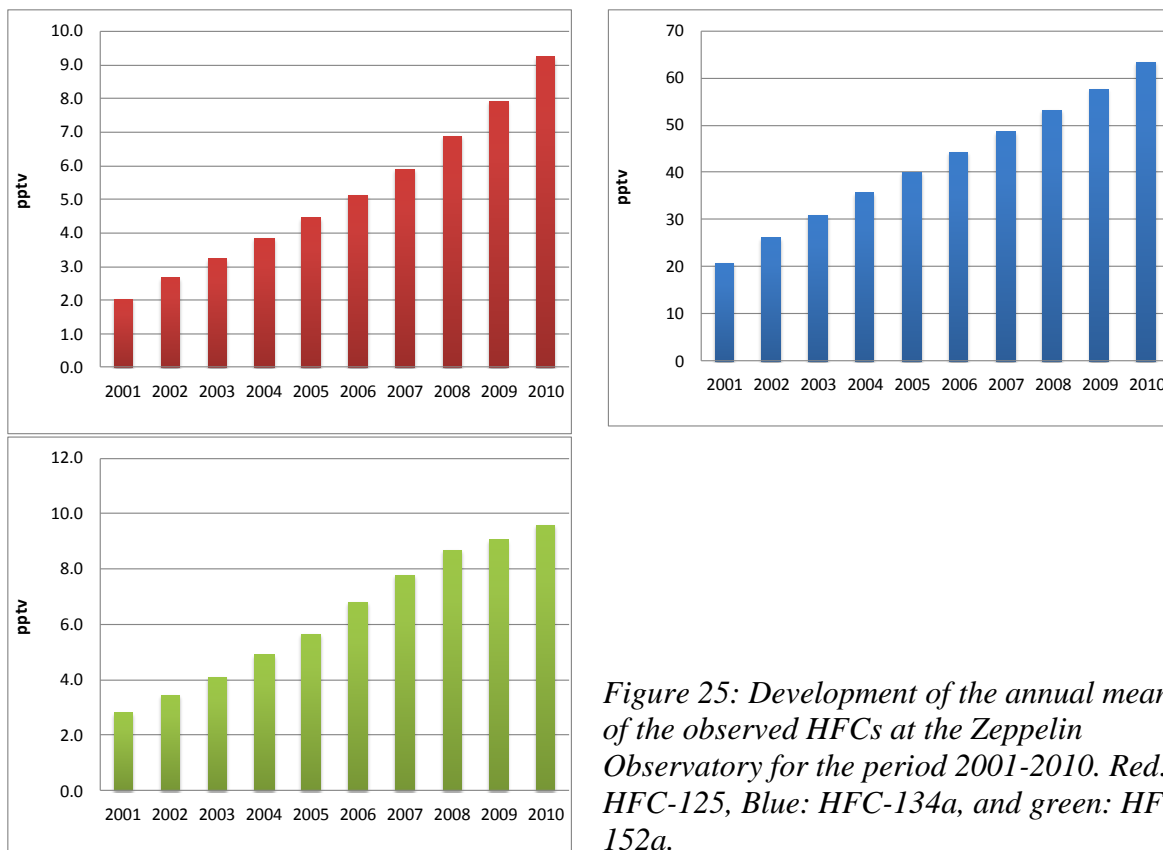


Figure 25: Development of the annual means of the observed HFCs at the Zeppelin Observatory for the period 2001-2010. Red: HFC-125, Blue: HFC-134a, and green: HFC-152a.

Due to the large increase in these compounds it is relevant to calculate the radiative forcing of these observed changes. Based on the assumption that these changes are homogeneous distributed and the same at all locations (constant geographical distribution) we find that the total radiative forcing for these three gases since the start of the emissions is 0.013 W m^{-2} . Thus the contribution from the recent man made emissions of these gases is still considered as small. This is explained by the (still) low mixing ratios of the compounds. It is important to follow the development of these gases in the future due to the rapid annual growth.

4.2.4 Observations of halons in the period 2001-2010

Halons include the following components: H-1301, H-1211. These climate gases contain bromine, also contributing to the depletion of the ozone layer. Actually, bromine is even more effective in destroying ozone than chlorine. The halons are regulated through the Montreal protocol, and are now phased out. The main source of these substances was fire extinguishers. Figure 26 presents the daily average concentrations of the monitored halons at Zeppelin¹⁴.

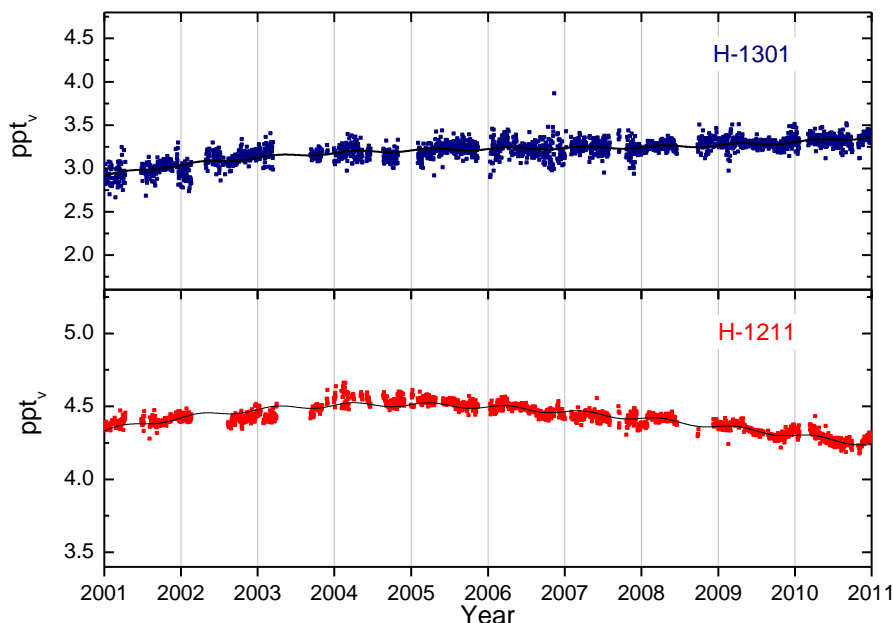


Figure 26: Daily average concentrations of the monitored halons: H-1301 (blue in the upper panel) and H-1211⁵ (Red in the lower panel) for the period 2001-2010 at the Zeppelin observatory. The solid lines are modelled background mixing ratio.

By use of the model described in Appendix I we have calculated the annual trends, and changes in trends, given in Table 2. The trends for the period 2001-2010 shows a small increase for both substances in total, with a very small reduction in the rates indicating that the trend is expected to be lower the next years (if there are no abrupt changes in sources and sinks).

¹⁴ The current instrumentation is not in accordance with recommendations and criteria of AGAGE for measurements of the Halon-1211 and there are larger uncertainties in the observations of this compound, see also Appendix I.

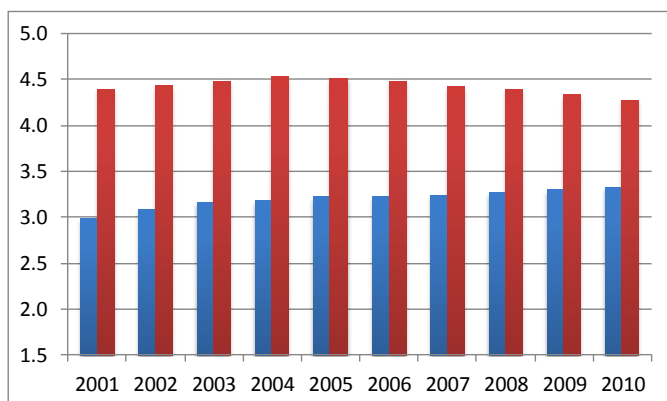


Figure 27: Development of the annual means the observed Halons at the Zeppelin Observatory for the period 2001-2010. Red: Halon-1211, Blue: H-1301.

atmospheric decrease in H-1211 was ~ 0.04 ppt in average in 2007-2008 and for H-1301 the increase was around ~ 1.2 ppt. Our observations in the Arctic region showed approximately no change from 2007-2008.

The development of the annual means are shown in the Figure to the left, and the mixing ratios are quite stable over the measured period explained by low emissions and relatively long lifetimes (11 years for H-1211 and 65 years for H-1301.) According to the last Ozone Assessment (WMO, 2011b) the total stratospheric Bromine concentration is no longer increasing, and Bromine from halons stopped increasing during the period 2005-2008. H-1211 decreased for the first time in this period, and H-1301 continued to increase, but at a slower rate than observed in 2003-2004. The global

4.2.5 Observations of other chlorinated hydrocarbons in the period 2001-2010

This section includes observations of the components: trichloromethane (also called methyl chloroform, CH_3CCl_3), dichloromethane (CH_2Cl_2), chloroform (CHCl_3), trichloroethylen (CHClCCl_2), perchloroethylene (CCl_2CCl_2). The main sources of all these substances are solvents. Note that Chloroform also has natural sources and the largest single source being in offshore sea water. The daily averaged concentrations are shown in Figure 28.

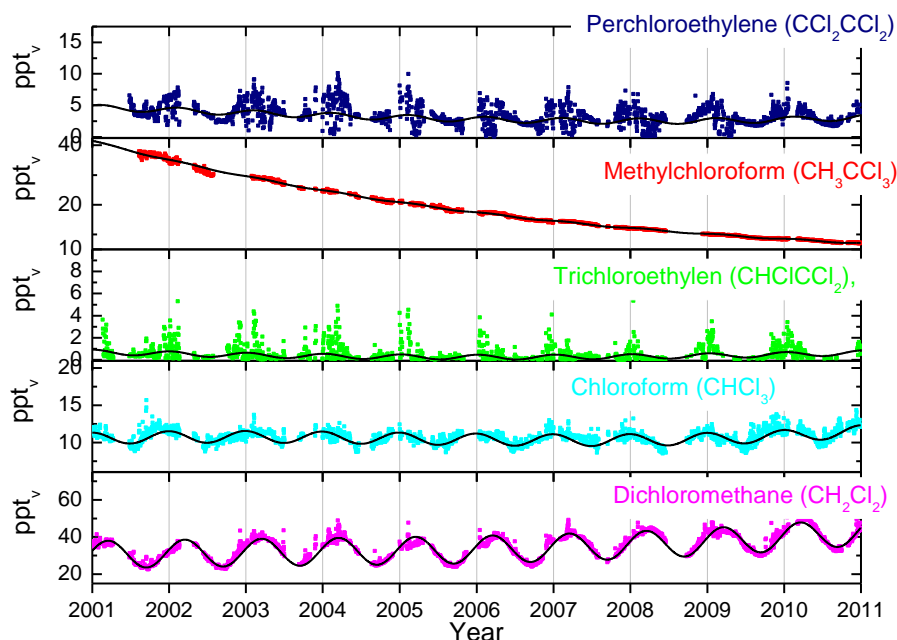


Figure 28: Daily average concentrations chlorinated hydrocarbons: From the upper panel: perchloroethylene (dark blue) methylchloroform (red), trichloroethylen (green), chloroform (light blue) and dichloromethane (pink) for the period 2001-2010 at the Zeppelin observatory. The solid lines are the modelled background mixing ratio.

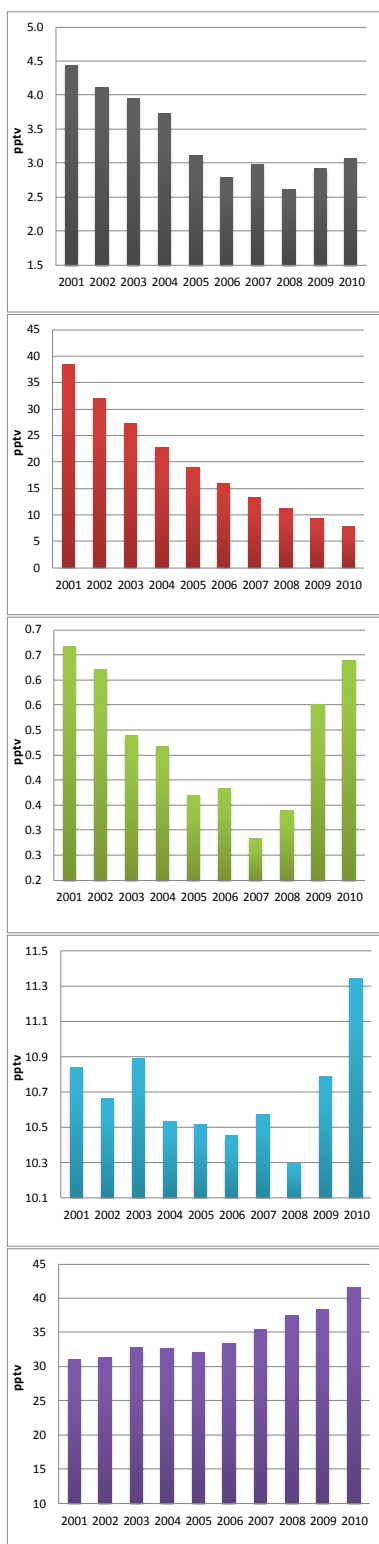


Figure 29: Annual means of the chlorinated hydrocarbons. From upper panel: perchloroethylene (grey), trichloromethane (red), trichloroethylene (green), chloroform (blue) and dichloromethane (violet) for the period 2001-2010

Methylchloroform (CH_3CCl_3) has continued to decrease and accounted only for 1% of the total tropospheric Chlorine in 2008, down from a mean contribution of 10% in the 1980s (WMO, 2011b). Globally averaged surface mixing ratios were around 10.5 ppt in 2008 (WMO, 2011b) versus 22 ppt in 2004 (WMO, 2007). Our measurements at Zeppelin show now that the component has further decreased to low levels, 8 ppt, a reduction of 80% since 2001.

It is worth noting the recent increase in trichloroethylene (green), chloroform (blue). A considerable increase in chloroform is evident at Zeppelin, and also at other sites (e.g. Mauna Loa at Hawaii and Barrow in Alaska). This is not expected and the reason for this is not yet clear. Large seasonal variations are observed for this component as the lifetime is only 1 year (see Figure 28).

The concentration of trichloroethylene is very low, and uncertainties and missing data might explain at least part of the variations.

4.2.6 Perfluorinated compounds

The only perfluorinated compound measured at Zeppelin is sulphurhexafluoride, SF_6 . This is an extremely strong greenhouse gas emitted to the atmosphere mainly from the production of magnesium and electronics industry. The atmospheric lifetime of this compound is as much as 3200 years, and the global warming potential is 22200, which means that the emission of 1 kg of this gas has a warming potential which is 22200 times stronger than 1 kg emitted CO_2 .

The other perfluorinated compounds are also very powerful greenhouse gases thus NILU has extended the monitoring with Carbon tetrafluoride (CF_4) and hexafluoroethane (C_2F_6) from 2010, as we have new and improved instrumentation installed at Zeppelin. However, these compounds are not a part of the national monitoring programme.

The current instrumentation is not well suited for measurements of SF₆ thus there are larger uncertainties for this compounds mixing ratios than for most of the other compounds reported¹⁵. The daily averaged concentration of SF₆ is presented in Figure 30. The compound is increasing with a rate of 0.3 ppt/year, and has increased by ca 45% since the start in 2001. Note that the variations through the year is not due to seasonal variations, but rather to instrumental adjustments⁸.

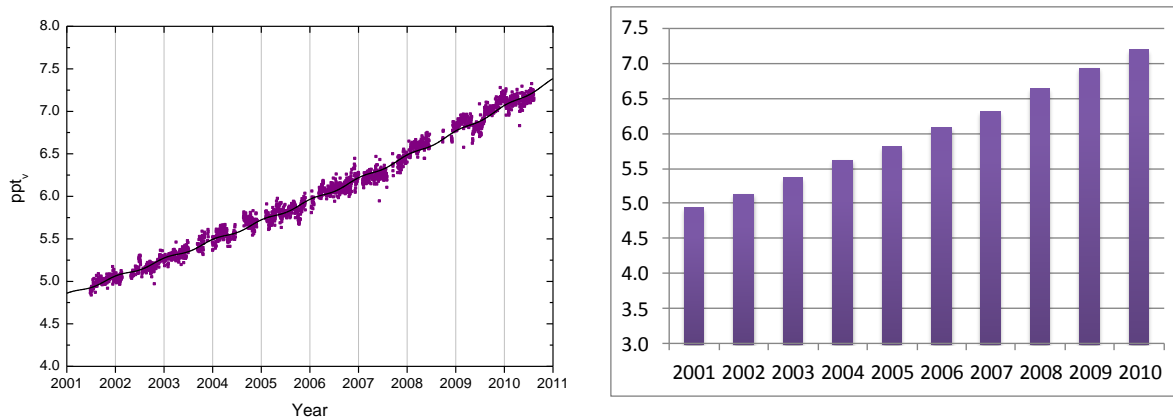


Figure 30: Daily average concentrations of SF₆ for the period 2001-2010⁸ to the left, and the development of the annual mean concentrations in the right panel.

¹⁵ The current instrumentation is not in accordance with recommendations and criteria of AGAGE for measurements of the SF₆ and there are larger uncertainties in the observations of this compound, see also Appendix I.

5. Observations of greenhouse gases at the Birkenes Observatory in Aust-Agder

In 2009 NILU upgraded and extended the observational activity at the Birkenes Observatory in Aust-Agder. Until 2009 the only Norwegian site measuring LLGHG greenhouse gases was Zeppelin, but from mid May 2009 there are also continues measurements of CO₂ and CH₄ at Birkenes. The results from the start and to 2010 are presented below.

The upper panel shows the daily (black line) and hourly (grey line) variations in CO₂. It is clear that the variations are largest during the summer months. In this period there is a clear diurnal variation with high values during the night and lower values during daytime. This is mainly due to the plant respiration, but also the meteorological situation during summer contributes to larger variations in the compound. In the lower panel is the CH₄ measurements shown. The diurnal variation for this compound is smaller, but the variations are still largest during summer and early autumn. In addition to the diurnal variations, there are also episodes with higher levels of both components due to transport of pollution from various regions. In general there are high levels when the meteorological situation results in transport from Central Europe.

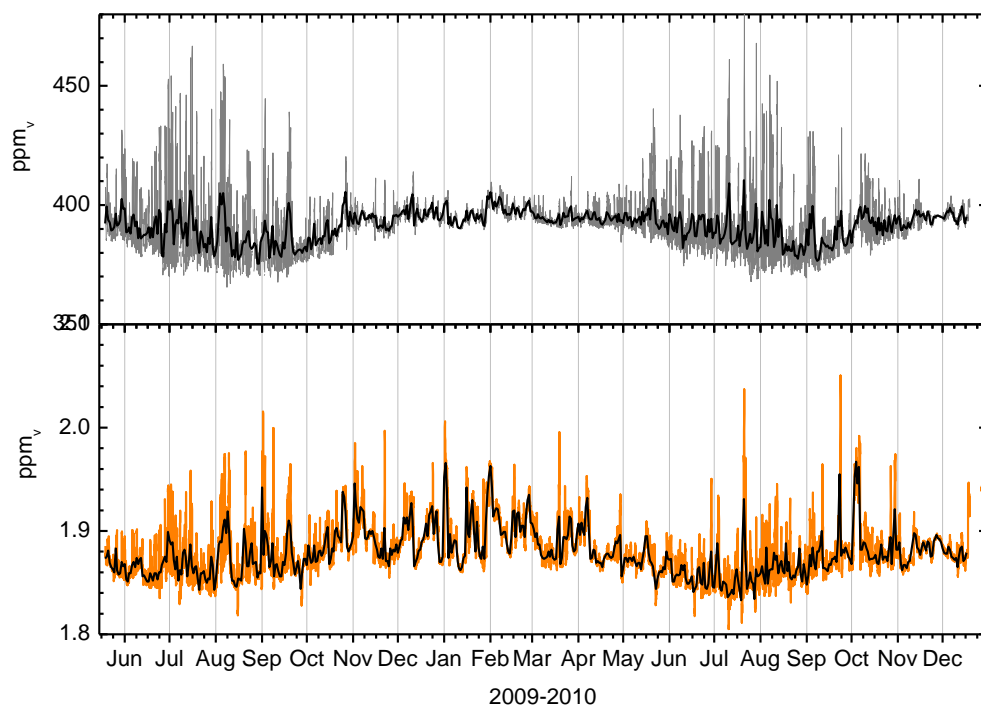


Figure 31: Greenhouse gas measurements at Birkenes Observatory from 19. May to 31. December 2010. Upper panel: CO₂ measurements, grey line: hourly mean, black line: daily mean. Lower panel: CH₄ from Birkenes, orange line: hourly mean, black line: daily mean.

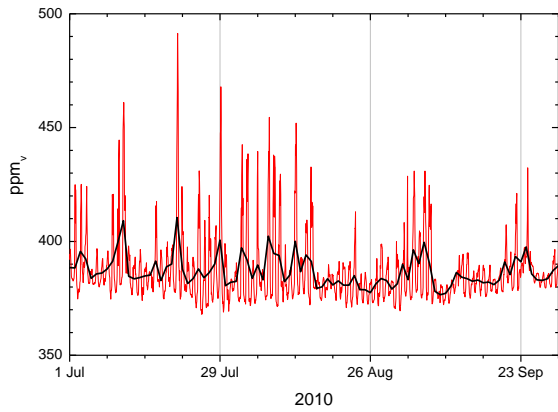


Figure 32: CO₂ measurements at Birkenes Observatory for July-September. Red line: hourly mean, black line: daily mean.

The highest CO₂ measurements are during summer and particularly warm periods. Figure 32 shows variations during summer with a mixture of episodes due to transport and strong diurnal variations due to photosynthesis.

The maximum value of CH₄ is on 22nd December. This strong episode is explained by long range transport of air from northern Russia and Scandinavia. The change in air mass transport to the Observations in this period is shown in Figure 33. During episodes with long range transport, both components are elevated, but particularly CH₄ in this episode.

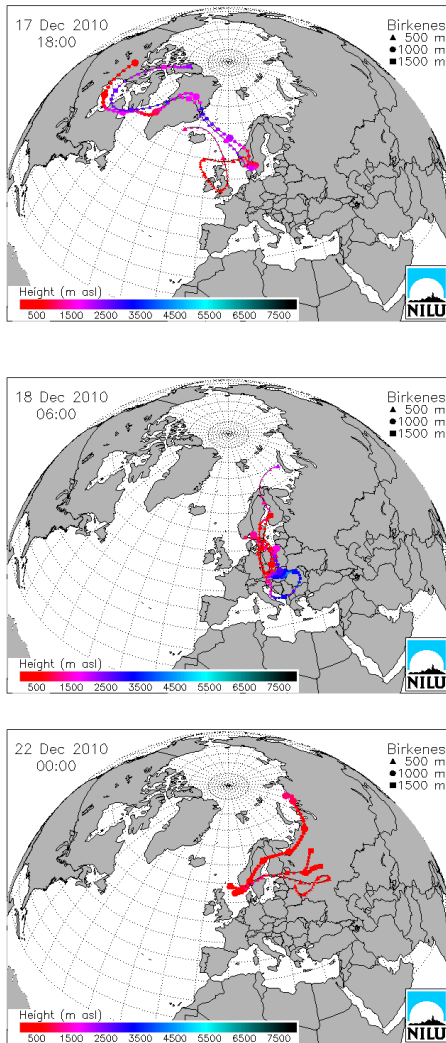


Figure 33: Transport pattern of air to Birkenes at 17. - 22. December 2010.

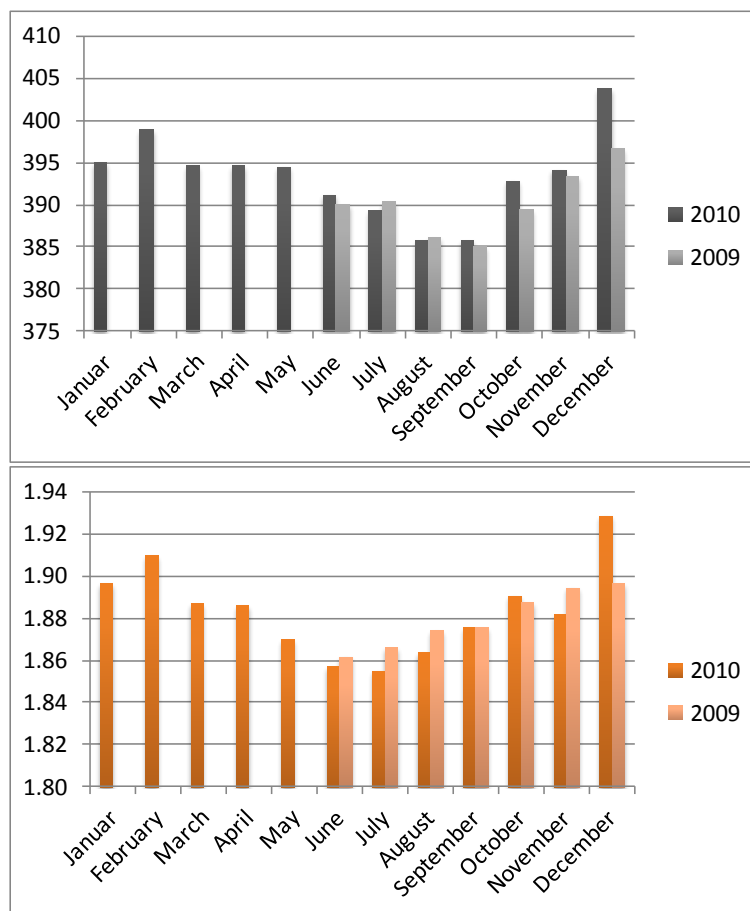


Figure 34: Monthly mean variations for CO₂ (upper panel) and CH₄ (lower panel) at Birkenes Observatory

Figure 34 show the monthly mean variations for both CO₂ and CH₄ at Birkenes. There is a clear minimum in the summer months and a maximum in the fall/winter as expected.

6. Aerosols and climate: Observations from Zeppelin and Birkenes Observatory

In the investigations of climate change, aerosols are of vital interest, as they cause significant effects on the radiative balance of the Earth, both directly, through scattering and absorption radiation, and indirectly, by acting as condensation nuclei. Calculations of the effects of aerosols still have a high level of uncertainty despite the huge scientific focus during the last decades (IPCC, 2007). For atmospheric aerosol, the longest continuous time series date back not more than around 4 decades. The total direct aerosol climate effect is cooling, but if the aerosols itself absorb solar radiation, e.g. if it consists partly of light absorbing carbon or light absorbing minerals, the aerosols have local or regional heating effect. The aerosol radiative effect depends on a number of aerosol properties, e.g. particle size distribution, chemical composition, optical properties, morphology in addition to the concentration and evolution in time. The ratio between aerosol and surface reflectivity in turn determines the aerosol's direct radiative forcing. Especially over bright surfaces such as snow, absorbing aerosols may have a net warming effect, even though the direct aerosol climate effect is cooling on a global average.

Aerosols are short-lived climate forcers that vary considerably by regions and respond quickly to changes in emissions as their lifetime is short, in the order of days-weeks. Major sources of anthropogenic aerosols are fossil fuel and biomass burning. Aerosols like sulphate, biomass burning aerosols and fossil fuel organic carbon result in negative radiative forcing (cooling), while black carbon from fossil fuel and fires has a positive forcing (warming effect). Natural aerosol loads like sea salt, dust and sulphate and carbon aerosols from natural emissions might increase as a feedback to climate change.

Atmospheric aerosols also affect the reflectivity and lifetime of clouds, which is termed the indirect aerosol climate effect. Also here, the effect can be cooling as well as warming of the atmosphere and climate, but in most cases, the cloud reflectivity and lifetime are increased, leading to a cooling effect. The indirect effect is much less understood than the direct effect. In the current scientific debate, it is discussed whether the indirect effect is determined only by the concentration of particles larger than a threshold diameter, or whether the particle chemical composition is also important (Dusek et al, 2006; McFiggans et al., 2006). If particle chemical composition affects the indirect effect, it will be most pronounced in stratiform cloud cover with low updraft velocities, i.e. at boreal and polar latitudes where cloud cover is larger than at lower latitudes (Kreidenweis et al., 2009).

When discussing the aerosol climate effects, there are a few aspects to keep in mind:

- **Better understanding and more exact quantification of the aerosol climate effects are a prerequisite for more accurate climate predictions and thus targeted mitigation and adaption strategies.**

The low understanding of the atmospheric aerosols influence on climate is one of the reasons for the large uncertainty range of the global average surface temperature increase predicted in the IPCC 4th assessment report, e.g. a range of 1.4 – 6.4°C by 2100 in the rapid economic growth scenario A1. Aerosols mask the observed warming from greenhouse gases with an unknown strength over the industrial era resulting in high uncertainty in the climate sensitivity (e.g. the temperature effect of a doubling of CO₂). Climate models with strong aerosol climate forcing predict temperature increases on the upper end of the uncertainty range, and vice versa (Andreae et al., 2005; Kiehl, 2007).

Thus, a better quantification of the aerosol climate effects translates directly into more accurate and reliable climate predictions. Comprehensive aerosol measurements at selected supersites are necessary for improving the knowledge of aerosol composition and change to be used in modelling of aerosol climate interaction. These types of observations are included in the national monitoring program from 2009 at the Birkenes Observatory.

- **Climate predictions are best improved by utilising sites with sufficient and statistically representative observations.**

To calibrate models for predicting climate, long and statistically significant time series of climate parameter observations, as well as corresponding time series of properties of climate forcing agents (greenhouse gases, atmospheric aerosol) are needed. These observations will be most efficient in improving prediction accuracy in the geographical vicinity of the observation. Relevant observations therefore need to have a sufficient and carefully selected geographical distribution both on continental as well as global scale.

- **Polar Regions are highly affected by both direct and indirect aerosol climate effects, but the indirect aerosol climate effect may potentially be large in boreal regions with high population density as well.**

It has been stressed that the Arctic is more exposed to climate change due to the combined effects of greenhouse gas warming and direct effect warming due to absorbing aerosol over bright snow surfaces (Law and Stohl, 2007). However, it needs to be pointed out that the climate forcing contribution of the indirect aerosol effect is poorly understood and potentially large as well (IPCC, 2007). This has significant implications for boreal and polar latitudes due to high cloud cover. For boreal latitudes, it is the poorly understood influence of emissions of precursors for secondary organic aerosol (SOA), both biogenic and anthropogenic, on the indirect aerosol effect in stratiform cloud decks that causes the main uncertainty. Thus, better quantification of the indirect aerosol effect is mandated in boreal as well as polar regions.

6.1 Observations of climate relevant aerosol properties: recent developments in Norway and internationally

NILU contributes to the international effort of improving climate predictions by better representation of aerosol climate effects in several ways. Both Zeppelin and Birkenes are EMEP sites following EMEP monitoring strategy for aerosols¹⁶ in accordance with UNECE (United Nation Economic Commission for Europe) and the “Convention on Long-range Transboundary Air Pollution”. The EMEP program is harmonised with WMO Global Atmosphere Watch (GAW) and this strengthen global harmonisation of aerosol observations and the link with the climate modelling community. The three sites Birkenes, Zeppelin (see section 3) and Troll in the Antarctica are each covering all EMEP and GAW aerosol core parameters and most of the recommended parameters. The observations at Birkenes and Zeppelin will be further developed in the EU-project ACTRIS described in section 3.1. The chemical composition of aerosols at various sites in Norway is more thoroughly discussed in Aas et al. (2011).

¹⁶ The monitoring strategy for the Cooperative Programme for Monitoring and Evaluation of the Long-range Transmission of Air Pollutants in Europe (EMEP) for 2010- 2019
<http://www.unece.org/env/documents/2009/EB/ge1/ece.eb.air.ge.1.2009.15.e.pdf>

Table 3: Aerosol observations at the Zeppelin, Birkenes and Troll Observatory following the EMEP and GAW recommendations.

	Zeppelin/Ny-Ålesund	Birkenes	Troll
Particle Number Size Distribution	fine mode ($0.01 \mu\text{m} < D_p < 0.8 \mu\text{m}$) in collaboration with Stockholm University	fine and coarse mode ($0.01 \mu\text{m} < D_p < 10 \mu\text{m}$)	fine mode ($0.03 \mu\text{m} < D_p < 0.8 \mu\text{m}$)
Aerosol Scattering Coefficient	spectral at 450, 550, 700 nm, in collaboration with Stockholm University	spectral at 450, 550, 700 nm	spectral at 450, 550, 700 nm
Aerosol Absorption Coefficient	single wavelength at 525 nm, in collaboration with Stockholm University	single wavelength at 525 nm, to be upgraded to 3 wavelengths in 2012	single wavelength at 525 nm
Aerosol Optical Depth	spectral at 368, 412, 500, 862 nm in collaboration with WORCC	spectral at 340, 380, 440, 500, 675, 870, 1020, 1640 nm, in collaboration with Univ. Valladolid	spectral at 368, 412, 500, 862 nm
Aerosol Chemical Composition	main components (ion chromatography), heavy metals (inductively-coupled-plasma mass-spectrometry)	main components (ion chromatography), heavy metals (inductively-coupled-plasma mass-spectrometry)	main components (ion chromatography), discontinued from 2011 due to local contamination.
Particle Mass Concentration	---	PM _{2.5} , PM ₁₀	PM ₁₀ , discontinued from 2011 due to local contamination
Cloud Condensation Nuclei	size integrated number concentration at variable supersaturation in collaboration with Korean Polar Research Institute	number size distribution at variable supersaturation, to be installed in 2012	---

The locations of the atmospheric observatories Zeppelin, Birkenes, Troll as well as their aerosol measurement programme, are chosen based on the EMEP and GAW recommendations, see also section 3.

In addition to operating aerosol supersites, NILU also operates the GAW World Data Centre for Aerosol (WDCA). Work in the context of the GAW-WDCA has recently focussed on the following tasks:

Improving the local and temporal coverage of the data holdings: In the last year before the WDCA was moved to NILU, 22 annual instrument datasets (data of one instrument at one station) were collected. This number increased to 112 annual instrument datasets in 2009.

Improving the local coverage of the GAW aerosol near-real-time (NRT) network: The NRT is targeted towards applications in air quality forecast and improvement of numerical weather forecast, e.g. quantitative precipitation forecast. The number of participating instrument datasets was increased from 11 in 2009 to 36 in 2010. A gateway to the European Centre for Medium Range Weather Forecast (ECMWF) was established.

Improving the service for both, data providers and data users: a website with detailed instructions on how to process and format data to be submitted to WDCA has been set up. The web-interface for browsing and downloading the data holdings has been improved in response time and work flow.

This report covers the observations marked in green in Table 3 as the analysis (but not the measurements and maintenance) of these variables are funded by KLIF.

6.2 Optical aerosol properties measured at Birkenes in 2010

Figure 35 summarises the optical properties of the dry PM₁₀ aerosols measured at Birkenes in 2010. The top panel shows the time series of the aerosol scattering coefficient σ_{sp} , which is the fraction of an incident light beam that is scattered by the particles in a unit volume of aerosol. It depends on the particle size distribution and particle chemical composition, and is a function of the incident radiation's wavelength. The integrating nephelometer measuring σ_{sp} provides three wavelengths across the visible spectrum. Values of σ_{sp} around 8 Mm⁻¹ are common in remote locations, whereas averages around 40 Mm⁻¹ and peaks above 100 Mm⁻¹ can be found in the continental background (see Delene & Ogren, 2002) for a comprehensive climatology of aerosol optical properties). The second panel depicts the time series of the aerosol absorption coefficient σ_{ap} , which is, analogously, the fraction of an incident light beam that is absorbed by the particles in a unit volume of aerosol. While the filter absorption photometer that measures σ_{ap} operates at 525 nm wavelength, the wavelength has been shifted to 550 nm for consistent comparison with the nephelometer assuming an absorption Ångström coefficient of -1. This adds a systematic uncertainty of 2% to σ_{ap} . The σ_{ap} values span a common range between 0.1 Mm⁻¹ in remote locations and 8 Mm⁻¹ in the continental background. Both, σ_{sp} and σ_{ap} , scale with the particle concentration in the aerosol (extensive property). The third and fourth panels show properties commonly derived from the measured optical aerosol properties that don't scale with the particle concentration (intensive property), but rather describe "the average" particle and allow for an easier and more intuitive assessment of the aerosol type observed. In the third panel, we see the time series of the scattering Ångström coefficient \hat{a} . The Ångström coefficient depends strongest on the particle size distribution, and decreases if the average optically active particle size increases. Values of \hat{a} around 2 are common for continental background aerosol, which is dominated by sub-micron aerosol particles, whereas aerosol with a marine component and thus a significant fraction of larger particles exhibit values of \hat{a} smaller than 1. In the fourth panel, the 2010 time series of the single scattering albedo ω_0 at 550 nm wavelength is displayed. The single scattering albedo states the fraction of incident radiation interacting with the aerosol particle phase that is scattered rather than absorbed by the particles, i.e. it decreases if the average aerosol particle becomes more absorbing. Values for ω_0 of close to 1 can be observed in pristine polar regions, whereas values around 0.92 are normal for continental background conditions, and even values below 0.8 can be found closer to sources of light-absorbing carbon such as fossil fuel or wood burning.

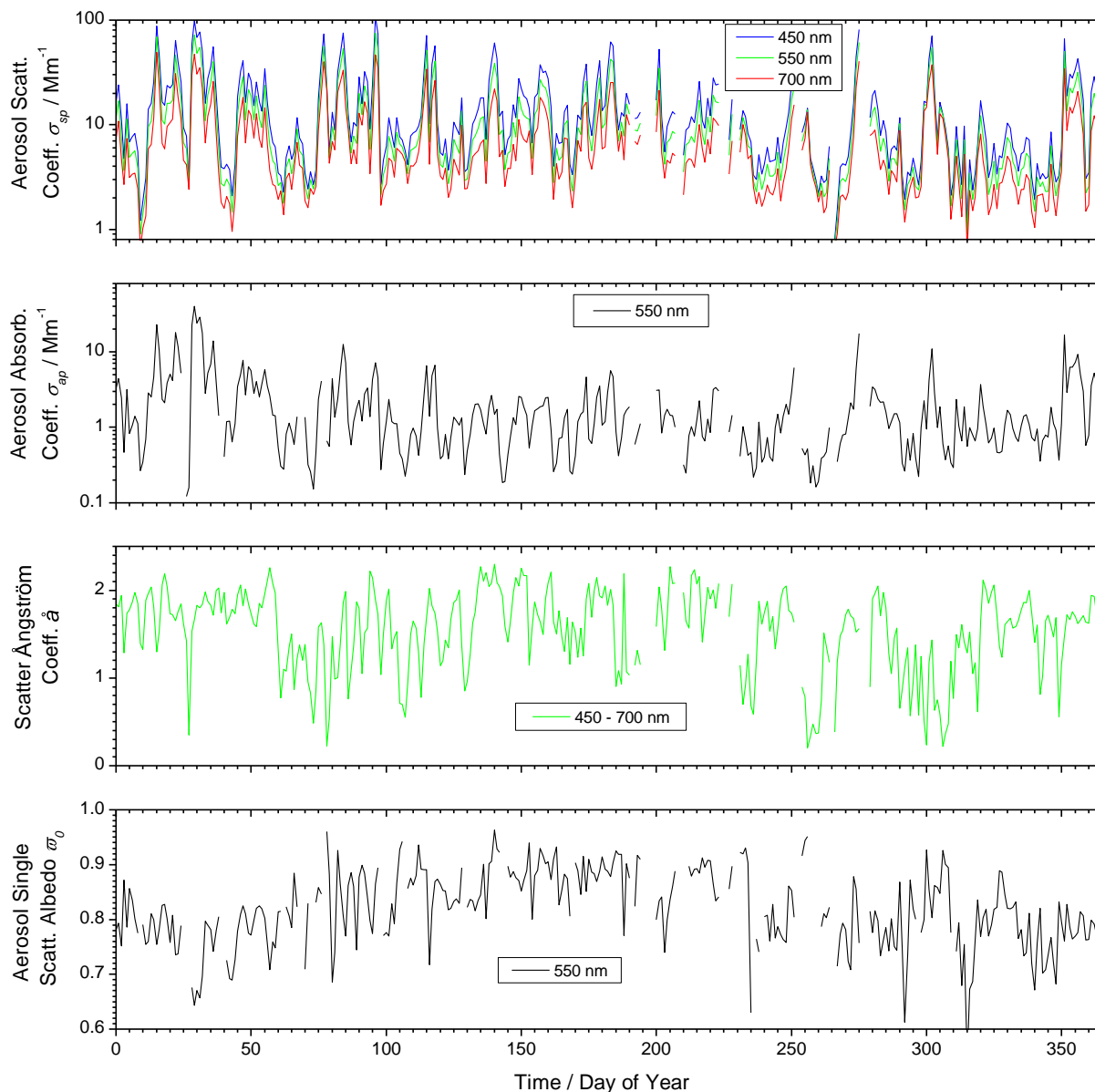


Figure 35: Time series of aerosol optical properties daily means measured in 2010 at Birkenes. The top panel shows the aerosol scattering coefficient σ_{sp} at 450, 550, and 700 nm wavelength measured by integrating nephelometer. The second panel depicts the aerosol absorption coefficient σ_{ap} at 550 nm wavelength measured by filter absorption photometer, shifted from the instrument wavelength at 525 nm to 550 nm for consistent comparison assuming an absorption Ångström coefficient of -1. The third and fourth panels show the scattering Ångström coefficient Å and the single scattering albedo ω_0 as derived properties, respectively.

When interpreting the upper 3 panels of Figure 35, no obvious annual cycle is apparent. Aerosol scattering and absorption coefficients as well as scattering Ångström coefficient vary within their ranges expected at a continental background location with shifts in the predominant air mass origin, with low values for σ_{sp} and σ_{ap} and high values for Å in air masses of Northern Atlantic or Arctic origin. High values for σ_{sp} and σ_{ap} can be found in air masses of continental European origin or influenced by marine sources. Aerosol of marine origin shows lower values of Å in addition due to a higher fraction of super-micron particles.

When interpreting the annual time series of ϖ_0 however, a clear annual cycle can be detected. Only in summer, ϖ_0 values around 0.92 are found which would be expected in a remote continental location like Birkenes. In winter however, ϖ_0 values around 0.78 are common, which are expected only closer to sources of absorbing aerosols. Autumn and spring represent transition periods between the extremes in summer and winter.

6.3 Estimating the local, instantaneous direct aerosol radiative effect

The direct aerosol climate effect is normally quantified by the corresponding radiative forcing ΔF_{ae} when there is a change over time in a climate forcer (e.g. the effect of change in aerosol concentration from preindustrial time and present aerosol concentration), see Figure 2 and footnote on page 11. A full scale calculation of this parameter requires the use of climate and radiative transfer models, which is far beyond the scope of this report. However, there exist methods for estimating the local radiative effect of aerosols $\Delta F_{ae}/\delta$. This is the radiative effect per unit aerosol optical depth. Since the spectral aerosol optical depth (AOD), (see section 6.5) is also measured at Birkenes, there are methods for estimating ΔF_{ae} available. Here, the formula of Haywood and Shine (1995, eq. 3) as applied in Sheridan and Ogren (1999) is used, which implies the following assumptions:

- a constant fractional day length of 0.5
- a constant atmospheric transmissivity of 0.76 above the aerosol layer assumed to be located in the boundary layer.
- a constant fractional cloud cover of 0.6
- a constant surface albedo of 0.15
- an integration of ΔF_{ae} across the solar spectrum by using the aerosol optical property values at 550 nm wavelength where the spectral intensity of the solar radiation reaching the earth surface is highest.
- neglecting the fact that all ground-based instruments measure the aerosol optical properties for the dry-state aerosol (relative humidity < 40%), whereas the AOD is measured for ambient conditions of relative humidity.

The above list of assumptions explains that the estimated direct aerosol radiative forcing is not suitable for further calculations, e.g. comparison with other radiative forcings such as those of greenhouse gases (assumes no snow during winter time, homogenous distribution of aerosols in the column above the site, no effects of relative humidity variations etc.). However, it is based only on directly measurable parameters, and allowing to study the radiative effects of the aerosols only varying due to changes of the atmospheric aerosol properties at a site.

Figure 36 visualises the annual time series measured at Birkenes of: 1) the aerosol optical depth (AOD) at 550 nm wavelength, $\delta_{550\text{ nm}}$ (upper panel); 2) the aerosol radiative forcing efficiency $\Delta F_{ae}/\delta$, which is calculated from ground-based in situ instruments; 3) the estimated direct aerosol radiative effect ΔF_{ae} , i.e. the product of $\delta_{550\text{ nm}}$ and $\Delta F_{ae}/\delta$. The time series of $\delta_{550\text{ nm}}$ shows gaps in winter since the sun photometer can measure rarely this time of year due to frequent cloud cover. The gap in the beginning of the year extending into spring is due to scheduled calibration of the instrument. As with the other measured extensive aerosol properties, the time series of $\delta_{550\text{ nm}}$ doesn't show any annual cycle, but variations with origin of air masses. In the time series of $\Delta F_{ae}/\delta$ and ΔF_{ae} however, the effect of the annual cycle in ϖ_0 becomes visible. Due to the higher concentration of light absorbing material in the winter aerosols, the aerosol radiative forcing at Birkenes is less cooling in winter than in summer.

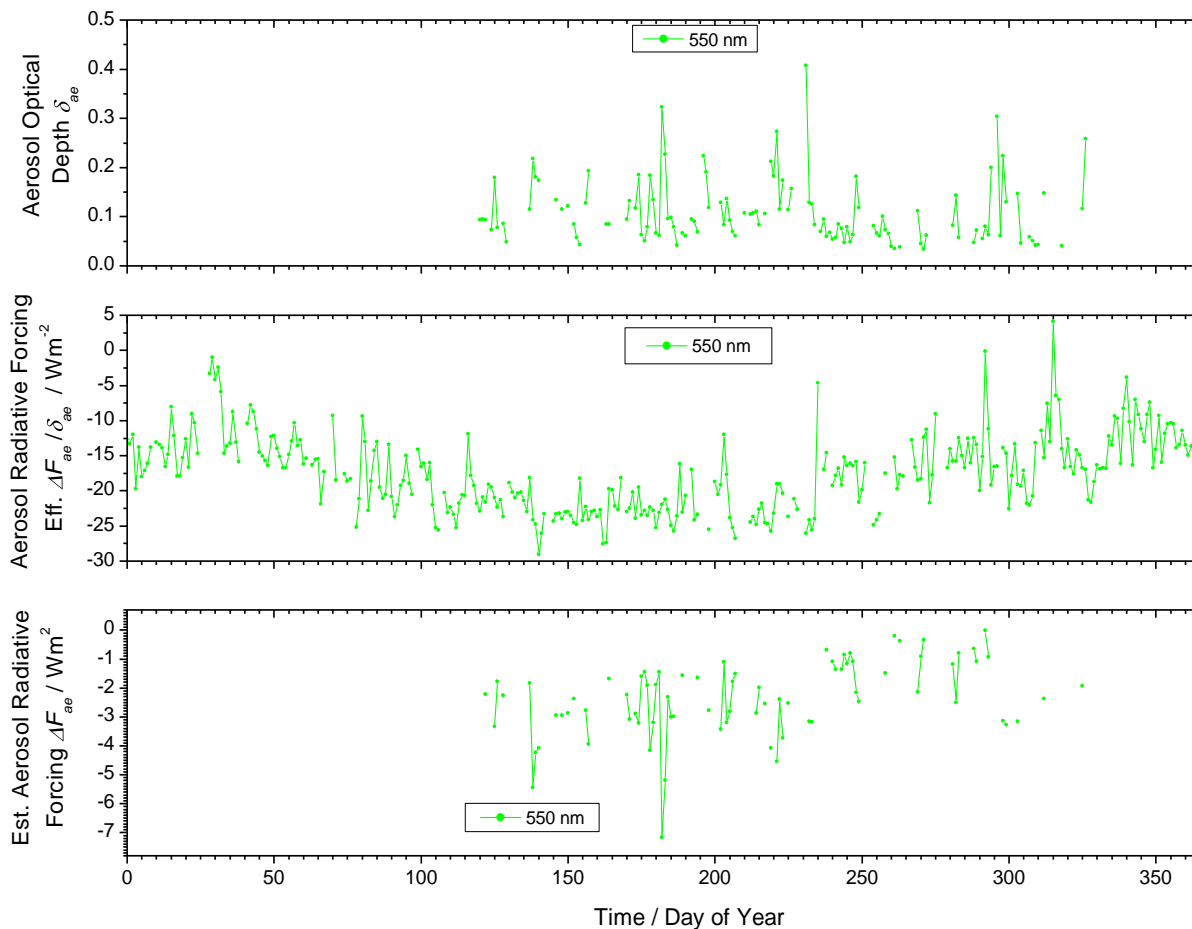


Figure 36: Time series of the cloud-screened aerosol optical depth (AOD) at 550 nm wavelength in the atmospheric column above Birkenes (upper panel), as well as the radiative forcing efficiency $\Delta F_{ae}/\delta$ (middle panel) and the estimated local, instantaneous, solar aerosol radiative forcing ΔF_{ae} .

Over a bright, high albedo snow surface in winter, the direct aerosol radiative forcing may well turn locally into a net warming effect.

6.4 Physical aerosol properties measured at Birkenes in 2010

The physical aerosol properties covered here include the particle number size distribution in the particle diameter range $30 \text{ nm} < D_p < 550 \text{ nm}$ measured by a Differential Mobility Size Spectrometer (DMPS). The data collected in 2010 by the DMPS is displayed in Figure 37 as colour contour plot, where the x-axis marks the time of measurement, the logarithmic y-axis the particle diameter, and the logarithmic colour code the particle number concentration per logarithmic size interval. This way of plotting time series of particle number size distribution is commonly used since both particle size and particle concentration span several orders of magnitude.

The particle number size distribution is not uniquely, but fairly characteristic for the origin and fate of an air mass, and thus shifts with shifting weather situation. Already in last year's report, the most common types of air masses occurring at Birkenes and their particle size distribution characteristics were discussed, which include (omitting special cases of long-range transport):

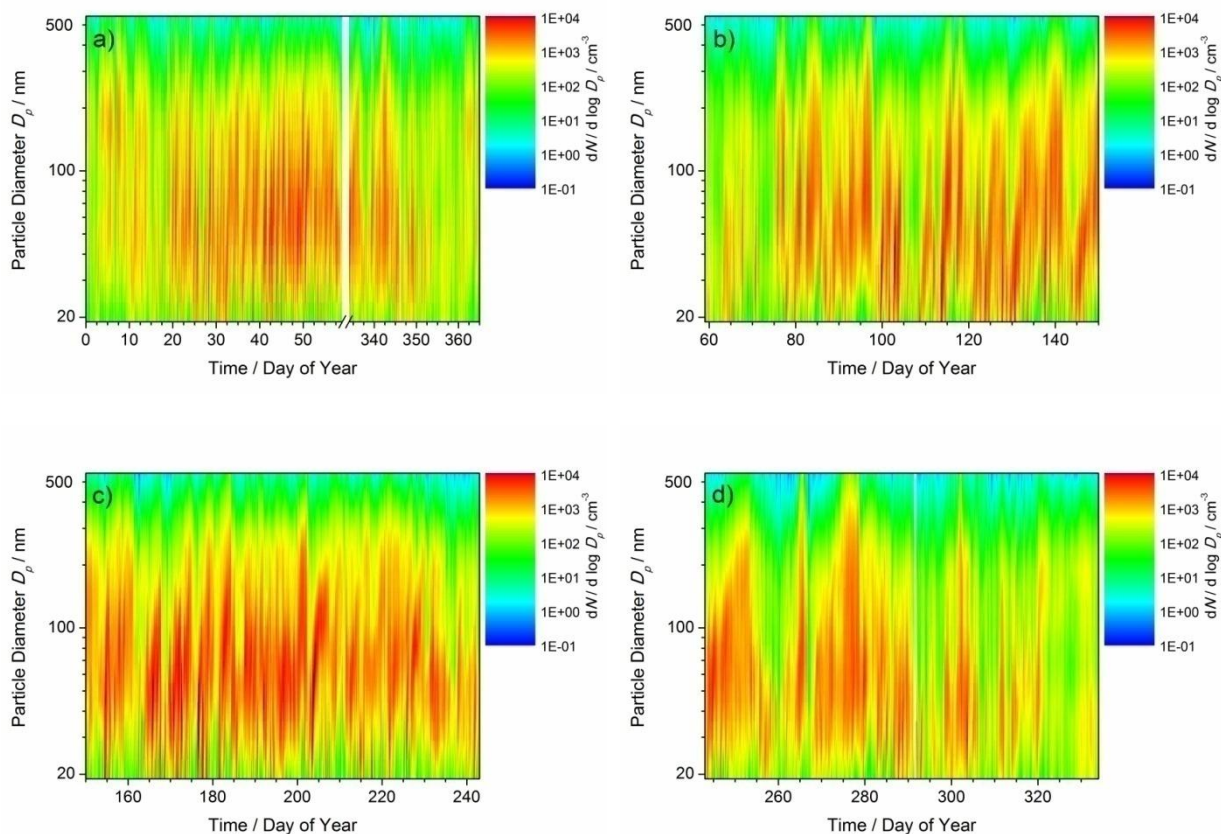


Figure 37: 2010 time series of particle number size distribution at Birkenes, panel a) winter, panel b) spring, panel c) summer, panel d) autumn.

- **Clean Arctic background aerosol**, characterised by a distinct accumulation mode (size mode peaking in the particle diameter range $100 \text{ nm} < D_p < 1000 \text{ nm}$) peaking at 150 nm particle diameter, with peak particle concentrations of 200 cm^{-3} .
- **Continental aerosol**, characterised by an accumulation mode peaking between $150 - 240 \text{ nm}$ particle diameter, depending on how long the aerosol had time to self-process, and peak particle concentrations between $1000 - 1500 \text{ cm}^{-3}$, in addition to the presence of an Aitken-mode (size mode peaking in the particle diameter range $10 \text{ nm} < D_p < 100 \text{ nm}$).
- **Arctic haze**, characterised by the absence of an Aitken-mode, and an accumulation mode peaking at 200 nm particle diameter, with peak particle concentrations of 1500 cm^{-3} .

All these aerosol types can be superimposed by additional modes in the particle size distribution within the Aitken-size range of $10 \text{ nm} < D_p < 100 \text{ nm}$. Particles in the Aitken-size range have an atmospheric lifetime of a couple of hours (Seinfeld & Pandis, 1998) before they either grow larger by mass uptake from the gas-phase, or coagulate with particles in the accumulation mode size range. Particles in the Aitken-size range are therefore relatively young, and have to be of local or regional origin, where a locally generated Aitken-mode peaks around 30 nm particle diameter, a regionally generated around 70 nm particle diameter.

At least two possible sources for such particles are known for continental background locations like Birkenes:

- **Biogenic aerosol**, generated from condensing oxidised precursor gases, e.g. terpenes, emitted by vegetation. Events of heavy biogenic aerosol formation are characterised by the formation of new particles. These events show by the appearance of a new mode in the particle size distribution that first quickly grows from particle diameters below 10 nm, then with decelerating velocity to particle diameters of about 60 nm.
- **Wood combustion aerosol**, generated usually by domestic heating with wood burning stoves.

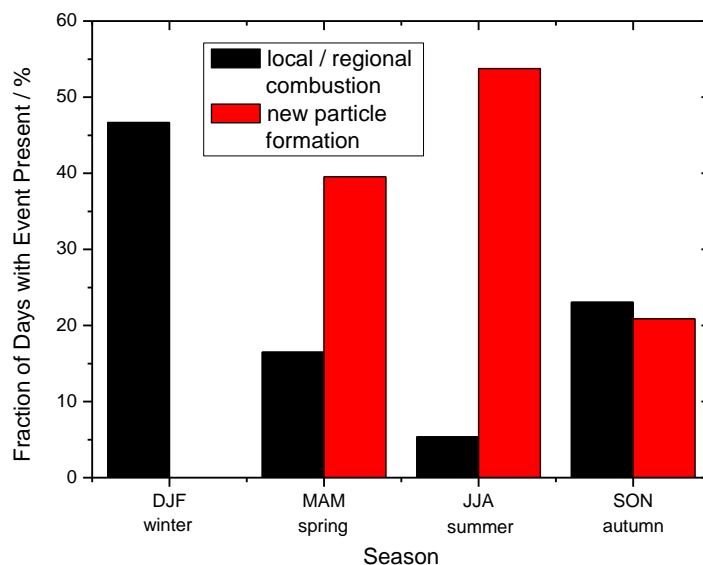


Figure 38: Frequency of occurrence of influence by local or regional combustion, as well as occurrence of new particle formation in Birkenes in 2010 as determined by combined analysis of particle number size distribution and single scattering albedo.

However, wood combustion aerosol is distinguished by another characteristic. It contains significant amounts of light absorbing carbon, and therefore has a single scattering albedo of below 0.85.

In this analysis, these characteristics are used to learn something about the reasons for the annual cycle of the aerosol single scattering albedo ϖ_0 , which was discussed in the previous section. To this end, the frequency of occurrence of particle formation events (characterised by the distinctly growing nucleation mode) and of wood combustion aerosol (characterised by a distinct Aitken-mode in the particle size distribution and a value of ϖ_0 below 0.85) have been determined as a function of season. If the annual cycle of ϖ_0 is associated with local or regional emissions of wood combustions aerosol, its frequency of occurrence should exhibit the same annual cycle.

Figure 38 visualises thus the determined frequency of occurrence of particle formation events and local or regional combustion events as bar graph. It is obvious that in summer, the Aitken mode in the aerosol at Birkenes, often present, most likely consists of newly formed particles, and here likely of biogenic origin. In winter however, no such event occurred in 2010. For biomass combustion events, the situation is exactly opposite. Here, the likelihood of the

Aitken-mode being due to biomass combustion is maximised in winter, and minimised in summer. For both types of events, spring and autumn are transition periods.

With all due caution due to the limited statistical significance of a one-year data series, it can be stated that the annual cycle of τ_{0} observed at Birkenes is very likely due to local and regional emissions of domestic biomass burning. Further studies on archived filter samples from Birkenes that use levoglucosan as tracer for biomass burning are currently being conducted to confirm this finding. It can thus be stated further that emissions of domestic biomass burning very likely have a significant effect on the direct aerosol radiative forcing in the Agder region in making it less cooling, in cases of snow covered surface maybe even positive, i.e. warming, in contrast to the global average.

6.5 Observations of the total aerosol load above Zeppelin and Birkenes observatories

The aerosol optical depth (AOD) is a quantitative measure of the extinction of solar radiation by aerosol scattering and absorption between the point of observation and the top of the atmosphere. It is determined by the total concentration of particulates in the atmosphere. The wavelength dependence of AOD, described by the Ångström exponent (α) is a qualitative indicator of the particle size and contains information about the aerosol type. The larger the exponent the smaller the size of the particles measured.

During the last years the number of stations measuring AOD has increased significantly. Figure 39 shows the development of the networks of sun-photometer in Scandinavia (Toledano et al., 2012). Photos of the standard instruments used in Ny-Ålesund and Birkenes, and their characteristics are shown in Figure 49 on page 74.

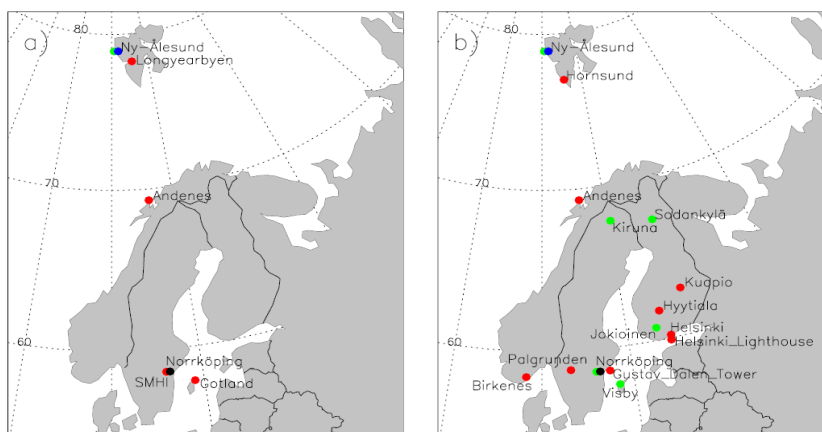


Figure 39: Location of sun photometer sites in the European Arctic sector and Scandinavia: (a) Until 2003; (b) From 2004 onward. Color symbols denote networks: AERONET sites (red), GAW-PFR (green), Polar-AOD (blue) [this Figure is equal to Figure 1 from Toledano et al., 2012].

In Ny-Ålesund, aerosol optical depth observations have been performed by the German Alfred Wegener Institute since 1991 (Herber et al., 2002). In 2002, PMOD/WRC in collaboration with NILU, started AOD observations, as part of the global network of AOD observations, which started in 1999 on behalf of the WMO GAW program. Since then, classic

extinction measurements at the recommended 4 WMO wavelengths 368, 415, 500 and 862 are performed as collaboration between PMOD/WRC and NILU, using a Precision Filter Radiometer (PFR, *Wehrli*, 2000 and 2005). Calibration is performed annually at PMOD/WRC. NRT data are displayed at www.pmodwrc.ch/worcc and can also be downloaded from the WDCA site (ebas.nilu.no)

In spring 2009 a CIMEL type CE-318 sun-photometer (#513) has been put in operation at the new Birkenes observatory. The instrument is an automatic sun and sky radiometer, with spectral interference filters centered at selected wavelengths: 340, 380, 440, 500, 675, 870, 1020, and 1640 nm, which is a standard instrument of the Aerosol Robotic Network AERONET network (*Holben et al.*, 1998; *NASA*, 2011). Measurements are made in collaboration with the University of Valladolid (Spain), who also perform the annual calibration (RIMA-AERONET sub-network). The data processing is centrally performed by AERONET. NRT and analyzed data are displayed at AERONET website (see aeronet.gsfc.nasa.gov).

The associated AOD uncertainty is 0.01-0.02 (larger for shorter wavelengths). The Ångström exponent (AE), indicative of size predominance is obtained from the AOD at different wavelengths. It depends on the spectral range used in the retrieval. The wavelength region for calculation AE from PFR measurements is 368-862 nm. This is slightly different from the one used for calculation of Ångström exponent within AERONET, which uses the range between 440 and 870 nm.

6.5.1 Measurements of the total aerosol load above Ny-Ålesund

NILU's measurements of the aerosol optical depth in Ny-Ålesund started in May 2002. Due to low aerosol load in Polar region, accuracy requirements for AOD measurements are more stringent than those usually encountered in established sun photometer networks. To jointly utilize and compare polar measurements, within the international polar year (IPY), the measurements contributed to the POLAR-AOD network was founded. Measurements from Ny-Ålesund were part of this network. First results can be found in *Tomasi et al.* (2007). Additional results from two inter-comparison campaigns, which were held during spring 2006 at Ny-Ålesund (Svalbard) and autumn 2008 at Izaña (Tenerife) within the framework of the IPY POLAR-AOD project, are recently published by *Mazzola et al.* (2012).

The Ny-Ålesund sun-photometer is located on the roof of the Sverdrup station. The instrument type is a Precision Filter Radiometer (PFR, *Wehrli*, 2000 and 2005), which measures the direct solar radiation in four narrow spectral bands at 862, 501, 411, and 368 nm. Samples are recorded with one minute time resolution. Data quality control includes instrumental control like detector temperature and solar pointing control as well as objective cloud screening. SCIAMACHY TOSOMI ozone columns and meteorological data from Ny-Ålesund were used in the retrieval of the aerosol optical depth. Ångström coefficients are derived for each set of measurements using all four PFR channels Annual calibration is performed at PMOD/WRC during winter-time.

In Ny-Ålesund the polar night lasts from 26th October to 16th February, leading to a relatively short observational seasons. In Table 4 and Table 5 monthly mean and sunlight-season average values of AOD at 500 nm and Ångström coefficients measured in Ny-Ålesund between 2002 and 2010 are summarized. The data are visualized in Figure 40 and Figure 41. In 2010 measurements started March 12 and stopped September 9 (only 2 hours, therefore we do not give a monthly average). Monthly mean data are calculated from hourly averaged

values with more than 10% of valid observations included. The results show a clear inter-annual variability. Individual episodes have a large impact on observed monthly averages. Huge emissions from boreal forest fires in North America are likely to explain the elevated AOD levels end of July 2004 (Stohl et al. 2006). Agricultural fires in Eastern Europe resulted in elevated pollution levels in Arctic in spring 2006 (Stohl et al., 2007; Myhre et al., 2007). The 2010 AOD observations indicate that 2010 was a relative clear year with relative low aerosol content, especially during spring. This is in agreement with lidar observations made by Alfred-Wegener Institute (Ritter et al., oral presentation at 10th Ny-Ålesund seminar, 2011).

Table 4: Monthly mean and sunlight-season average values of AOD at 500 nm measured in Ny-Ålesund between 2002 and 2010. The values given are mean and standard deviation.

Month / Year	2002	2003	2004	2005	2006	2007	2008	2009	2010	2002-2010
March		0.15±0.12	0.06±0.00	0.08±0.03	0.12±0.03		0.14±0.07		0.11±0.03	0.11±0.05
April	0.06±0.01	0.11±0.05	0.12±0.08	0.12±0.07	0.16±0.07	0.10±0.05	0.15±0.08		0.08±0.03	0.11±0.06
May	0.08±0.03	0.15±0.06	0.13±0.09	0.10±0.03		0.10±0.12	0.15±0.05	0.11±0.03	0.08±0.01	0.11±0.06
June	0.06±0.02	0.10±0.03	0.06±0.01	0.05±0.02	0.04±0.00	0.07±0.03	0.06±0.02	0.08±0.02	0.06±0.01	0.06±0.02
July	0.07±0.12	0.04±0.01	0.10±0.07	0.05±0.02	0.05±0.02	0.05±0.01	0.06±0.03	0.11±0.04	0.05±0.01	0.06±0.04
August	0.07±0.08	0.05±0.02	0.05±0.02	0.04±0.03	0.05±0.04	0.05±0.02		0.10±0.02	0.05±0.01	0.06±0.03
September	0.06±0.05	0.06±0.03	0.04±0.02	0.03±0.01	0.04±0.03	0.04±0.03		0.09±0.01		0.05±0.02
Mar – Sep	0.07±0.05	0.09±0.06	0.08±0.07	0.08±0.05	0.09±0.07	0.07±0.06	0.12±0.07	0.13±0.05	0.08±0.03	0.08±0.04

Table 5: Monthly mean and sunlight-season average values of Ångström coefficient AE measured in Ny-Ålesund in the period between 2002 and 2010. The values given are mean and standard deviation.

Month / Year	2002	2003	2004	2005	2006	2007	2008	2009	2010	2002-2010
March		0.9±0.5	1.3±0.1	1.1±0.3	0.9±0.1		1.4±0.3		1.0±0.03	1.1±0.3
April	0.9±0.1	1.3±0.3	1.2±0.3	1.4±0.4	0.9±0.3	1.4±0.4	1.3±0.3		1.4±0.02	1.2±0.3
May	1.4±0.1	1.3±0.2	1.4±0.5	1.0±0.2		1.4±0.6	1.4±0.2	1.3±0.4	1.3±0.02	1.4±0.3
June	1.2±0.3	1.5±0.1	1.7±0.2	1.6±0.3	1.7±0.2	1.7±0.2	1.5±0.4	1.4±0.2	1.3±0.03	1.5±0.2
July	1.2±0.2	1.5±0.3	1.6±0.4	1.7±0.2	1.4±0.3	1.6±0.2	1.5±0.3	1.3±0.3	1.4±0.02	1.4±0.3
August	1.3±0.4	1.4±0.5	1.5±0.3	1.4±0.7	1.3±0.6	1.7±0.3		1.2 ±0.1	1.0±0.01	1.4±0.4
September	1.2±0.5	1.4±0.3	1.3±0.3	1.5±0.4	1.4±0.3	1.5±0.4		1.1±0.1		1.3±0.3
Mar-Sep	1.3±0.3	1.3±0.4	1.4±0.4	1.3±0.4	1.2±0.4	1.5±0.4	1.4±0.3	1.3±0.3	1.2±0.3	1.3±0.3

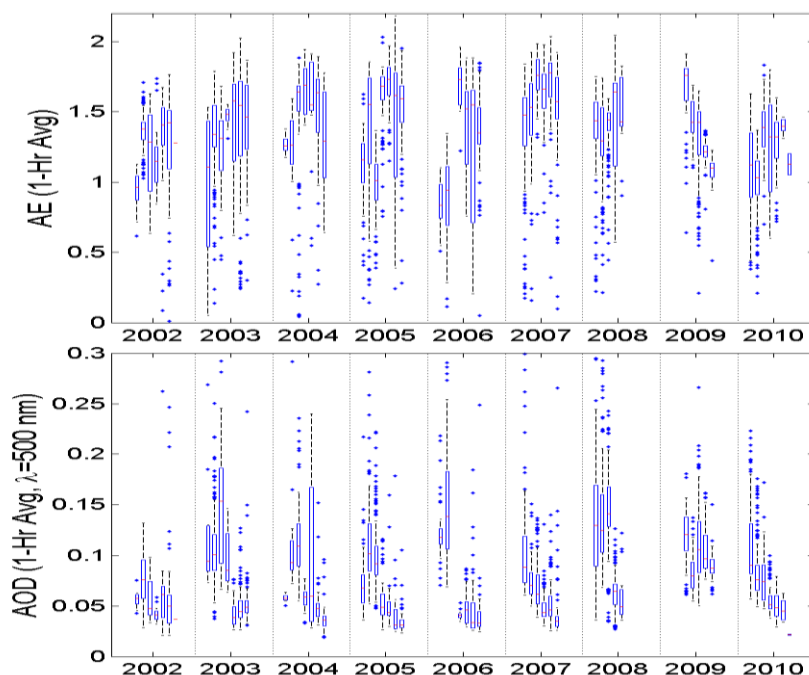


Figure 40: Monthly average Ångström exponent (upper panel) and aerosol optical depth (AOD at 500 nm) (lower panel) measured in Ny-Ålesund during the sunlight time periods in 2002 - 2010. On each box, the central mark is the median, the edges of the box are the 25th and 75th percentiles, the whiskers extend to the most extreme data points not considered outliers, and outliers (in terms of monthly averages, although not considered outlier in terms of pollution events with high aerosol loads) are plotted individually.

Seasonal variations for AOD and Ångström coefficient are shown in Figure 41. For comparison measurements from Hornsund, which is an AERONET site, are shown. The measurements reveal the expected pattern, larger AOD (about 0.12 at 500 nm wavelength), equivalent to higher aerosol-load during the Arctic haze period in spring than in summer (about 0.06), where background conditions were seen with low aerosol column concentration. According to the analysis of aerosol transport into the Arctic, Stohl et al. (2006) demonstrated that the region north of 70°N is isolated from mid-latitude sources in summer, whereas in winter and spring the sources with larger potential impact are located in Eurasia (rather than North America or East Asia). During summer the aerosol removal processes are likely more active in Svalbard.

The Ångström exponent in Svalbard does not show such a clear seasonal pattern as the AOD. Apparently there is a minimum in May at the end of the haze season, and then the AE increases slightly during the summer. In any case the multi-annual monthly means were above 1.0, thus indicating dominance of fine particle. The AE standard deviation in March is much higher than during rest of the months, which is due to the variability of Arctic haze transport events. The AOD differences in March between Ny-Ålesund and Hornsund cannot be considered relevant due to the different temporal periods in each dataset.

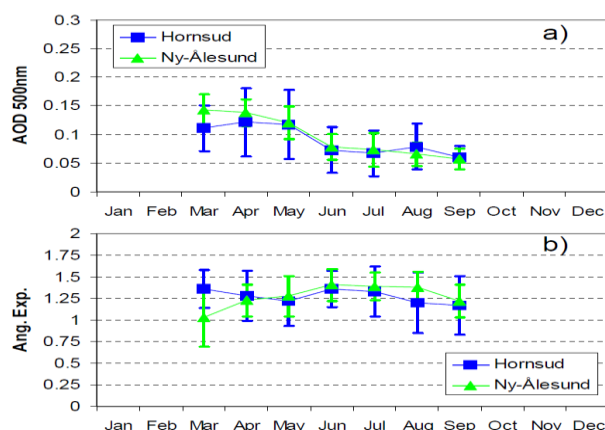


Figure 41: Multi-annual monthly means of (a) aerosol optical depth (500 nm) and (b) Ångström exponent at the high Arctic sun photometer sites in Svalbard: Ny-Ålesund (2002-2010); Hornsund (2004-2010). Error bars give standard deviation [this Figure is equal to Figure 2 from Toledano et al., 2012].

6.5.2 Measurements of the total aerosol load above the Birkenes observatory

Aerosol optical depth measurements started at the new Birkenes observatory in spring 2009, utilizing an automatic sun and sky radiometer (CIMEL type CE-318). During the first year of operations, measurements were made in the time period 30 April to 19 October 2009. The retrieval method is that of the AERONET version 2 direct sun algorithm (for details, see <http://aeronet.gsfc.nasa.gov>). Level 2 data are available for 2009. In 2010 measurements were made between May and December. The late start was caused due to calibration in Spain and delays connected with the transport of the instrument back to Norway.

The time-series of the total AOD in 2009 is given in Figure 42¹⁷ (left panel). Besides the total AOD, the coarse mode AOD is shown. Low coarse mode AOD is observed especially during the summer months, which can also be expressed as predominance of fine mode fraction. The yearly averaged fine mode fraction for 2009 was 71 ± 15 %. Values were clear above 80% during the summer months. The AOD and coarse mode fraction show a clear seasonality, with higher total AOD and lower coarse mode AOD in summer 2009. On top of stable spring background conditions with low AOD between 0.05 and 0.01, several episodes with high aerosol load can be seen. The seasonality seen is similar in 2010¹⁸. In summer the fine mode AOD is higher (monthly average of 76%) than in autumn (65%).

¹⁷ The data displayed are from the AERONET-SDA Version 4.1 data set (for a description of the Spectral Deconvolution Algorithm see O'Neill et al, 2003), which are derived from pre- and post-field calibrated and manually inspected AOD data

¹⁸ Note that 2010 data are not fully quality assured by AERONET yet (level 1.5 data),

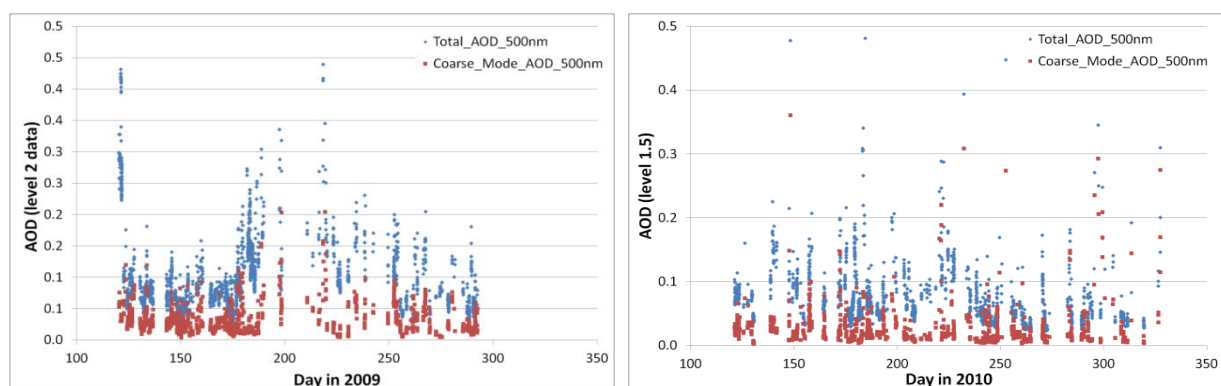


Figure 42: Time-series of total and coarse mode AOD measured during the first tow year of operation, in 2009 (left panel, level 2 data) and 2010 (right panel, level 1.5 data), at the Birkenes observatory.

Monthly mean averages of AOD at 500 nm, the Ångström exponent, precipitable water (PW), the associated standard deviations (σ), and the number of days (N) in 2009 and 2010 are given in Table 6. The data are visualized in Figure 43.

Table 6: Aerosol optical depth at 500 nm, Ångström exponent ($\alpha_{440-870}$), precipitable water (PW), the associated standard deviations (σ), the number of days (N) in 2009 (Level 2 data) and 2010 (Level 1.5, no post-calibration, cloud-screened, no AERONET QA).

Averages of	AOD _{a500}	$\alpha_{440-870}$	PW	N	Averages of	AOD _{a500}	$\alpha_{440-870}$	PW	N
MAY 2009	0.09±0.05	1.16±0.31	0.97±0.28	22	MAY 2010	0.10	1.33	1.11	13
JUN 2009	0.09±0.05	1.42±0.27	1.26±0.38	25	JUN 2010	0.09	1.38	1.33	16
JUL 2009	0.18±0.06	1.43±0.44	2.02±0.25	11	JUL 2010	0.10	1.43	1.73	18
AUG 2009	0.17±0.07	1.14±0.20	1.57±0.44	13	AUG 2010	0.15	1.37	1.63	16
SEP 2009	0.10±0.04	0.96±0.24	1.32±0.30	15	SEP 2010	0.05	1.29	1.18	16
OCT 2009	0.08±0.03	1.05±0.18	0.75±0.19	12	OCT 2010	0.08	1.16	0.73	11
					NOV 2010	0.07	1.08	0.58	8

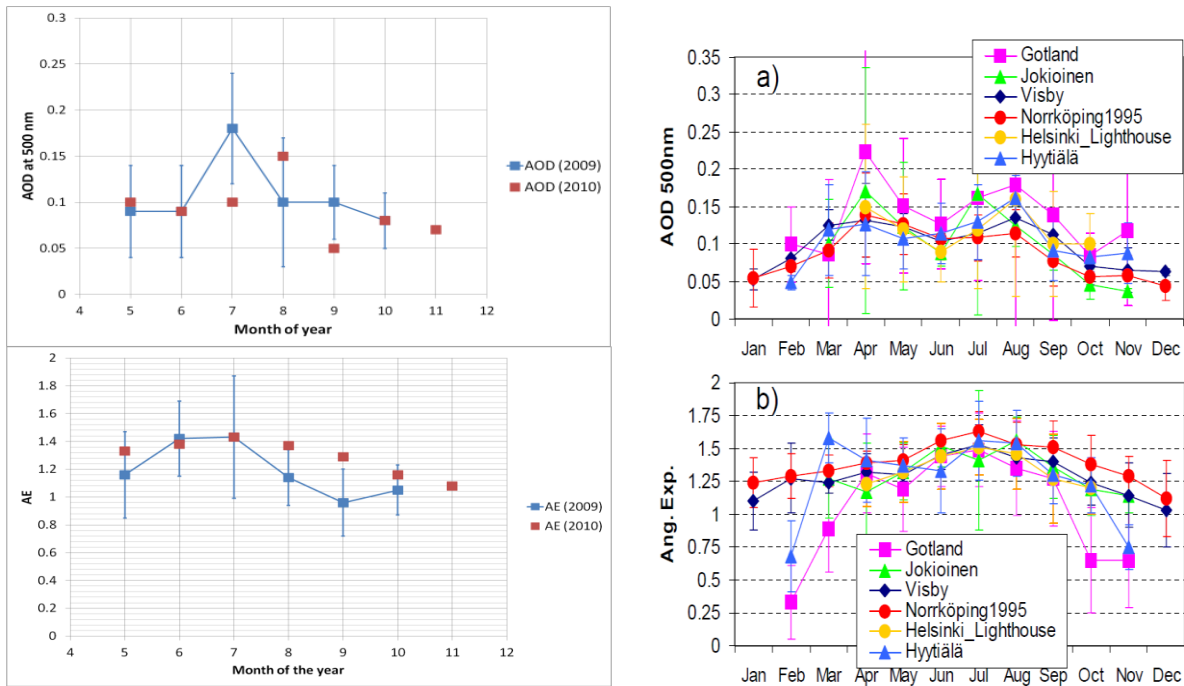


Figure 43: Left panel: Monthly mean values (\pm standard deviation) of Ångström exponent (upper panel) and Aerosol Optical Depth in 2009 and 2010 (lower panel). Blue: level 2 data from 2009; Brown: level 1.5 data for 2010. Right panel: seasonal variation for AOD and AE for selected Scandinavian sites [this figure is equal to Figure 4 in Toledano et al., 2012]

The monthly averaged data show a maximum aerosol load (high AOD) during summer period, July and August, which is consistent with what is seen in the rest of Southern Scandinavia. So far, the data set is not large enough to confirm the occurrence of the second AOD maxima. The larger Ångström exponent between May and July indicate a predominance of fine particulates in Southern Norway during early summer June and July. The Ångström exponent decreased towards winter-time, indicating larger particles. The annual cycle can be linked to long-range transport patterns from e.g. the European continent. During the coming years, the two year dataset will be complemented with more data, esp. during the beginning of the year. This will enable us to draw more general conclusions about the seasonality of the aerosol total column, the particle characteristics and origin at Birkenes.

7. Transport of pollution to the Zeppelin Observatory

We have performed an analysis and assessment of the source regions of the air masses arriving at Zeppelin in the period 2001-2010. Analyses of the air mass origin are important for the understanding of the observed levels of the gases and aerosols. We have analysed the origin of the air arriving at Zeppelin in 2010. Air mass trajectories are calculated using the FLEXTRA trajectory model (<http://www.nilu.no/trajectories/>) and using meteorological data provided from European Centre for Medium Range Weather Forecasts (ECMWF). 7 days backward trajectories from ECMWF have been used to investigate the major transport pathways into the region.¹⁹ The origin of the air arriving at Zeppelin is categorised in following 6 sectors:

- **Arctic region:** Clean Arctic air: Air mass trajectories with all trajectory points north of 65°N
- **Atlantic sector:** Clean marine air: Air mass trajectories with all trajectory points between 10°W and 70°W and from south of 65°N.
- **North American sector:** Polluted air: If at least 50% of the trajectory points are between 70°W and 180°W, and from south of 65°N.
- **European sector:** Polluted air: If at least 50% of the trajectory points were between 10°W and 30°E, and from south of 65°N.
- **Russian sector:** Polluted air: If air mass trajectories with all points between 30°E and 180°E and from south of 65°N.
- **Undefined sector:** 20% the trajectories do not come from a distinct sector.

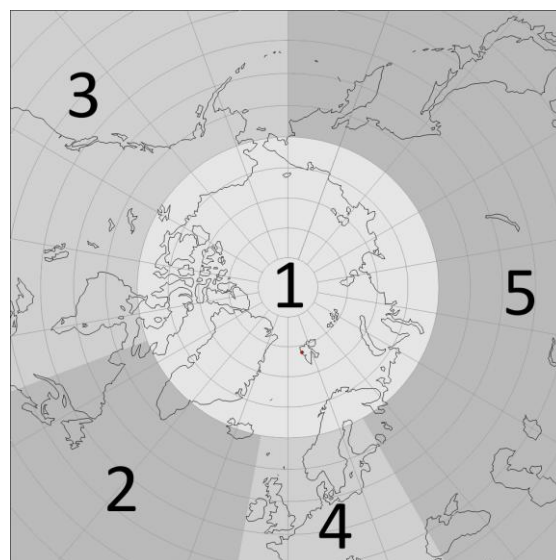


Figure 44: The sectors used to classify the air arriving at the Zeppelin Observatory. 1 is Arctic sector, 2 is Atlantic sector, 3 is North American sector, 4 is European sector and 5 is Russian sector.

Air from the Arctic and Atlantic sector is assumed to contain minimal influence of pollution. There are almost no industrial sources in these areas, and one can say that the air is ‘clean’. Background values of the greenhouse gases components are defined from those ‘clean air’ areas with 6 out of 8 trajectories (sampling day +/- 12 hours) within the sector, as described above.

Figure 45 shows the share of polluted and clean air arriving at the Zeppelin observatory for the years 2001-2010. The most striking result of this analysis is that in particularly 2007 and

¹⁹ The spatial resolution is T106, which correspond to a latitude/longitude resolution of 1x1 degrees, the temporal resolution is 6 hours, and 91 levels (60 levels before February 2006) are available in the vertical direction. The data sets used are so-called analysis, which is a combination of observations and numerical calculations. This includes measurements from satellites, radio sondes, buoys, weather stations, etc. which are assimilated into a meteorological model that produce an estimate of the state of the atmosphere at a given time.

2008 the fraction of air arriving at Zeppelin categorized as clean marine and Arctic air was clearly higher than the previous years. As described in section 4.1 the CH₄ concentration has increased since 2005. This can point in the direction of a possible Arctic source or accumulation of methane in the Arctic, particularly during late summer and autumn. Also the year 2003 with high methane concentration had a large fraction of clean air arriving at Zeppelin. 2009 is a somewhat different. In 2009 there were many episodes with polluted air transported to Zeppelin but no episodes as extreme as the record one observed in spring 2006 (Stohl et al., 2007; Myhre et al 2007). In contrast to the last years the site experienced higher influence of polluted air masses from central Europe and from the Russian sector in 2009. Clean arctic marine air dominated only on 59% of the days which is considerable lower than previous years. At the same time the category with mixed air from various sectors has increased slightly, thus the results are connected with uncertainty. 2010 show similar results to several previous years with large fraction of clean air, but fewer episodes from the Russian sector.

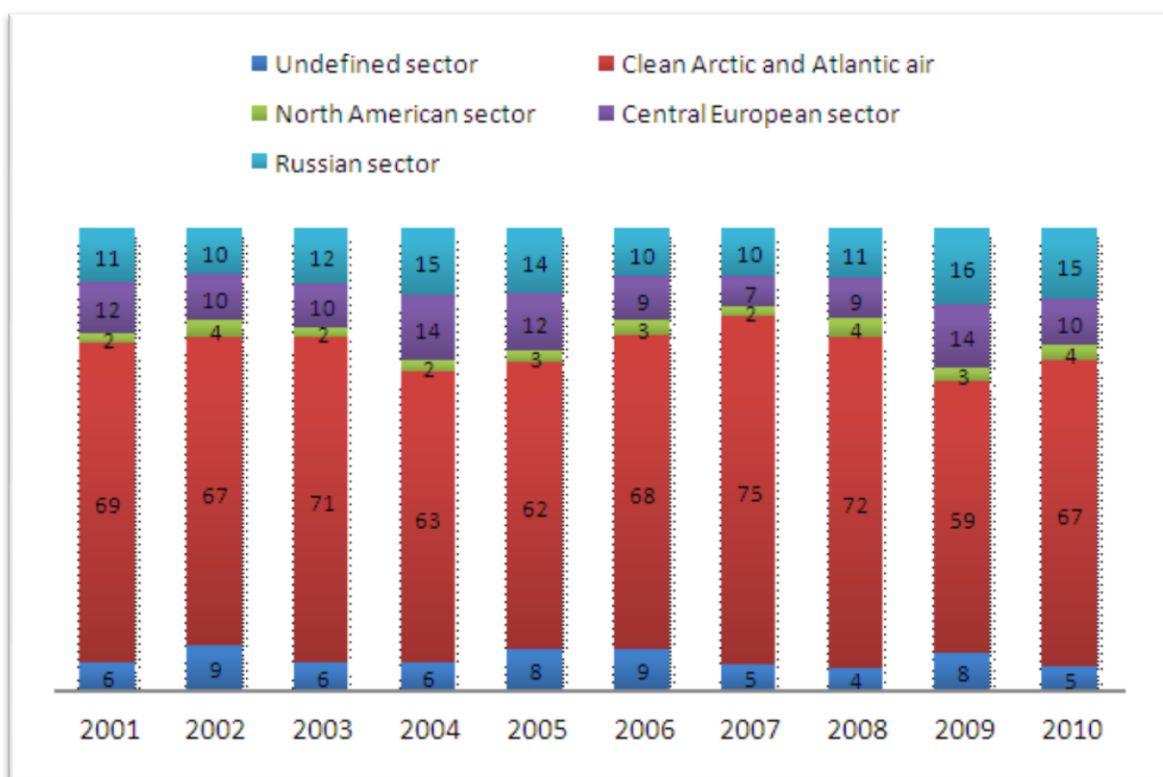


Figure 45: The percentage of polluted and clean air arriving at Zeppelin in the period 2001-2010 from the various sectors.

8. References

- Aas, W., Solberg, S., Manø, S., Yttri, K.E. (2011) Monitoring of long-range transported air pollutants. Annual report for 2010. [In Norwegian]. Kjeller, Norwegian Institute for Air Research (Statlig program for forurensningsovervåking. Rapport 1099/2011. TA-2812/2011) (NILU OR 29/2011).
- Andreae, M.O., Jones, C.D., Cox, P.M. (2005) Strong present-day aerosol cooling implies a hot future. *Nature*, *435*, 1187–1190.
- Bousquet, P., Ringeval, B., Pison, I., Dlugokencky, E. J., Brunke, E.-G., Carouge, C., Chevallier, F., Fortems-Cheiney, A., Frankenberg, C., Hauglustaine, D. A., Krummel, P. B., Langenfelds, R. L., Ramonet, M., Schmidt, M., Steele, L. P., Szopa, S., Yver, C., Viovy, N., Ciais, P. (2011) Source attribution of the changes in atmospheric methane for 2006–2008. *Atmos. Chem. Phys.*, *11*, 3689–3700, doi:10.5194/acp-11-3689-2011
- Delene, D.J., Ogren, J.A. (2002) Variability of aerosol optical properties at four North American surface monitoring sites. *J. Atmos. Sci.* *59*, 1135 – 1150.
- Dusek, U., Frank, G.P., Hildebrandt, L., Curtius, J., Schneider, J., Walter, S., Chand, D., Drewnick, F., Hings, S., Jung, D., Borrmann, S., Andreae, M.O. (2006) Size matters more than chemistry for cloud-nucleating ability of aerosol particles. *Science*, *312*, 1375–1378.
- Fisher, R.E., Sriskantharajah, S., Lowry, D., Lanoisellé, M., Fowler, C.M.R., James, R.H., Hermansen, O., Myhre, C.L., Stohl, A., Greinert, J., Nisbet-Jones, P.B.R., Mienert, J., Nisbet, E.G. (2011) Arctic methane sources: Isotopic evidence for atmospheric inputs. *Geophys. Res. Lett.*, *38*, L21803, doi:10.1029/2011GL049319
- Forster, P., Ramaswamy, V., Artaxo, P., Berntsen, T., Betts, R., Fahey, D.W., Haywood, J., Lean, J., Lowe, D.C., Myhre, G., Nganga, J., Prinn, R., Raga, G., Schulz, M., Van Dorland, R. (2007) Changes in atmospheric constituents and in radiative forcing. In: *Climate Change 2007: The physical science basis. Contribution of Working Group I to the fourth assessment report of the Intergovernmental Panel on Climate Change*. Ed. by S. Solomon, D. Qin, M. Manning, Z. Chen, M. Marquis, K.B. Averyt, M. Tignor, H.L. Miller. Cambridge, Cambridge University Press.
- Haywood, J.M., Shine, K.P. (1995) The effect of anthropogenic sulfate and soot aerosol on the clear sky planetary radiation budget. *Geophys. Res. Lett.*, *22*, 603–606.
- Herber, A., Thomason, L.W., Gernandt, H., Leiterer, U., Nagel, D., Schulz, K., Kaptur, J., Albrecht, T., Notholt, J. (2002) Continuous day and night aerosol optical depth observations in the Arctic between 1991 and 1999. *J. Geophys. Res.*, *107* (NO. D10) 4097, doi:10.1029/2001JD000536
- Holben, B., Eck, T., Slutsker, I., Tanré, D., Buis, J., Setzer, A., Vermote, E., Reagan, J., Kaufman, Y. (1998) AERONET- a federated instrument network and data archive for aerosol characterization. *Remote Sens. Environ.*, *66*, 1-16.
- IPCC (2007) Summary for Policymakers. In: *Climate Change 2007: The physical science basis. Contribution of Working Group I to the Fourth Assessment Report of the Intergovernmental Panel on Climate Change*. Ed. by S. Solomon, D. Qin, M. Manning, Z. Chen, M. Marquis, K.B. Averyt, M. Tignor, H.L. Miller. Cambridge, Cambridge University Press.
- Isaksen, I.S.A., Hov, Ø. (1987) Calculation of trends in the tropospheric concentration of O₃, OH, CO, CH₄ and NO_x. *Tellus*, *39B*, 271-285.

- Keppler, F., Hamilton, J.G., Bra, M., Röckmann, T. (2006) Methane emissions from terrestrial plants under aerobic conditions. *Nature*, 439, 187-191.
- Kiehl, J.T. (2007) Twentieth century climate model response and climate sensitivity. *Geophys. Res. Lett.*, 34, L22710, doi:10.1029/2007GL31383
- Kreidenweis, S.M., Petters, M.D., Chuang, P.Y. (2009) Cloud particle precursors. In: *Clouds in the perturbed climate system: Their relationship to energy balance, atmospheric dynamics, and precipitation*. Ed. by J. Heintzenberg, R.J. Charlson. Cambridge, MA, MIT Press.
- Law, K., Stohl, A. (2007) Arctic air pollution: Origins and impacts. *Science*, 315, 1537-1540.
- Mazzola, M., Stone, R.S., Herber, A., Tomasi, C., Lupi, A., Vitale, V., Lanconelli, C., Toledano, C., Cachorro, V.E., O'Neill, N.T., Shiobara, M., Aaltonen, V., Stebel, K., Zielinski, T., Petelski, T., Ortiz de Galisteo, J.P., Torres, B., Berjon, A., Goloub, P., Li, Z., Blarel, L., Abboud, I., Cuevas, E., Stock, M., Schulz, K.-H., Virkkula, A. (2012) Evaluation of sun photometer capabilities for retrievals of aerosol optical depth at high latitudes: The POLAR-AOD intercomparison campaigns. *Atmos. Environ.*, 52, 4-17, doi:10.1016/j.atmosenv.2011.07.042
- McFiggans, G., Artaxo, P., Baltensperger, U., Coe, H., Facchini, M.C., Feingold, G., Fuzzi, S., Gysel, M., Laaksonen, A., Lohmann, U., Mentel, T.F., Murphy, D.M., O'Dowd, C.D., Snider, J.R., Weingartner, E. (2006) The effect of physical and chemical aerosol properties on warm cloud droplet activation. *Atmos. Chem. Phys.*, 6, 2593–2649, doi:10.5194/acp-6-2593-2006.
- Myhre, C.L., Toledano, C., Myhre, G., Stebel, K., Yttri, K.E., Aaltonen, V., Johnsrud, M., Frioud, M., Cachorro, V., de Frutos, A., Lihavainen, H., Campbell, J.R., Chaikovsky, A.P., Shiobara, M., Welton, E.J., Tørseth, K. (2007) Regional aerosol optical properties and radiative impact of the extreme smoke event in the European Arctic in spring 2006. *Atmos. Chem. Phys.*, 7, 5899-5915.
- NASA (2011) NASA Goddard Space Flight Center, AERONET Aerosol Robotic Network. URL: <http://aeronet.gsfc.nasa.gov/> [Accessed 2011-06-09].
- O'Neill, N.T., Eck, T.F., Smirnov, A., Holben, B.N., Thulasiraman, S. (2003) Spectral discrimination of coarse and fine mode optical depth. *J. Geophys. Res.*, 108, 4559, doi:10.1029/2002JD002975
- Prather, M. et al. (2001) Atmospheric chemistry and greenhouse gases. In: *Climate Change 2001: The Scientific Basis, Contribution of Working Group I to the Third Assessment Report of the Intergovernmental Panel on Climate Change*. Ed. by J.T. Houghton et al. Cambridge, Cambridge University Press. pp. 239-287.
- Repo, M.E., Susiluoto, S., Lind, S.E., Jokinen, S., Elsakov, V., Biasi, C., Virtanen, T., Pertti, J., Martikainen, P.J. (2009) Large N₂O emissions from cryoturbated peat soil in tundra. *Nature Geosci.*, 2, 189–192.
- Rigby, M., Prinn, R.G., Fraser, P.J., Simmonds, P.G., Langenfelds, R.L., Huang, J., Cunnold, D.M., Steele, L.P., Krummel, P.B., Weiss, R.F., O'Doherty, S., Salameh, P.K., Wang, H.J., Harth, C.M., Mühle, J., Porter, L.W. (2008) Renewed growth of atmospheric methane. *Geophys. Res. Lett.*, 35, L22805, doi:10.1029/2008GL036037
- Schuur, E., Abbot, B. (2011) High risk of permafrost thaw. *Nature*, 480, 32-33.
- Seinfeld, J., Pandis, S. (1998) Atmospheric chemistry and physics: From air pollution to climate change. New York, Wiley-Interscience.

- Sheridan, P.J., Ogren, J.A. (1999) Observations of the vertical and regional variability of aerosol optical properties over central and eastern North America. *J. Geophys. Res.*, *104*, No. D14, 16793–16805.
- Simmonds, P.G., Manning, A.J., Cunnold, D.M., Fraser, P.J., McCulloch, A., O'Doherty, S., Krummel, P.B., Wang, R.H.J., Porter, L.W., Derwent, R.G., Grealley, B., Salameh, P., Miller, B.R., Prinn, R.G., Weiss, R.F. (2006) Observations of dichloromethane, trichloroethene and tetrachloroethene from the AGAGE stations at Cape Grim, Tasmania, and Mace Head, Ireland. *J. Geophys. Res.*, *111*, D18304, doi:10.1029/2006JD007082
- Stohl, A (2006) Characteristics of atmospheric transport into the Arctic troposphere. *J. Geophys. Res.*, *111*, D11306, doi:10.1029/2005JD006888
- Stohl, A., Berg, T., Burkhardt, J.F., Fjæraa, A.M., Forster, C., Herber, A., Hov, Ø., Lunder, C., McMillan, W.W., Oltmans, S., Shiobara, M., Simpson, D., Solberg, S., Stebel, K., Ström, J., Tørseth, K., Treffeisen, R., Virkkunen, K., Yttri, K.E. (2007) Arctic smoke – record high air pollution levels in the European Arctic due to agricultural fires in Eastern Europe in spring 2006. *Atmos. Chem. Phys.*, *7*, 511-534.
- Toledano, C., Cachorro, V., Gausa, M., Stebel, K., Aaltonen, V., Berjón, A., Ortiz de Galisteo, J.P., de Frutos, A.M., Bennouna, Y., Blindheim, S., Myhre, C.L., Zibordi, G., Wehrli, C., Kratzer, S., Hakansson, B., Carlund, T., de Leeuw, G., Herber, A., Torres, B. (2012) Overview of sun photometer measurements of aerosol properties in Scandinavia and Svalbard. *Atmos. Environ.*, *52*, 18-28, doi:10.1016/j.atmosenv.2011.10.022
- Tomasi, C., Vitale, V., Lupi, A., Di Carmine, C., Campanelli, M., Herber, A., Treffeisen, R., Stone, R.S., Andrews, E., Sharma, S., Radionov, V., von Hoyningen-Huene, W., Stebel, K., Hansen, G.H., Myhre, C.L., Wehrli, C., Aaltonen, V., Lihavainen, H., Virkkula, A., Hillamo, R., Ström, J., Toledano, C., Cachorro, V.E., Ortiz, P., de Frutos, A.M., Blindheim, S., Frioud, M., Gausa, M., Zielinski, T., Petelski, T., Yamanouchi, T. (2007) Aerosols in polar regions: A historical overview based on optical depth and in situ observations. *J. Geophys. Res.*, *112*, D16205, doi:10.1029/2007JD008432
- Wehrli, C. (2000) Calibrations of filter radiometers for determination of atmospheric optical depth. *Metrologia*, *37*, 419-422.
- Wehrli, C. (2005) GAWPFR: A network of Aerosol Optical Depth observations with Precision Filter Radiometers. In: *WMO/GAW Experts workshop on a global surface based network for long term observations of column aerosol optical properties*. Geneva, World Meteorological Organization (GAW Report No. 162, WMO TD No. 1287).
- WMO (2009) Greenhouse Gas Bulletin. The state of greenhouse gases in the atmosphere using global observations through 2008. Geneva, World Meteorological Organization (Bulletin No. 5, 23 November 2009). **URL:** http://www.wmo.int/pages/prog/arep/gaw/ghg/documents/ghg-bulletin2008_en.pdf
- WMO (2011a) Greenhouse Gas Bulletin. The state of greenhouse gases in the atmosphere using global observations through 2010. Geneva, World Meteorological Organization (Bulletin No. 7, 21 November 2011). **URL:** http://www.wmo.int/pages/prog/arep/gaw/ghg/documents/GHGbulletin_7_en.pdf
- WMO (2011b) Scientific assessment of ozone depletion: 2010. Global Ozone Research And Monitoring Project – Report No. 52. Geneva, World Meteorological Organization.

Appendix I: Description of instruments, methods and trend analysis

In this appendix are the instrumental methods used for the measurements of the various greenhouse gases presented. Additionally we explain the theoretical methods used in the calculation of the trends. In the end of the section we show how the annual mean values presented in Table 2 are calculated.

Details about greenhouse gas measurements and recent improvement and extensions

NILU performs measurements of halogenated greenhouse gases as well as methane and carbon monoxide using automated gas chromatographs with high sampling frequencies at Zeppelin. A mass spectrometric detector is used to determine more than 20 halogenated compounds, automatically sampled 6 times per day. Methane and CO are sampled 3 times per hour. This high sampling frequency gives valuable data for the examination of episodes caused by long-range transport of pollutants as well as a good basis for the study of trends and global atmospheric change. Close cooperation with AGAGE-partners on the halocarbon instrument and audits on the methane and CO-instruments (performed by EMPA on the behalf of GAW/WMO) results in data of high quality.

At the Birkenes Observatory a very different approach is used. At this site Picarro Cavity Ring-Down Spectroscopy (CRDS) is employed. This is a state of the art infrared spectrometer for field measurements with very high time resolution and precision. The Picarro CRDS are utilizing a near-infrared laser to measure spectral signatures of the molecule. Gas is introduced in an optical measurement cavity with an effective path length of up to 20 km making it possible to measure very low concentrations. The CRDS technology allows monitoring of CO₂ and CH₄ in moist air. During post-processing concentrations are re-calculated for dry air. This is required to remove the variability of moisture in the atmosphere, and to make the monitoring results comparable with traditional FTIR monitoring methods.

Table 7: Instrumental details for greenhouse gas measurements at Zeppelin and Birkenes.

Component		Instrument and method	Time res.	Calibration procedures	Comment
Methane (Birkenes)	CH ₄	Picarro CRDS G1301 CO ₂ /CH ₄ /H ₂ O	5 s	Waiting for calibration gases from NOAA. Currently only initial calibration from Picarro.	Measurements started 19. May 2009
Methane (Zeppelin)	CH ₄	GC-FID-	15 min	Hourly, working std. calibrated vs. GAW std.	Data coverage 2010: 70% (97% for daily values). Low coverage due to a problem with the ventilation system in the station building causing contamination of samples during last part of the year.
Nitrous oxide (Zeppelin)	N ₂ O	GC--ECD	15 min	Hourly, working std. calibrated vs. GAW std.	Data coverage 2010: 77%. Measurements started 02.04.2010.
Carbon monoxide	CO	GC-MgO/UV	20 min	Every 2 hours, working std. calibrated vs. GAW std.	Data coverage 2010: 70%
Carbon dioxide (Zeppelin)	CO ₂		1 h		CO ₂ measurements performed by ITM Stockholm University (SU)
Carbon dioxide (Birkenes)	CO ₂	Picarro CRDS G1301 CO ₂ /CH ₄ /H ₂ O	5 s	Waiting for calibration gases from NOAA. Currently only initial calibration from Picarro.	Measurements started 19. May 2009.
CFC-11 CFC-12 CFC-113 CFC-115 HFC-125 HFC-134a HFC-152a HFC-365mfc HCFC-22 HCFC-141b HCFC-142b H-1301 H-1211	CFCl ₃ CF ₂ Cl ₂ CF ₂ ClCFCl ₂ CF ₃ CF ₂ Cl CHF ₂ CF ₃ CH ₂ FCF ₃ CH ₃ CHF ₂ CF ₃ CH ₂ CHF ₂ CH ₃ CHF ₂ Cl CH ₃ CFCl ₂ CH ₃ CF ₂ Cl CF ₃ Br CF ₂ ClBr	ADS-GCMS	4 h	Every 4 hours, working std. calibrated vs. AGAGE std.	Data coverage 2010: ca 70% The measurements of the CFCs have higher uncertainty and are not within the required precision of AGAGE. See next section for details.

Table 7, cont.

Component		Instrument and method	Time res.	Calibration procedures	Comment
Methyl Chloride	CH ₃ Cl				
Methyl Bromide	CH ₃ Br				
Methylenedichloride	CH ₂ Cl ₂				
Chloroform	CHCl ₃				
Methylchloroform	CH ₃ CCl ₃				
TriChloroethylene	CHClCCl ₂				
Perchloroethylene	CCl ₂ CCl ₂				
Sulphurhexafluoride	SF ₆				
Tetrafluormethane	CF ₄	Medusa-GCMS	2 h	Every 2	Start September
PFC-116	C ₂ F ₆	No. 19		hours,	2010. The instrument
PFC-218	C ₃ F ₈			working std.	will run in parallel with
PFC-318	c-C ₄ F ₈			calibrated vs.	ADS-GC-MS for one
Sulphurhexafluoride	SF ₆			AGAGE std	year. The precision is
Sulfuryl fluoride	SO ₂ F ₂				improved and more
HFC-23	CHF ₃				components are
HFC-32	CH ₂ F ₂				measured compared
HFC-125	CHF ₂ CF ₃				to the ADS-GC-MS.
HFC-134a	CH ₂ FCF ₃				
HFC-143a	CH ₃ CF ₃				
HFC-152a	CH ₃ CHF ₂				
HFC-227ea	CF ₃ CHFCF ₃				
HFC-236fa	CF ₃ CH ₂ CF ₃				
HFC-245fa	CF ₃ CH ₂ CHF ₂				
HFC-365mfc	CF ₃ CH ₂ CHF ₂ CH ₃				
HCFC-22	CHF ₂ Cl				
HCFC-124	CHClFCF ₃				
HCFC-141b	CH ₃ CFC ₂				
HCFC-142b	CH ₃ CF ₂ Cl				
CFC-11	CFCl ₃				
CFC-12	CF ₂ Cl ₂				
CFC-113	CF ₂ CICFCl ₂				
CFC-114	CF ₂ CICF ₂ Cl				
CFC-115	CF ₃ CF ₂ Cl				
H-1211	CF ₃ Br				
H-1301	CF ₂ ClBr				
H-2402	CF ₂ BrCF ₂ Br				
Methyl Chloride	CH ₃ Cl				
Methyl Bromide	CH ₃ Br				
Methyl Iodide	CH ₃ I				
Methylenedichloride	CH ₂ Cl ₂				
Chloroform	CHCl ₃				
Methylchloroform	CH ₃ CCl ₃				
Dibromomethane	CH ₂ Br ₂				
Bromoform	CHBr ₃				
TriChloroethylene	TCE				
Perchloroethylene	PCE				
Ethane	C ₂ H ₆				
Benzene	C ₆ H ₆				
Carbonyl Sulfide	COS				
Ozone	O ₃		5 min		

CO₂ measurements performed by ITM Stockholm University (SU)

At the Zeppelin station carbon dioxide (CO₂) and atmospheric particles are measured by Stockholm University (Institute of Applied Environmental Research, ITM).

SU maintains a continuous infrared CO₂ instrument, which has been monitoring since 1989. The continuous data are enhanced by the weekly flask sampling programme in co-operation with NOAA CMDL. Analysis of the flask samples provides CH₄, CO, H₂, N₂O and SF₆ data for the Zeppelin station.

Data quality and uncertainties

In general the ADS-GCMS can measure a wide range of hydrochlorofluorocarbons, hydrofluorocarbons (HCFC-141b, HCFC-142b, HFC-134a etc.), methyl halides (CH₃Cl, CH₃Br, CH₃I) and the halons (e.g. H-1211, H-1301) with a good scientific quality. The system can also measure other compounds like the chlorofluorocarbons, but the quality and the precision of these measurements are not at the same level. Table 8 shows a list over those species measured with the ADS-GCMS at Zeppelin Observatory. The species that are in blue are of acceptable scientific quality and in accordance with recommendations and criteria of AGAGE for measurements of halogenated greenhouse gases. Those listed in red have higher uncertainty and are not within the required precision of AGAGE. There are various reasons for this increased uncertainty; unsolved instrumental problems e.g. possible electron overload in detector (for the CFC's), influence from other species, detection limits (CH₃I, CHClCCl₂) and unsolved calibration problems (CHBr₃).

Table 8: ADS-GCMS measured species. Good scientific quality data in Blue; Data with reduced quality data in Red. The data are available through <http://ebas.nilu.no>. Please read and follow the stated data policy upon use.

Compound	Typical precision (%)	Compound	Typical precision (%)
SF ₆	1,5	H1301	1,5
HFC134a	0,4	H1211	0,4
HFC152a	0,6	CH ₃ Cl	0,6
HFC125	0,8	CH ₃ Br	0,8
HFC365mfc	1,7	CH ₃ I	5,1
HCFC22	0,2	CH ₂ Cl ₂	0,4
HCFC141b	0,5	CHCl ₃	0,3
HCFC142b	0,5	CHBr ₃	15
HCFC124	2,3	CCl ₄	0,5
CFC11	0,3	CH ₃ CCl ₃	0,6
CFC12	0,3	CHClCCl ₂	1,2
CFC113	0,2	CCl ₂ CCl ₂	0,7
CFC115	0,8		

New Medusa instrument installed at Zeppelin and improved air inlet system

To have the suitable and necessary scientific quality of the GHG measurements and fulfill the requirements of AGAGE, NILU installed a new Medusa at the Zeppelin Observatory Autumn 2010. The instrument is developed to provide more accurate measurements of halocarbon gases and also extending the range of compounds monitored.

The new Medusa instruments not only extend the number of species measured by original ADS instruments to 40 species, but also improve the quality and precision in measurements of most of the species, especially the CFC's. But even though the improvements, there are still a few issues related to the measurements of the CFC's and a few others of the 40 species that are unresolved. Therefore, the AGAGE network has decided to report their CFC data measured with their old GC-MD system from the AGAGE stations that both have a GC-MD and a Medusa.

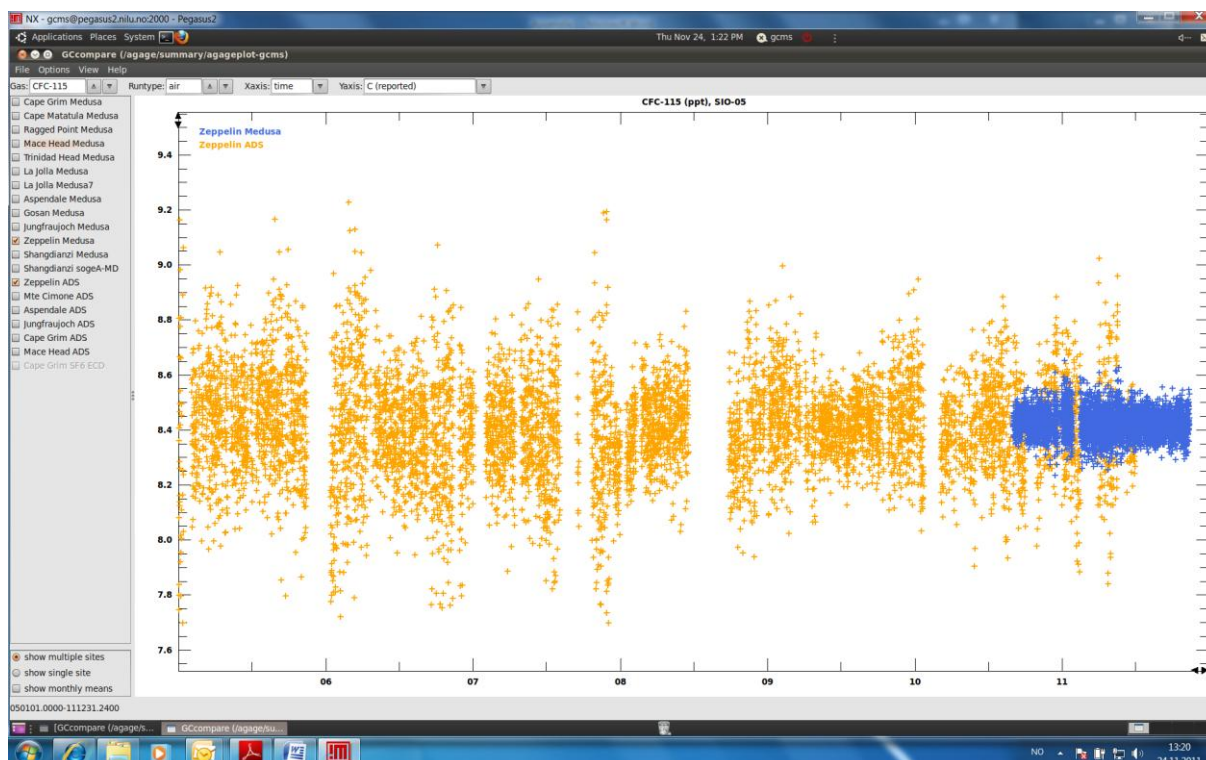
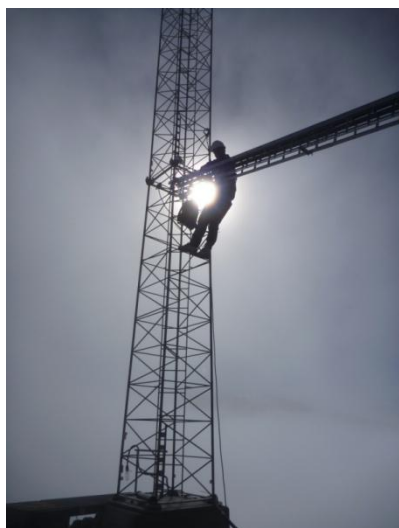


Figure 46: Measurements of CFC-115 at Zeppelin Observatory. The measurement precision improves when using results from the Medusa-GCMS (in blue) compared to the ADS-GCMS (in yellow).

Table 9 gives an overview over the species measured with the Medusa and GC-MD systems at the AGAGE stations and the typical precision with the different instruments. After the installation of the Medusa instrument and implementation of the same calibration scale and QA/QC routines as the rest of the AGAGE station, the Zeppelin Observatory is considered as an AGAGE station and the measurements performed meet the same criteria as shown in Table 9.

There has also been improved air inlet for the GHG observations at Zeppelin to reduce possible influence from the station and visitors at the stations.



NILU engineer Are Bäcklund about to install a new air inlet for the Medusa instrument.
Photo: Ove Hermansen, NILU

Table 9: AGAGE measured species. *Medusa in Blue; GC-MD green; Both: Red.*

Compound	Typical precision (%)	Compound	Typical precision (%)
CF ₄	0.15	H1301	1.5
C ₂ F ₆	0.9	H1211	0.5
C ₃ F ₈	3	H2402	2
SF ₆	0.4	CH ₃ Cl	0.2
SO ₂ F ₂	1.6	CH ₃ Br	0.5
HFC23	0.7	CH ₃ I	2
HFC32	5	CH ₂ Cl ₂	0.8
HFC134a	0.4	CHCl ₃	0.6
HFC152a	1.2	CHBr ₃	0.6
HFC125	1	CCl ₄	1
HFC143a	1.2	CH ₃ CCl ₃	0.7
HFC365mfc	10	CHClCCl ₂	2.5
HCFC22	0.3	CCl ₂ CCl ₂	0.5
HCFC141b	0.4	C ₂ H ₂	0.5
HCFC142b	0.6	C ₂ H ₄	2
HCFC124	2	C ₂ H ₆	0.3
CFC11	0.15	C ₆ H ₆	0.3
CFC12	0.05	C ₇ H ₈	0.6
CFC13	2	GC-MD only*	
CFC113	0.2	CH ₄	0.05
CFC114	0.3	N ₂ O	0.05
CFC115	0.8	CO	0.2
		H ₂	0.6

*CO and H₂ are measured by GC-MD at Mace Head and Cape Grim only
(ppt = parts per trillion, ppb = parts per billion)

To improve the quality of the ongoing ADS-GCMS measurements at Zeppelin Observatory, the two instruments (Medusa and ADS-GCMS) will be run in parallel for at least 6 months. Results from the comparison between the two will be used to improve the quality of the species measured with the ADS-GCMS so far.

New instrument for monitoring of methane and nitrous oxide

A new gas chromatograph (GC) for measurements of CH₄ and N₂O was installed at the Zeppelin station late 2009. After a period of tuning and verification, methane measurements with the new instrument were started early 2010. Measurements of N₂O were started early April 2010. The new gas chromatograph is a dual channel system equipped with a Flame Ionization Detector for CH₄ -measurements and an Electron Capture Detector for N₂O -measurements. The new system enables better control of the calibration process and increased frequency for calibration against reference standards. Precision on methane measurements calculated from working standards over a 24 hour period of normal measurements is improved from ~0.2% to ~0.1%. The old and the new instrument show good agreement when run in parallel.

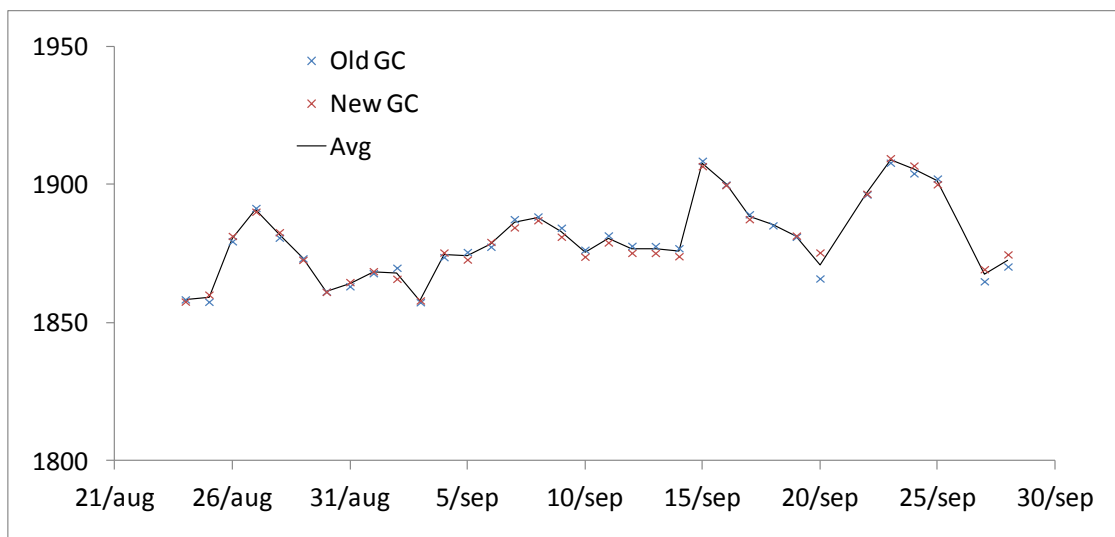


Figure 47: Comparison of old and new measurements of methane at Zeppelin.



Figure 48: The new Gas Chromatograph for Methane and Nitrous Oxide measurements (left) side by side with the old system for Methane measurements.

Details about aerosol optical depth measurements

The amount of particles in the air is monitored by use of a Precision-Filter-Radiometer (PFR) sun photometer (NILU) in Ny-Ålesund and a Cimel instrument at Birkenes, see details below.

<p>AERONET - Cimel C-318</p> <ul style="list-style-type: none"> • Sun (9 channels) and sky radiances • Wavelength range:: 340-1640 nm nm • 15 min sampling • No temperature stabilized • AOD uncertainty: 0.01-0.02 	<p>PFR-GAW - Precision Filter Radiometer</p> <ul style="list-style-type: none"> • Direct sun measurements (4 channels) • Wavelength range: 368-862 nm • Continuous sampling (1 min) • Temperature stabilized • AOD uncertainty: 0.01
<p>Figure 49: Photos and typical features of the standard instrument of the AERONET (left panel) and GAW PFR network instruments (right panel) (adapted from Toledano et al., 2012).</p>	

Aerosol optical depth measurements started at the new Birkenes observatory in spring 2009, utilizing an automatic sun and sky radiometer (CIMEL type CE-318), with spectral

interference filters centered at selected wavelengths: 340, 380, 440, 500, 675, 870, 1020, and 1640 nm. The measurement frequency is approximately 15 minutes (depends on the air-mass and time). Calibration was performed in Izaña in the period 13 May to 24 of July 2008 (RIMA-AERONET sub-network). Between 11 December 2009 and 26 January 2010 and between 16 September and November 2011, at Autilla del Pino (Palencia, Spain), the operational calibration platform managed by GOA for RIMA-AERONET sun photometers. The data analysis is centralized and performed by AERONET. At present, quality assured data (AERONET level 2.0) are available only for 2009. The 2009 data-set is pre and post field calibrated, automatically cloud cleared and manually inspected. Due to post-calibration performed in autumn 2011, for 2010 no quality assured level 2.0 data are available yet. The data were automatically cloud cleared, but the final calibration has not been applied (AERONET Level 1.5).

The PFR measurements in Ny-Ålesund are part of the global network of aerosol optical depth (AOD) observations, which started in 1999 on behalf of the WMO GAW program. The instrument is located on the roof of the Sverdrup station, Ny-Ålesund, close to the EMEP station on the Zeppelin Mountain (78.9°N, 11.9°E, 474 m asl). The PFR has been in operation since May 2002. In Ny-Ålesund the polar night lasts from 26th October to 16th February, leading to short observational seasons. However during the summer it is possible to measure day and night if the weather conditions are satisfactory. The instrument measures direct solar radiation in four narrow spectral bands centred at 862, 501, 411, and 368 nm. Data quality control includes instrumental control like detector temperature and solar pointing control as well as objective cloud screening. Measurements are made at full minutes are averages of 10 samples for each channel made over a total duration of 1.25 seconds. SCIAMACHY TOSOMI ozone columns and meteorological data from Ny-Ålesund were used in the retrieval of the aerosol optical depth.

Outlook on observations of aerosol properties in Ny-Ålesund in and beyond 2011

To better characterize the total aerosol content in Ny-Ålesund, especially in the boundary layer, and distinguish between local and long-range transported contributions, in collaboration with the Alfred-Wegener Institute, for the first time, a sun-photometer has been operated at Zeppelin mountain to determine the optical depth above the site, and by comparison with ground-level observations in Ny-Ålesund, to determine the AOD of the first 450 m of the atmosphere. After a successful test-period in 2011, this collaboration will continue in 2012.

Status and outlook on observations of aerosol properties at Birkenes in 2010 and 2011

Up to 2009, the instrumentation for observing properties of atmospheric aerosol particles at Birkenes consisted of a Differential Mobility Particle Sizer (DMPS), a single-wavelength Particle Soot Absorption Photometer (PSAP), and a PM_{2.5} and PM₁₀ filter samplers for collecting samples for chemical analysis. A DMPS measures the particles number size distribution, usually in the range of about 0.02 – 0.8 µm particle diameter. After putting the aerosol particle phase into a defined state of charge by exposing them to an ionised atmosphere in thermal equilibrium, the DMPS uses a cylindrical capacitor to select a narrow size fraction of the particle phase. The particle size in the selected size fraction is determined by the voltage applied to the capacitor. The particle number concentration in the selected size fraction is then counted by a Condensation Particle Counter (CPC). A mathematical inversion that considers charge probability, transfer function of the capacitor, and counting efficiency of the CPC is then used to calculate the particle number size distribution. A PSAP measures the aerosol absorption coefficient by measuring the decrease in optical transmissivity of a filter while the filter is loaded with the aerosol sample. The transmissivity time series is subsequently translated into a absorption coefficient time series by using Lambert-Beer's law,

the same law also used in optical spectroscopy. The $PM_{2.5}$ and PM_{10} filter samples of the aerosol particle phase are analysed by ion chromatography to reveal the chemical speciation.

From 2010, all instruments measuring aerosol properties in Birkenes listed in section 6.1 were in full operation. This now also includes a 3-wavelength integrating nephelometer and an Optical Particle Counter (OPC). The integrating nephelometer measures the aerosol scattering coefficient at three wavelength across the visible spectrum by illuminating an aerosol-filled confined volume with a Lambertian light source, and collecting the light scattered by the particles in the volume. This observation is complementary to the measurements of the aerosol absorption coefficient by PSAP, can be used to increase the accuracy of the PSAP measurements. The OPC measures the particle number size distribution in the size range of 0.25 – 10 μm particle diameter, and is thus complementary to the DMPS measurements. Together, DMPS and OPC cover the full particle size range commonly considered by atmospheric aerosol observations. In the OPC, the particles in the sample pass through a laser beam. By correlating the amplitude of the peak of scattered light generated while passing the laser beam with particle size, the particle size distribution is measured.

Moreover, the measurement programme at Birkenes is due to be extended in 2011 with a multi-wavelength absorption photometer and a cloud condensation nucleus counter (CCNC). The absorption photometer will measure the aerosol absorption coefficient at three wavelength across the visible spectrum, and will, after an intercomparison period, replace the old single wavelength instrument used so far. The information on spectral particle absorption will allow conclusion about the nature of the absorber, and its distribution with particle size. The CCNC will measure the number of particles available for acting as cloud condensation nuclei as a function of particle size and water vapour supersaturation. The instrument achieves this by exposing the sample to an “artificial cloud” of defined user-selectable supersaturation. This will ultimately allow statements not only on the direct, but also the indirect aerosol climate effect.

This full picture will not only allow a better source apportionment of the aerosol observed. The full set of optical properties will also facilitate an estimate of local, instantaneous direct aerosol radiative forcing, and a comparison with the radiative forcing of greenhouse gases at the site.

Model studies: calculation of trends

To calculate the annual trends the observations have been fitted as described in Simmonds et al. (2006) by an empirical equation of Legendre polynomials and harmonic functions with linear, quadratic, and annual and semi-annual harmonic terms:

$$f(t) = a + b \left(\frac{N}{12} \right) \cdot P_1 \left(\frac{t}{N} - 1 \right) + \frac{1}{3} \cdot d \left(\frac{N}{12} \right)^2 \cdot P_2 \left(\frac{t}{N} - 1 \right) + c_1 \cdot \cos \left(\frac{2\pi t}{N} \right) + s_1 \sin \left(\frac{2\pi t}{N} \right) + c_2 \cdot \cos \left(\frac{4\pi t}{N} \right) + s_2 \sin \left(\frac{4\pi t}{N} \right)$$

The observed f can be expressed as functions of time measures from the 2N-months interval of interest. The coefficient a defines the average mole fraction, b defines the trend in the mole fraction and d defines the acceleration in the trend. The c and s define the annual and inter-annual cycles in mole fraction. N is the mid-point of the period of investigation. P_i are the Legendre polynomials of order i .

Determination of background data

Based on the daily mean concentrations an algorithm is selected to find the values assumed as clean background air. If at least 75% of the trajectories within +/- 12 hours of the sampling day are arriving from a so-called clean sector, defined below, one can assume the air for that specific day to be non-polluted. The remaining 25% of the trajectories from European, Russian or North-American sector are removed before calculating the background.

Appendix II: Acknowledgments and affiliations of external authors

We gratefully acknowledge the work of the station personnel from the Norwegian Polar Institute for taking care of the observations in Ny-Ålesund. The authors acknowledge the NOAA Air Resources Laboratory (ARL) for the provision of the HYSPLIT transport and dispersion model and/or READY website (arl.noaa.gov/ready.php). Analyses and visualization used in this report were produced with the Giovanni online data system, developed and maintained by the NASA GES DISC. We also acknowledge the MODIS mission scientists and associated NASA personnel for the production of the data used here. SCIAMACHY TOSOMI ozone overpass data were obtained from the TEMIS website (temis.nl/protocols/o3field/overpass_scia.html), Meteorological data for Ny-Ålesund were received via eKlima (www.eklima.no), the web portal from the Norwegian Meteorological Institute. We greatly acknowledge the personnel for obtaining the data and making them publically available.

Christoph Wehrl and Carlos Toledano are acknowledged due to their contributions with the aerosol observations, quality assurance and interpretations.

Christoph Wehrl
WORCC, PMOD/WRC, Dorfstrasse 33, Davos Dorf
CH-7260, Switzerland

Carlos Toledano
Grupo de Óptica Atmosférica
Universidad de Valladolid
Prado de la Magdalena s/n
47071 Valladolid, Spain



KLIMA- OG
FORURENSNINGS-
DIREKTORATET

Klima- og forurensningsdirektoratet
Postboks 8100 Dep, 0032 Oslo
Besøksadresse: Strømsveien 96
Telefon: 22 57 34 00
Telefaks: 22 67 67 06
E-post: postmottak@klif.no
Internett: www.klif.no

Utførende institusjon NILU – Norwegian Institute for Air Research NILU project no.: O-99093 NILU report no.: OR 14/2012	ISBN-nummer 978-82-425-2493-5 (trykt) 978-82-425-2494-2 (elektronisk)
--	--

Oppdragstakers prosjektansvarlig Cathrine Lund Myhre	Kontaktperson i Klif Harold Leffertstra	TA-nummer 2902/2012
		SPFO-nummer 1117/2012

	År 2012	Sidetall 78	Klifs kontraktnummer 4011022
--	------------	----------------	---------------------------------

Utgiver NILU – Norsk institutt for luftforskning	Prosjektet er finansiert av Klima- og forurensningsdirektoratet (Klif) og NILU – Norsk institutt for luftforskning
---	---

Forfatter(e) C.L. Myhre, O. Hermansen, A.M. Fjæraa, C. Lunder, M. Fiebig, N. Schmidbauer, T. Krognæs, K. Stebel
Tittel - norsk og engelsk Overvåking av klimagasser og partikler på Svalbard og Birkenes: Årsrapport 2010 Monitoring of greenhouse gases and aerosols at Svalbard and Birkenes: Annual report 2010
Sammendrag – summary Rapporten presenterer aktiviteter og måleresultater fra klimagassovertvåkingen ved Zeppelin observatoriet på Svalbard for årene 2001-2010 og klimagassmålinger og klimarelevante partikkelmålinger fra Birkenes for 2010. Overvåkingsprogrammet utføres av NILU – Norsk institutt for luftforskning og er finansiert av Statens forurensningstilsyn (SFT) (nå Klima- og forurensningsdirektoratet (Klif)) og NILU – Norsk institutt for luftforskning. The report summaries the activities and results of the greenhouse gas monitoring at the Zeppelin and observatory situated on Svalbard in Arctic Norway during the period 2001-2010 and the greenhouse gas monitoring and aerosol observations from Birkenes for 2010. The monitoring programme is performed by the NILU – Norwegian Institute for Air Research and funded by the Norwegian Pollution Control Authority (SFT) (now Climate and Pollution Agency) and NILU – Norwegian Institute for Air Research.

4 emneord Drivhusgasser, partikler, Arktis, halokarboner	4 subject words Greenhouse gases, aerosols, Arctic, halocarbons
---	--



Klima- og forurensningsdirektoratet

Postboks 8100 Dep,
0032 Oslo

Besøksadresse: Strømsveien 96

Telefon: 22 57 34 00

Telefaks: 22 67 67 06

E-post: postmottak@klif.no

www.klif.no

Om Statlig program for forurensningsovervåking

Statlig program for forurensningsovervåking omfatter overvåking av forurensningsforholdene i luft og nedbør, skog, vassdrag, fjorder og havområder. Overvåkingsprogrammet dekker langsiktige undersøkelser av:

- overgjødsling
- forsuring (sur nedbør)
- ozon (ved bakken og i stratosfæren)
- klimagasser
- miljøgifter

Overvåkingsprogrammet skal gi informasjon om tilstanden og utviklingen av forurensningssituasjonen, og påvise eventuell uheldig utvikling på et tidlig tidspunkt. Programmet skal dekke myndighetenes informasjonsbehov om forurensningsforholdene, registrere virkningen av iverksatte tiltak for å redusere forurensningen, og danne grunnlag for vurdering av nye tiltak. Klima- og forurensningsdirektoratet er ansvarlig for gjennomføringen av overvåkingsprogrammet.

SPFO-1117/2012

TA-2902/2012

ISBN 978-82-425-2493-5 (trykt)

ISBN 978-82-425-2494-2 (elektronisk)